GENETIC VARIATION IN THE UNCOUPLING PROTEIN AND FATTY ACID BINDING PROTEIN GENE FAMILIES: A MULTI-LOCUS APPROACH TO INVESTIGATING OBESITY AND TYPE 2 DIABETES

by

Coleen Mae Damcott

Associates in Applied Science, SUNY Alfred, 1995

Bachelor of Science, Cornell University, 1997

Submitted to the Graduate Faculty of

The Graduate School of Public Health in partial fulfillment

of the requirements for the degree of

Doctor of Philosophy

University of Pittsburgh

2002

UNIVERSITY OF PITTSBURGH

GRADUATE SCHOOL OF PUBLIC HEALTH

This dissertation was presented

by

Coleen Mae Damcott

It was defended on

April 17, 2002

and approved by

Robert Ferrell, PhD,
Department of Human Genetics

Eleanor Feingold, PhD,
Department of Human Genetics

David Finegold, MD,
Department of Pediatrics

Michael Barmada, PhD,
Department of Human Genetics

Dissertation Director:
Robert Ferrell, PhD,
Department of Human Genetics

GENETIC VARIATION IN THE UNCOUPLING PROTEIN AND FATTY ACID BINDING PROTEIN GENE FAMILIES: A MULTI-LOCUS APPROACH TO INVESTIGATING OBESITY AND TYPE 2 DIABETES

Coleen Mae Damcott, PhD

University of Pittsburgh, 2002

Obesity and type 2 diabetes are heterogeneous conditions caused by a combination of genetic and environmental factors. A number of candidate gene families have been identified that influence obesity- and diabetes-related traits, including the uncoupling proteins (UCPs) and fatty acids binding proteins (FABPs). The UCPs are mitochondrial transport proteins that promote proton leakage across the inner mitochondrial membrane, uncoupling oxidative phosphorylation from ATP production and releasing energy as heat. The FABPs are intracellular transporters of fatty acids that facilitate lipid metabolism and gene transcription regulation. The UCPs and FABPs influence energy metabolism, fuel substrate partitioning, glucose and lipid metabolism, and insulin action. In this study, we identified variation in UCP and FABP genes, explored the influence of that variation on phenotype through multi-locus analyses, and assayed the functional consequences of promoter variation on gene expression. Using the multi-locus analysis approach, we constructed regression models that explained a relatively large portion of the variation in phenotypes in comparison to the individual effects of single loci. Several of the models explained upwards of 10% of the variation in traits. This suggests that a multi-locus approach to studying complex disease is

much more informative than considering single loci individually. In addition to the statistical analyses, functional studies were performed to assess the effects of promoter variation on gene expression. Variation in the FABP2 promoter region was associated with levels of promoter activity, suggesting a biological explanation for effects of this polymorphism on phenotype. This exploratory analysis identified a number of interesting multi-locus genetic effects on traits related to obesity and type 2 diabetes, suggesting that consideration of multiple gene effects is a more comprehensive approach to understanding complex disease.

TABLE OF CONTENTS

LIST OF TABLES

LIST OF FIGURES

I. SPECIFIC AIMS

The purpose of this study is to explore the genetic contributions to the development of obesity and type 2 diabetes. Two families of candidate genes, the uncoupling proteins and the fatty acid binding proteins, were chosen for study. The uncoupling proteins (UCPs) are inner mitochondrial transport proteins that influence energy homeostasis, insulin action, fuel substrate partitioning, and substrate oxidation. The fatty acid binding proteins (FABPs) are intracellular transporters of fatty acids that facilitate lipid metabolism and gene transcription regulation. The FABPs influence transcription of the UCP genes and themselves by acting as transporters of ligands (fatty acids) for the peroxisome proliferator-activated receptor (PPAR) family of ligand-activated transcription factors. These gene families interact in a biological pathway to influence traits related to obesity and type 2 diabetes. Due to the complex nature of both obesity and type 2 diabetes and the genetic pathways influencing them, it is important to explore the effects of variation in these gene families through a multi-locus approach. This study will examine the impact of genetic variation in the UCP and FABP gene families on obesity and type 2 diabetes by fulfilling the following investigational plan:

1. Screen the coding regions and promoter sequence of UCP1, UCP2, UCP3, FABP2, FABP3, and FABP4 to identify polymorphic variation.

2. Genotype 764 participants of the San Luis Valley Diabetes Study for the variants identified in the six genes listed in Aim 1.

3. Use analysis of variance (ANOVA) and multiple linear regression analyses to identify associations between the variants and traits related to obesity and type 2 diabetes, exploring single locus and multi-locus effects.

4. Perform promoter activity assays to determine functional effects of chosen promoter variants.

II. INTRODUCTION AND BACKGROUND

A. OBESITY

Obesity is a common condition most prevalent in Westernized societies, with approximately 20-30% of adults affected in the United States (Friedman 2000; Lönnqvist et al. 1999). The most commonly used measure of overweight and obesity is body mass index (BMI), which is calculated as weight in kilograms divided by square of the height in meters. The World Health Organization proposed a classification system in which a BMI measure of 18.5-25 kg/m^2 indicates "healthy" weight, a BMI measure of 25-30 kg/m^2 signifies overweight, and a BMI measure greater than 30 kg/m^2 characterizes obesity. By the year 2030, an estimated 45% of the US population will meet the criterion for obesity. Obesity is a major risk factor for common diseases including type 2 diabetes, hypertension, atherosclerosis, and various forms of cancer. Thus, obesity leads to increased morbidity and mortality, placing a large burden on the US healthcare system (Kopelman 2000).

Obesity is a multifactorial disorder encompassing various genetic and environmental components manifesting in imbalances in energy intake and expenditure (Kopelman 2000). On the physiological level, genetic and environmental influences act upon body weight through alterations in energy balance. Body weight is regulated by the coordination of energy intake and expenditure. Intake is simply the mass of calories that enter the body. Expenditure is composed of three factors: resting energy expenditure (50% to 60% of daily energy expenditure), physical activity, and adaptive thermogenesis (Solanes et al. 1997; Flier and Lowell 1997). Resting energy

expenditure is the energy required for cellular and organ function (Taber 1997), and adaptive thermogenesis is the response to environmental changes such as food intake, cold exposure, and infection (Ricquier and Bouillaud 2000). Energy homeostasis is maintained by signals from feedback loops linked to mechanisms such as food intake, energy expenditure, glucose metabolism, and fat metabolism. Thus, modification of the genes controlling these pathways could influence the development of obesity and its complications.

B. TYPE 2 DIABETES MELLITUS

Glucose homeostasis in mammals is imperative to proper metabolism and is maintained, primarily, by pancreatic β cells, which secrete insulin in response to increasing concentrations of glucose. Insulin lowers blood glucose by stimulating glucose uptake into skeletal muscle and adipose tissue and by suppressing glucose production by the liver. Diabetes mellitus is a condition in which hyperglycemia occurs as a result of disruptions in insulin production or action. Type 1 diabetes mellitus is characterized by the destruction of the pancreatic islet cells, resulting in extremely low levels of insulin or complete absence if insulin. Type 2 diabetes mellitus is characterized by impaired insulin sensitivity (inability to lower blood glucose levels) in combination with pancreatic β cell dysfunction (inability to sense blood glucose levels and secrete appropriate quantities of insulin in response). As a result, β cells are unable to meet the demand for increased insulin secretion induced by insulin resistance, resulting in hyperglycemia due to a relative deficiency in circulating insulin levels (Zhang et al. 2001; Fujimoto 2000). Ninety percent of diabetic cases are type 2 (Birnbaum 2001).

Type 2 diabetes is the most common metabolic disorder, reaching epidemic proportions worldwide. The global trend demonstrates that increases in prevalence accompany migration of ethnic groups from underdeveloped areas to more westernized regions and adoption of westernized diets. In the US, the overall prevalence of type 2 diabetes is ~6-7% (Kahn et al. 1996) with virtually every other ethnic group showing a higher prevalence than the European Caucasian population. Mexican American and Pima Indian populations in the US reach prevalence levels of ~14% and ~45%,

respectively (Fujimoto 2000). Diabetes is the leading cause of blindness, renal failure, nerve damage, and limb amputation in adults. Diabetes is also a major risk factor for cardiovascular disease and stroke (Brownlee 2001). In 1995, an estimated 135 million people suffered from diabetes. By 2025, that number is expected to soar to about 300 million. Thus, diabetes is a major public health concern (Fujimoto 2000).

Obesity and type 2 diabetes are heterogeneous conditions caused by a combination of genetic and environmental factors. A strong genetic component is suggested for both conditions based on family studies. A large meta-analysis of monozygotic versus dizygotic twin pair studies estimated the heritability for BMI to be 50-90% (Barsh et al. 2000). The concordance rate for type 2 diabetes in monozygotic twins ranges from 50%-90% (Kahn et al. 1996). A strong environmental influence is evident in the differences in prevalence of obesity and/or diabetes among populations with similar genetic background living in different areas (eg. individuals of Japanese descent living in Seattle have an ~3-fold increase in prevalence of type 2 diabetes compared to those living in Tokyo; Fujimoto 2000). A number of mouse models representing monogenic forms of both obesity and diabetes have been identified (eg. *ob/ob*, *db/db*, *tub/tub*); however, monogenic forms of obesity (eg. Prader-Willi, Cohen, and Bardet-Biedl syndromes) and diabetes (eg. MODY) in humans are rare, so they are unable to explain the genetic causes of obesity and diabetes in the population as a whole (Barsh et al. 2000; Kahn et al. 1996). Linkage and association studies in both humans and rodents have identified a number of candidate genes influencing both conditions; however, they give variable results, perhaps due to the existence of many small gene effects interacting to create a phenotype or susceptibility to a phenotype.

Thus, a reasonable approach to studying complex diseases such as obesity and diabetes is to consider a biological model in which gene products interact to accomplish a specific function, screen for variation in the genes, and assay the effects of the variation on phenotype through a multi-locus analysis.

C. THE SAN LUIS VALLEY DIABETES STUDY

The individuals chosen for this study are participants of the San Luis Valley Diabetes Study (SLVDS). The SLVDS was established in 1983 as a case-control study of type 2 diabetes prevalence, risk factors and complications in Hispanic and non-Hispanic white subjects living in the San Luis Valley of Colorado. The age adjusted prevalence rates for type 2 diabetes in the study area are shown in Table 1. Over the course of the study, the SLVDS has evolved into a cohort study with the purpose of investigating genetic and environmental risk factors for type 2 diabetes and cardiovascular disease.

Table 1: Age adjusted prevalence of type 2 diabetes in the San Luis Valley

	Males	Females
Hispanic	4.4%	6.2%
Non-Hispanic White	2.1%	1.3%

Criteria for inclusion in the study at baseline (1984-1988: Phases I and II) included: residence in the study area, use of Spanish or English, age 20-74, and self reported race as Hispanic or non-Hispanic white. Diabetics were identified by review of medical records and through advertisement. New cases of diabetes were identified in the population sample by a standard oral glucose tolerance test. The non-diabetic controls were identified through a census-type process and randomly chosen. The participants returned for two cycles of follow-up visits in the years 1988-1992 (Phase III) and 1997-1998 (Phase IV) to identify the development of impaired glucose tolerance

(IGT), type 2 diabetes, cardiovascular disease, diabetic complications, and mortality. Measures of body composition, diet, physical activity, medical history, and blood components (eg. glucose, insulin, cholesterol) were obtained at each visit (Hamman et al. 1989). For the current study, 764 individuals (321 Hispanics/443 Non-Hispanic whites) from a non-diabetic control group, a subset of the SLVDS, were genotyped for the polymorphisms identified in the UCP genes and the FABP genes.

D. THE UNCOUPLING PROTEIN FAMILY

1. Mitochondrial Energy Metabolism

Mitochondria are organelles within the cytoplasm of the cell described as the "cellular powerhouses." The mission of the mitochondria is to carry out cellular respiration, producing the ATP energy required for cellular and subsequently whole organism function. Efficient ATP production is largely dependent on the electrochemical gradient generated across the highly selective inner mitochondrial membrane during substrate oxidation. The gradient is formed as protons are pumped into the intramembrane space from the matrix by the flow of electrons along the electron transport chain. This protonmotive force facilitates the production of ATP by driving protons back into the mitochondrial matrix through ATP synthase, the inner membrane protein complex responsible for ADP phosphorylation. Since protons cannot enter the matrix through ATP synthase in the absence of ADP, proton reentry is coupled to phosphorylation of ADP to ATP. Natural inefficiencies in ATP production occur in the form of proton "leaks" that dissipate the gradient by circumventing ATP synthase, thereby uncoupling fuel substrate oxidation from ATP production and releasing energy as heat (Harper and Himms-Hagen 2001; Adams 2000; Dalgaard et at. 2001b).

Uncoupling activity is imperative to the whole organism for its roles in thermoregulation and substrate oxidation efficiency. Thermoregulation is the ability of an organism to adjust to environmental changes in temperature through production and/or dissipation of heat to maintain body temperature (Harper and Himms-Hagen 2001). In rodents and other small mammals, thermoregulation is primarily achieved

through uncoupling-mediated non-shivering thermogenesis, taking place in the highly specialized brown adipose tissue (BAT; Stuart et al. 2001). Brown adipocytes are laden with mitochondria, increasing their capacity for oxidative phosphorylation and hence the opportunity for heat production through uncoupling activity. In humans, BAT stores are abundant in newborns to facilitate acclimation to temperatures outside the womb. By adulthood, however, only small quantities of BAT remain, weakening its potential as a major thermogenic tissue in humans (Harper et al. 2001). Mitochondria in several other tissues have also been shown to possess significant levels of uncoupling activity, including skeletal muscle, the major tissue of thermogenesis in humans. In fact, Brand et al. (1999) estimated that the proton leak in tissues other than BAT accounts for ~20-50% of total energy expenditure.

The role of uncoupling activity in the efficient oxidation of fuel substrates revisits the simple concept of energy balance. In the event that energy intake chronically exceeds energy expenditure, excess calories are stored as fat, leading to obesity. The uncoupling of fuel substrate oxidation from ATP production results in the release of heat and subsequent burning of calories. In that capacity, uncoupling activity potentially modulates resistance to obesity (Harper et al. 2001).

2. The Uncoupling Proteins

The uncoupling proteins (UCPs) are a family of mitochondrial transport proteins that promote proton leakage across the inner mitochondrial membrane, uncoupling proton transfer from ATP production and initiating thermogenesis (Klaus et al. 1991).

Due to the involvement of the uncoupling proteins in thermogenesis, this protein family has been implicated as mediators of energy metabolism and regulators of body weight.

a) Uncoupling Protein-1

Uncoupling protein-1 (UCP1) is expressed exclusively in BAT, the major site of cold-induced non-shivering thermogenesis and diet-induced thermogenesis in most mammals (Dalgaard et al. 2001a). The UCP1 protein is found abundantly in the inner mitochondrial membrane of BAT mitochondria. UCP1 expression is influenced by cold exposure, fasting, and high fat diet and regulated by thyroid hormone, leptin, insulin, glucocorticoids, β_3-adrenergic agonists, peroxisome proliferator-activated receptor agonists, purine nucleotides (ATP, ADP, GTP, GDP) and free fatty acids (Dalgaard et al. 2001a; Silva et al. 1997; Solanes et al. 1997; Bao et al. 1998; Boss et al. 2000). In adult humans, BAT stores are minimal, arguing against the involvement of UCP1 as a major player in energy balance in humans. Thus, recently identified homologues of this BAT specific protein, UCP2 and UCP3, have become a focal point in human thermogenesis.

b) Uncoupling Protein-2

UCP2 is widely expressed in human tissues, including: brown adipose tissue, white adipose tissue, skeletal muscle, heart, lungs, stomach, liver, kidney, pancreas and the immune system (Fleury et al. 1997; Bao et al. 1998; Tu et al. 1999). UCP2 expression is regulated differently among the various tissues by cold exposure, high fat diet, fasting, β_3-adrenergic agonists, peroxisome proliferator-activated receptor agonists,

free fatty acids, leptin, glucocorticoids and thyroid hormone (Dalgaard et al. 2001a; Walder et al. 1998).

c) Uncoupling Protein-3

UCP3 expression is exclusive to skeletal muscle, a major site of thermogenesis, energy homeostasis, and substrate oxidation in humans (Boss et al. 1997, Gong et al. 1997, Vidal-Puig et al. 1997). It is also found in the BAT of rodents. Expression of UCP3 is modulated differently between its two sites of expression. In BAT, UCP3 expression is upregulated by cold exposure, leptin, and thyroid hormone; moderately stimulated by high fat diet, insulin, and β_3-adrenergic agonists; and downregulated by fasting, chronic exercise, and glucocorticoids. In skeletal muscle, UCP3 expression is upregulated by high fat diet, fasting, free fatty acids, leptin, glucocorticoids, thyroid hormone, β_3-adrenergic agonists, and peroxisome proliferator-activated receptor agonists; moderately stimulated by insulin and cold exposure; and downregulated by chronic exercise (Dalgaard et al. 2001a; Walder et al. 1998; Gong et al. 1999; Gong et al. 1997; Weigle et al. 1998). Since UCP3 is exclusively expressed in these two thermogenically active tissues, as opposed to the wide distribution of UCP2, it is suggested that UCP3 plays a major role in thermogenesis in humans.

Each member of the uncoupling protein family is approximately 300 amino acids long. Structurally, they consist of six transmembrane domains and exist as homodimers in their functional forms (Boss et al. 2000). UCP2 and UCP3 share 71% amino acid identity to one another and 55% and 57% identity, respectively, to UCP1 (Vidal-Puig et al. 1997; Boss et al. 1997). UCP1 is located on chromosome 4 (Cassard et al. 1990).

UCP2 and UCP3 have been mapped within 8kb of one another on chromosome 11q13 (Pecqueur et al. 1999; Boss et al. 1998c), a region linked to variation in obesity, resting energy expenditure, and hyperinsulinemia (Fleury et al. 1997; Bouchard et al. 1997). The syntenic region on mouse chromosome 7 is linked to obesity, resting energy expenditure, and type-2 diabetes mellitus (Fleury et al. 1997). The close proximity of these genes suggests that one arose from the other in a duplication event (Tu et al. 1999).

3. Mechanisms of Proton Transport by UCP1

The precise molecular mechanisms directing uncoupling activity are still under investigation; however, experiments involving UCP1 reveal information on the mechanisms of UCP-mediated mitochondrial proton leak. Proton transport across the inner mitochondrial membrane by UCP1 is initiated and presumably performed by free fatty acids. Two major hypotheses exist to explain the mechanism by which free fatty acids facilitate this process. The first hypothesis suggests that carboxyl groups of fatty acids residing within the walls of the transport channel formed by the UCP1 protein act as proton donor/acceptors, passing the protons through to the mitochondrial matrix. The second hypothesis proposes that fatty acid anions are passed outward to the cytosol through the transport channel where they are protonated. The protonated fatty acids return to the matrix by flip-flop through the membrane bilayer to release the proton. The final outcome of either mechanism is the dissipation of the proton gradient due to the displacement of protons into the matrix, causing the uncoupling of oxidative phosphorylation. This process results in the release of energy as heat and a

subsequent increase in fuel substrate oxidation. Proton transfer is inhibited by purine nucleotides, which bind to UCP1 on the cytosolic side (Boss et al. 2000; Klingenberg 1999).

4. Uncoupling Activity in UCP2 and UCP3

It has been demonstrated in several ion flux experiments using yeast and mammalian cell lines that both UCP2 and UCP3 lower mitochondrial membrane potential and increase cellular respiration rate, predicting a role in uncoupling activity (Fleury et al. 1997; Gimeno et al. 1997; Zhang et al. 1999; Boss et al. 1998a). In conjunction with demonstrated sequence and structural homology to UCP1, this evidence suggests that UCP2 and UCP3 do perform as true uncouplers (Boss et al. 2000; Lowell et al. 2000).

5. Transgenic Mouse Models

a) UCP1 Knockout Mouse

The UCP1 knockout mouse was developed by Harper, Kozak, and colleagues using homologous recombination with a deletion vector that disrupted exon 2 and part of exon 3, resulting in no UCP1 mRNA of normal size (Enerback et al. 1997). Due to the uncoupling activity displayed by UCP1 in BAT, a tissue imperative to energy balance, these mice were hypothesized to be obese and cold-sensitive. Surprisingly, they do not show increased susceptibility to obesity even on a high fat diet. They are, however, unable to maintain normal body temperature when exposed to 4^{o}C,

suggesting a defect in thermogenesis. UCP1 knockout mice also show an increase in interscapular BAT, the source of fuel for thermogenesis, and a blunted response in oxygen consumption to administration of a β_3-adrenergic agonist, both indicators of defective thermogensis (Enerback et al. 1997; Kozak et al. 2000; Harper et al. 2001).

UCP1 knockout mice display a 5-fold elevation in UCP2 mRNA levels in BAT without significant changes in expression levels in any other tissue, hinting at a role for UCP2 in compensatory mechanisms (Enerback et al. 1997; Kozak et al. 2000; Harper et al. 2001). UCP3 mRNA expression is unaltered (Harper et al. 2001). The sensitivity to cold, however, indicates that UCP2 and UCP3 are unable to compensate for the role of UCP1 in thermoregulation, which suggests further that UCP2 and UCP3 are regulated by different factors and perform alternative functions. Additional experiments by Monemdjou et al. (1999) demonstrate evidence of this at the molecular level. They show that the mitochondrial proton leak in BAT of UCP1 knockout mice is insensitive to the purine nucleotide, GDP, an effective UCP1 inhibitor. In wildtype control mice, GDP is able to inhibit overall mitochondrial proton leak in BAT by 50%, suggesting that UCP1 accounts for the majority of uncoupling in BAT. The residual proton leak seen in mitochondria of BAT, presumably facilitated by UCP2, UCP3, and other proteins with uncoupling ability, is regulated by alternative factors and is unable to reach levels of thermogenesis necessary for thermoregulation (Monemdjou et al. 1999).

A second study conducted by Monemdjou et al. (2000) examined proton leak in skeletal muscle mitochondria of UCP1-deficient mice. They observed an increase in proton leak in the muscle, suggesting a compensatory thermogenic mechanism by which these mice avoid obesity.

b) UCP2 Knockout Mouse

UCP2-deficient mice were generated by two groups, Arsenijevic et al. (2000) and Zhang et al. (2001), using homologous recombination to disrupt coding exons. Arsenijevic et al. (2000) observed that the UCP2 knockout mouse retained normal body weight homeostasis even on a high fat diet and normal response to cold exposure, suggesting that UCP2 is not imperative to cold- or diet-induced thermogenesis. However, UCP1 mRNA levels were elevated in WAT, raising the possibility of compensatory mechanisms. No change in UCP3 mRNA expression was observed. Mitochondrial proton leak was reduced in the transgenic mouse, providing further evidence that UCP2 does carry out uncoupling activity (Arsenijevic et al. 2000).

Upon examination of the UCP2-deficient mouse, Zhang et al. (2001) observed evidence that UCP2 influences β cell function. The UCP2 knockout mice exhibited elevated serum insulin levels and lower plasma glucose in comparison to wild-type mice, providing *in vivo* evidence of increased insulin secretion and glucose uptake. Cultured islet cells from UCP2 null mice produced more ATP and secreted more insulin in response to glucose than islets of control animals. This indicates that mitochondrial metabolism is tightly coupled to ATP synthesis in the absence of the uncoupling protein, providing the energy required for increased functional efficiency of the β cells (Zhang et al. 2001). In corroboration, normal rat islet cells overexpressing UCP2 experienced inhibition of glucose-stimulated insulin secretion and a 50% reduction in ATP content (Chan et al. 1999; Chan et al. 2001).

To further examine the effects of UCP2 deficiency, Zhang et al. (2001) crossed the UCP2 knockout mice with *ob/ob* mice, a leptin-deficient mouse model of obesity.

The phenotype of the *ob/ob* mouse includes hyperphagia, severe obesity, hyperinsulinemia, and development of diabetes. UCP2 mRNA expression is markedly upregulated in islets of *ob/ob* mice in comparison to islets of wild-type mice, suggesting a link between UCP2 and the *ob/ob* phenotype. The *ob/ob* mice lacking UCP2 were still severely obese; however, these mice showed increased insulin secretion, increased serum insulin levels, and greatly reduced serum glucose levels, suggesting partial rescue from the development of diabetes (Zhang et al. 2001). Thus, UCP2 seems to behave as a negative regulator of insulin action, influencing β cell glucose sensing and the ensuing insulin secretion.

c) UCP3 Knockout Mouse

Two groups simultaneously reported development of the UCP3 knockout mouse. Gong et al. (2000) and Vidal-Puig et al. (2000) created the transgenic mice using homologous recombination targeting exon 2, the first coding exon of UCP3. UCP3 knockout mice are healthy, lacking an enhanced susceptibility to obesity. They display normal responses in body temperature, metabolic rate, and respiratory quotient to fasting, cold exposure, thyroid hormone, and β_3-adrenergic agonist. Serum levels of insulin, free fatty acids, triglycerides, and leptin are also normal. The only apparent discrepancy in phenotype is reduced mitochondrial proton leak (Gong et al. 2000; Vidal-Puig et al. 2000; Harper et al. 2001). Gong et al. (2000) observed that mitochondrial proton leak was "greatly reduced in muscle, minimally reduced in BAT, and unaltered in liver mitochondria, suggesting that UCP3 is responsible for the majority of mitochondrial leak in skeletal muscle."

d) UCP3 Overexpressing Mouse

Clapham et al. (2000) developed UCP3 overexpressing mice through microinjection of a transgene, consisting of the UCP3 coding region driven by the α-skeletal actin promoter, into fertilized mouse eggs. These mice experienced a 66-fold increase in UCP3 mRNA expression accompanied by an increase in skeletal muscle mitochondrial proton leak, triggering increased energy expenditure. Mice overexpressing UCP3 are hyperphagic, enjoying a 50% increase in food intake, but weigh less than their wildtype littermates due, at least in part, to strikingly reduced adipose tissue mass. Leptin levels in the transgenic mice are not significantly different from control mice regardless of this reduction in adipose tissue. Despite an increase in food intake, plasma triglyceride and non-estrified fatty acid levels are also similar between overexpressing and control mice, indicating an increase in fatty acid oxidation. This increase in lipid oxidation is presumed useful for fueling increased metabolic rates. These mice also display decreased fasting plasma glucose and insulin, increased glucose clearance, and lower total cholesterol (Clapham et al. 2000; Moore et al. 2001; Harper et al. 2001).

6. UCP2 and UCP3 in Fuel Partitioning

A role in fuel substrate management has been proposed for UCP2 and UCP3 in skeletal muscle based on experiments revealing that increased levels of UCP2 and UCP3 mRNA levels correlate with increased levels of fat metabolism (Boss et al. 2000). Several fasting and refeeding experiments show evidence that UCP2 and UCP3 are

involved in lipid metabolism in skeletal muscle of rodents. In normal rats, UCP2 and UCP3 mRNA in skeletal muscle are upregulated during starvation, a period of fat store mobilization, and downregulated in response to refeeding, a period of fat store replenishment (Samec et al. 1998a; Brun et al. 1999; Samec et al. 1998b). In humans, fasting induced an increase in UCP2 and UCP3 mRNA expression in white adipose tissue (UCP2 only) and skeletal muscle (Millet et al. 1997). In addition, Boss et al. (2000) observed that UCP2 and UCP3 mRNA levels correlate with increased levels of fat metabolism. This suggests a role for UCP2 and UCP3 in fuel partitioning in skeletal muscle and adipose tissue.

7. Association Studies In Human Populations

a) UCP1

Oppert et al. (1994) identified an A to G base pair substitution at –3826 bp of the UCP1 transcription start site, which they found to be associated with body fat gain over time in participants of the Quebec Family Study. Subsequent studies concerning that polymorphism have been inconsistent. The A-3826G variant has been shown to be associated with weight gain and resistance to weight loss during dieting in obese French subjects (Clement et al. 1996; Fumeron et al. 1996) and BMI in overweight Australian women (Heilbronn et al. 2000). On the other hand, a few studies found no association with obesity-related phenotypes, weight gain over time, or diabetes (Urhammer et al. 1997a; Gagnon et al 1998; Shaffler et al. 1999; Evans et al. 2000). When the A-3826G variant was considered simultaneously with the Trp64Arg

polymorphism in the β-adrenergic receptor gene, interaction between the two polymorphic sites was consistently associated with weight gain and basal metabolic rate in obese individuals (Clement et al. 1996; Valve et al. 1998; Evans et al. 2000).

Urhammer et al. (1997a) identified a number of polymorphisms in the coding region of UCP1 including a G to A substitution in condon 64 of exon 2, resulting in an alanine to threonine amino acid change, and an A to T substitution in codon 229 of exon 5, causing a methionine to leucine amino acid change. Neither of these polymorphisms have been shown to contribute significantly to the development of obesity (Urhammer et al. 1997a; Hamann et al. 1998); however, Mori et al (2001) recently reported an association between type 2 diabetes in Japanese subjects and the Met229Leu variant, which is in high linkage disequilibrium with a UCP1 promoter variant (-112 bp) shown to affect promoter activity.

b) UCP2

Through mutational analysis of the coding region of UCP2, Urhammer et al. (1997b) identified an Ala55Val (C→T) substitution in exon 4 of UCP2. Otabe et al. (1998) reported a 45-base pair insertion/deletion polymorphism in the 3' untranslated region of exon 8. Genotype/phenotype studies of both of these variants are conflicting. Walder et al. (1998) reported association between both UCP2 polymorphisms and sleeping metabolic rate and between the exon 8 insertion/deletion variant and 24-hour metabolic rate in Pima Indians. The Ala55Val variant was also associated with enhanced metabolic efficiency and fat oxidation in Danish subjects (Astrup et al. 1999), while the insertion/deletion polymorphism was shown to be associated with BMI (Walder

et al. 1998; Cassell et al. 1999). A number of other studies showed no association with obesity- and diabetes-related phenotypes (Urhammer et al. 1997b; Otabe et al. 1998; Dalgaard et al. 1999).

c) UCP3

Urhammer et al. (1998) identified a T to C silent substitution in codon 99 in exon 3 of UCP3, which was found to be associated with BMI in morbidly obese diabetics (Otabe et al. 1999). A second polymorphism in exon 3 was identified by Argyropoulos et al. (1998), which consisted of a G to A substitution in codon 102, causing a valine to isoleucine amino acid change. Otabe et al. (1999) reported a C to T silent substitution in codon 210 in exon 5 of UCP3. The T/T genotype in that study of obese French patients was weakly associated with diabetic status, but not morbid obesity. Lanouette et al. (2002) recently reported suggestive linkage between the UCP3 codon 210 variant and BMI, fat mass, or leptin levels in black and white individuals. Schrauwen et al. (1999a) identified a variant in the promoter region of UCP3, a C to T substitution at –55bp. In the obese French cohort described above, T homozygosity for this variant was associated with higher BMI and resistance to beneficial effects of physical activity (Otabe et al. 2000). A contrasting study found no association between the –55bp polymorphism and BMI or percent body fat in obese and non-obese Danish subjects (Dalgaard et al. 2001b). The –55bp variant is located in the proximity of two important transcription factors, four base pairs downstream of a PPAR regulatory element and six base pairs upstream of a TATA box (Acín et al. 1999; Tu et al. 2000).

d) mRNA Expression

The uncoupling protein family has been implicated in regulation of energy homeostasis. Thus, inefficiencies in expression of the UCPs may disturb energy balance and lead to the development of obesity. Oberkofler et al. (1997; 1998) explored UCP1 and UCP2 mRNA expression in intra- and extraperitoneal fat stores. Intraperitoneal expression of both UCPs was significantly higher than extraperitoneal expression. Both UCP1 and UCP2 mRNA expression were significantly lower in the intraperitoneal adipose tissue of obese subjects in comparison to lean controls. Extraperitoneal expression was not significantly different between lean and obese individuals. These expression studies suggest that disruption of UCP1 and UCP2 mRNA expression in adipose tissue may play a role in the pathophysiology of obesity. Esterbauer et al. (1998) discovered that the A-3826G variant was associated with UCP1 mRNA expression levels in intraperitoneal fat stores in a dose dependent manner, suggesting a role for this polymorphism in regulation of UCP1 mRNA expression. Two UCP2 promoter variants in complete linkage disequilibrium, a G/A substitution at –866 bp and a T/A polymorphism at –2723 bp, were shown to be associated with UCP2 mRNA levels and obesity. These variants were also shown to affect promoter activity, indicating a role in UCP2 mRNA expression (Esterbauer et al. 2001).

Schrauwen et al. have extensively studied UCP2 and UCP3 mRNA expression in skeletal muscle, the major tissue of energy metabolism in humans. In male Pima Indians, UCP3 mRNA expression was positively correlated with sleeping metabolic rate and tended to correlate with 24-hour metabolic rate, supporting a role for UCP3 in energy metabolism. A negative correlation was shown between UCP3 mRNA levels

and BMI, and UCP3 expression tended to correlate with percent body fat. UCP2 mRNA expression did not correlate with any of the metabolic or obesity measures tested (Schrauwen et al. 1999b). These results suggest that the UCP2 variants observed by Walder et al. (1998) to be associated with sleeping metabolic rate may actually be marking a functional change in the UCP3 gene. In a subsequent study, Schrauwen et al. (1999a) identified the C-55T variant in the UCP3 promoter and determined that the T allele was associated with a 58% increase in UCP3 mRNA expression in skeletal muscle.

E. THE FATTY ACID BINDING PROTEIN FAMILY

1. Introduction

Long-chain fatty acids serve a number of important functions within the human body. They are substrates for metabolism, components of phospholipid membranes, precursors for signaling molecules, and ligands for transcription factors (Glatz et al. 2001). In order to carry out their diverse functions, fatty acids require efficient transport from extracellular depots to their intracellular targets. This transportation is facilitated, both extracellularly and intracellularly, by lipid binding proteins. These proteins bind to the hydrophobic fatty acids, enhancing their solubility and, subsequently, their ability to move through aqueous surroundings (Glatz et al. 1993; Glatz et al. 1995). Fatty acids are transported through the bloodstream to target organs bound to albumin or packaged as triglycerides (Glatz et al. 1997; Hamilton & Kamp 1999). A number of membrane-associated fatty acid transporters have been identified that facilitate transmembrane translocation of fatty acids including: plasma membrane fatty acid binding protein ($FABP_{pm}$), fatty acid translocase (FAT), and a family of fatty acid transport proteins (FATPs; Dutta-Roy 2000). Once inside the cell, the intracellular or cytoplasmic fatty acid binding proteins ($FABP_c$s) transport fatty acids to their intracellular targets(Glatz & Storch, 2001).

The fatty acid binding proteins (FABPs) are a family of cytoplasmic proteins involved in intracellular free fatty acid transport. Eight distinct members of this gene family have been identified and named based on their major tissues of expression: liver-FABP (FABP1), intestinal-FABP (FABP2), heart/muscle-FABP (FABP3), adipocyte-LBP

(FABP4; aP2), myelin-LBP, brain-FABP, ileal-LBP, and epidermal-FABP. Typically, expression of each of the binding proteins is confined to its major tissue of expression. FABP1 and FABP3, however, are more widely expressed. FABP1 is found in the liver and intestinal epithelium, while FABP3 is expressed in heart, skeletal muscle, mammary tissue, lung, brain, kidney, gonads, stomach, and adrenal tissues. Gene structure is highly conserved among the members of this gene family, while amino acid sequence shows higher homology among species than among the gene family members (Vassileva et al. 2000). FABP expression within tissues generally correlates with the rate of fatty acid utilization during periods of energy expenditure and storage. The FABPs are regulated further by dietary factors, hormones, and transcription factors, such as the peroxisome proliferator-activated receptors (PPARs), a superfamily of nuclear, ligand-activated transcription factors (Glatz et al. 1993; Glatz et al. 1995; Bernlohr et al. 1997).

2. Physiological Functions of the FABPs

In addition to the primary function, facilitation of intracellular fatty acid transport, several other roles have been suggested for the FABPs. The FABPs are believed to be involved in specific transport and uptake of fatty acids to intracellular organelles such as the mitochondria and peroxisomes for activation of lipid metabolism by fatty acids or fatty acid-sensitive enzymes. FABPs also compartmentalize pools of intracellular fatty acids to protect cellular membranes and enzymes from the toxic effects of fatty acids. Finally, the FABPs are believed to play a role in signal transduction by transporting fatty acids to the nucleus, where they form complexes with

peroxisome proliferator-activated receptors. These complexes bind to specific response elements in the promoter region of genes, such as the UCPs, to regulate gene expression (Glatz et al. 1993; Glatz et al. 1995; Bernlohr et al. 1997). These proposed functions suggest involvement of the FABPs in cellular lipid metabolism and regulation of gene expression by facilitating and directing fatty acid transport within the cell.

3. Transgenic Mouse Models

a) FABP2 Knockout Mouse

Intestinal-type FABP (FABP2) is highly and exclusively expressed in intestinal epithelial cells, suggesting a role in the uptake and transport of dietary fatty acids in the small intestine (Sweetser et al. 1987; Baier et al. 1995). Vassileva et al. (2000) developed the FABP2 knockout mouse to explore the role this gene in fatty acid transport. They hypothesized that if FABP2 were essential for dietary fatty acid uptake, then the null mice would not gain as much weight as their wild-type counterparts. Surprisingly, the null mice exhibited sex-specific alterations in body weight, with male knockout mice showing increased body weight regardless of dietary fat content. Female null mice, on the other hand, gained the same amount of weight as wild-type controls on a low fat diet and gained less weight than wild-type controls when fed a high fat diet. FABP2 null mice of both sexes developed hyperinsulinemia independent of differences in weight gain. These results indicate that FABP2 is not essential for dietary fat uptake; however, a role in lipid absorption, metabolism and/or secretion may not be ruled out (Vassileva et al. 2000; Glatz et al. 2001).

b) FABP3 Knockout Mouse

Heart-type or muscle-type FABP (FABP3) is highly expressed in cardiac and red skeletal muscle and represents the only FABP family member present in those tissues (Crisman et al. 1987; Claffey et al. 1987). To explore the physiological functions of FABP3 and its family members, the FABP3 knockout mouse was developed by Binas et al. (1999). The FABP3 knockout mouse appeared healthy with no overt morphological abnormalities. However, the FABP3 null mouse showed dramatic decreases in fatty acid uptake into the heart and skeletal muscle. In the cardiac tissue, where cells are normally fueled by fatty acid oxidation, there was a significant increase in glucose uptake and oxidation in the FABP3 knockout mouse, suggesting that glucose compensates as a fuel source. Plasma free fatty acids were increased, indicating reduced uptake and utilization. Glucose levels showed a greater reduction during fasting or feeding of high-fat diet in transgenic mice, suggesting an increase in peripheral glucose oxidation. The FABP3 knockout mouse also showed reduced exercise tolerance. At old age, FABP3-deficient mice develop cardiac hypertrophy characterized by the enlargement of myocyte nuclei, increased mean muscle fiber diameter, and an ~10% increase in heart weight. This knockout mouse model provides physiological evidence of a role for FABP3 in fatty acid transport and metabolism (Binas et al. 1999).

c) FABP4 Knockout Mouse

The adipocyte-type FABP (FABP4; aP2) knockout mouse was originally developed by Hotamisligil et al. (1996). Under normal laboratory conditions, there were

no overt phenotypic differences observed between the FABP4 knockout mouse and wild-type mice. When placed on a high fat diet, both knockout and wild-type mice developed obesity; however, the total weight gain was higher in the null mice. Circulating fatty acid levels in transgenic mice were not different, but plasma triglyceride levels were lower in the obese FABP4-deficient mice (Hotamisligil et al. 1996). Ribarik Coe et al. (1999) observed an ~40% reduction in basal lipolysis and a 3-fold increase in intracellular fatty acid levels. This suggests that FABP4 is not necessary for fatty acid uptake in adipocytes, but it may play a role in triglyceride synthesis and/or secretion. Obese wild-type mice developed hyperinsulinemia in response to obesity-induced insulin resistance. In contrast, FABP4-null mice had lower plasma insulin and glucose levels than wild-type mice, suggesting a role for FABP4 in the development of dietary obesity-induced insulin resistance. Lower glucose levels may also indicate preferential use of glucose as a fuel substrate peripherally and/or increased conversion of glucose to fatty acids in adipocytes (Hotamisligil et al. 1996). A marked increase in keratinocyte-type FABP is also observed in adipose tissue of FABP4 null mice, possibly providing partial compensation for the lack of FABP4 and preventing more dramatic phenotypic alterations (Hotamisligil et al. 1996; Ribarik Coe et al. 1999; Glatz et al. 2001)

4. Association Studies In Human Populations

The majority of the genotype/phenotype studies in the FABP gene family have focused on an alanine to threonine (G→A) substitution in codon 54 in exon 2 of FABP2 identified by Baier et al. (1995). Two studies showed an association between the Thr-encoding allele and increased lipid oxidation (Baier et al. 1995; Pihlajamäki et al. 1997).

In vitro expression studies revealed increased binding affinity and transport of long-chain fatty acids and more efficient secretion of triglycerides in Caco-2 cells (an immortalized human intestinal cell line) expressing the Thr-encoding allele (Baier et al. 1996). A number of study populations showed association between the Thr-encoding allele and elevated plasma cholesterol and triglycerides, particularly postprandially (Pihlajamäki et al. 1997; Agren et al. 1998; Carlsson et al. 2000; Georgopoulos et al. 2000; Galluzzi et al. 2001a). The Thr-encoding allele is associated with insulin resistance in Pima Indians (Baier et al., 1995) and in Japanese men (Yamada et al., 1997), two populations with genetic susceptibility to type 2 diabetes (Yamada et al., 1997). Evidence of impaired insulin action has also been observed in Caucasian carriers of the Thr-encoding allele (Chiu et al. 2001; Galluzzi et al. 2001b). These studies suggest that the Thr-encoding allele of the FABP2 codon 54 variant is associated with increased intestinal uptake of fatty acids, leading to the impairment of insulin action through increased plasma lipid levels.

F. PPAR:RXR/FABP/UCP TRANSCRIPTIONAL PATHWAY

1. Peroxisome Proliferator-Activated Receptors

The peroxisome proliferator-activated receptors (PPARs) are members of the nuclear receptor subfamily of ligand-activated transcription factors. Following ligand binding, the PPARs interact with members of another nuclear receptor subfamily, the retinoid X receptors (RXRs) to form heterodimers. The heterodimer binds to specific response elements in the transcription regulatory regions of target genes, modulating transcription. PPAR action is dependent upon formation of the heterodimer with RXR. There are three subtypes in the PPAR family, PPARα, PPARβ (also referred to as PPARδ and NUC1), and PPARγ (Kersten et al. 2000; Willson et al. 2000). Three isoforms of PPARγ have also been identified, PPARγ1, PPARγ2, and PPARγ3, which are products of alternate promoter usage. The γ1 and γ3 isoforms encode the same protein (Elbrecht et al. 1996; Willson et al. 2000). PPARα is highly expressed in BAT and liver and moderately expressed in kidney, heart, and skeletal muscle. PPARβ is expressed ubiquitously with highest levels of expression in the gut, kidney, and heart. PPARγ is mainly expressed in adipose tissue, and at lower levels in the colon, the immune system, and the retina (Kersten et al. 2000).

Each member of the PPAR gene family has been shown to regulate genes involved in lipid transport and metabolism pathways. In the liver, PPARα regulates genes involved in fatty acid uptake, binding, and oxidation within in the hepatocyte and lipoprotein packaging and transport out of the hepatocyte. PPARγ induces adipocyte

differentiation within fat stores. Little is known concerning PPARβ function; however, it has been linked to colon cancer (Kersten et al. 2000).

2. Free Fatty Acid-Mediated Regulation of UCP Expression

Several lines of evidence implicate free fatty acids in the regulation of UCP2 and UCP3 mRNA expression. In mice, exposure to a high fat diet for 2 weeks caused a marked increase in UCP2 mRNA in adipose tissue (Surwit et al. 1998). Lipid infusion in rats triggered an increase in UCP3 mRNA expression in skeletal muscle, paralleling the increase in circulating free fatty acids (Weigle et al., 1998). In newborn mouse pups, UCP3 mRNA expression in skeletal muscle was initiated by increased plasma free fatty acids induced by suckling (Weigle et al., 1998), with up-regulation continuing throughout lactation. Weaning onto a high-carbohydrate diet caused down-regulation of UCP3, while weaning onto a high-fat diet maintained the UCP3 up-regulation (Brun et al., 1999). UCP3 mRNA levels were also increased in rodent skeletal muscle by exercise, a period of increased plasma free fatty acid levels (Tsuboyama-Kasaoka et al., 1998; Cortright et al., 1999). Human studies also supported a role for fatty acids in UCP2 and UCP3 mRNA expression. In fasted obese humans, expression of UCP3 mRNA was correlated with increased levels of circulating free fatty acids (Boss et al., 1998b). Lipid infusion in humans caused an increase in expression of UCP3 mRNA, which paralleled increases in plasma free fatty acids and lipid oxidation (Khalfallah et al., 2000). Finally, in comparison to lean and obese controls, UCP2 and UCP3 mRNA expression is increased in the skeletal muscle of type-2 diabetics, a condition associated with increased plasma free fatty acids and triglycerides (Bao et al., 1998; Vidal et al., 1999).

Several *in vitro* studies have shown a role for the PPARs in free fatty acid-mediated transcription regulation of the UCPs (reviewed in Chevillotte et al. 2001). In addition, an *in vivo* study showed that in circumstances of increased fatty acid supply or treatment with a PPAR agonist, UCP3 mRNA expression was regulated by PPARα in the adult rodent heart (Young et al. 2001). The primary naturally occurring ligands for the PPARs are fatty acids (Willson et al. 2000). Since the PPARs are located in the nucleus of the cell (Dreyer et al. 1993), activation depends upon the transport of fatty acids to the nucleus. The FABPs direct intracellular trafficking of fatty acids, identifying them as candidates for the task. In fact, Helledie et al. (2000) found evidence that adipocyte lipid-binding protein (FABP4) and keratinocyte lipid-binding protein localize to the nucleus. Two other studies showed that the liver-specific FABP (FABP1) functions as a fatty acid transporter to the nucleus where the entire FABP/fatty acid complex directly interacts with the PPARs (Lawrence et al. 2000; Wolfrum et al. 2001). In addition, the proximal 5' region of FABP1 contains a PPAR regulatory element (Issemann et al. 1992), and PPARα and PPARβ have been shown to regulate FABP1 mRNA expression (Poirier et al. 2001). Thus, it follows that the PPARs regulate transcription of the UCPs through ligand-dependent activation by the FABP/fatty acid complex. This system, depicted in Figure 1, is further regulated by a feedback loop resulting from the influence of the PPARs over FABP transcription.

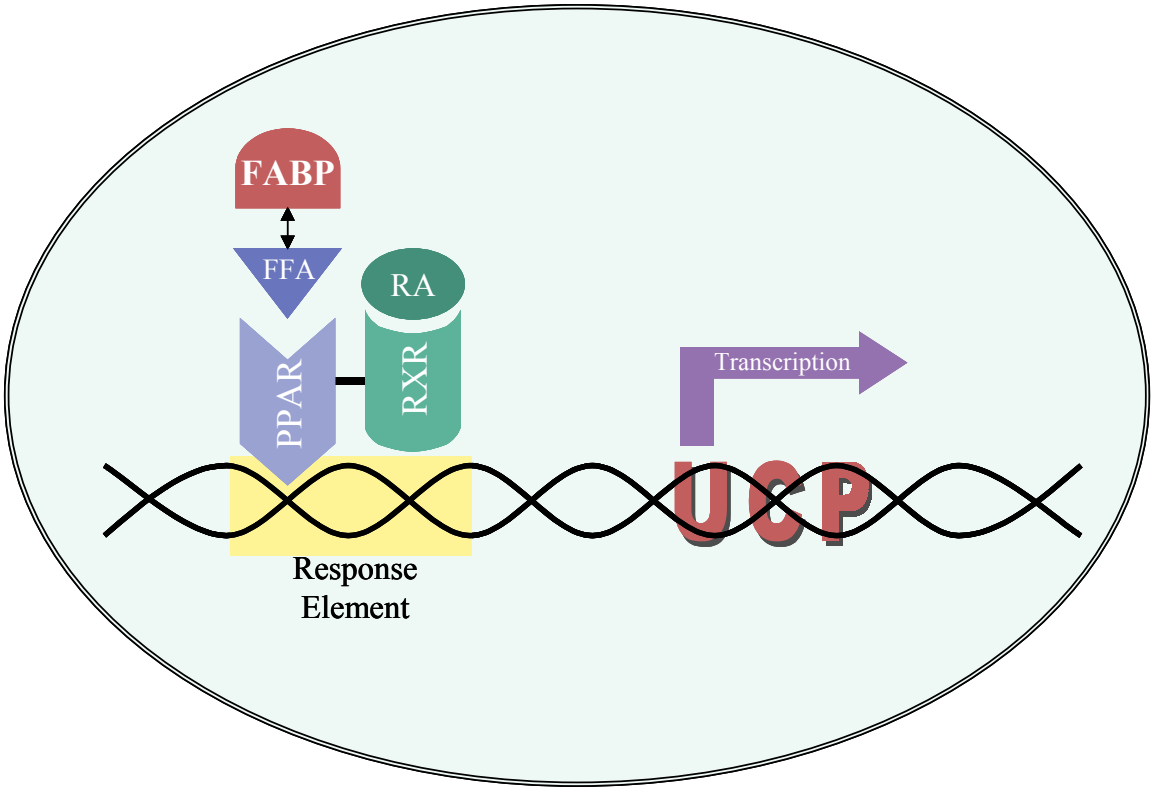

Figure 1: Fatty acid-mediated transcription regulation of the UCPs through activation of the PPAR:RXR complex by fatty acid bound FABP

The UCP gene family performs roles in thermogenesis, lipid metabolism, glucose metabolism and fuel partitioning. The FABPs facilitate and direct the action of fatty acids in relation to lipid metabolism, cell signaling, and regulation of gene expression. Factors negatively affecting the efficiency of energy metabolism and substrate utilization influence the development of obesity and its related complications (ie. type 2 diabetes, heart disease, etc.). Thus, it is important to consider variation in the UCP and FABP

gene families when analyzing the genetic components of obesity. The interactions between the UCPs, FABPs, and PPARs present a pathway of substrate utilization and gene regulation that may prove interesting in constructing genetic models of susceptibility to obesity and/or type 2 diabetes.

III. MATERIALS AND METHODS

A. SCREENING FOR VARIATION

The majority of the mutational screening for this study was accomplished through direct sequencing; however, the seven exons of UCP3 were initially screened using single-stranded conformational polymorphism (SSCP) analysis. SSCP is a method of mutational screening in which polymorphisms are detected based upon conformational differences in folding patterns of single-stranded DNA run on polyacrylamide gels. The conformational changes in the DNA folding patterns alter the electrophoretic mobility of the DNA, which is observed as disparate banding patterns on the gel (Razzaghi et al. 2001). Twelve control samples were used for the screening efforts.

Primers were chosen for the exons of UCP3 from the flanking intronic sequence (Genbank #AF032871, #AF012196, #Af012197, #AF012198, #AF012199, #AF012200, #AF012201, and #AF012202). Primers and amplification conditions for each exon are shown in Table 40 of Appendix A. For SSCP, DNA fragments should ideally be 200-250 bp. Thus, PCR products larger than 250 bp were digested with restriction enzymes prior to performing the procedure. The restriction enzymes used are listed in Table 40 of Appendix A with their corresponding exonic fragment. The DNA fragments were denatured by adding 3.75µl of denaturing solution to 7.5µl of the PCR product followed by incubation at 42^{o}C for 10 minutes. 3.75µl of formamide dye was added to each sample. The samples were loaded into pre-cast 20% polyacrylamide gels and run at 150V on Mighty Small II Gel Electrophoresis Units (Hoefer) using a programmable

temperature controller (PolyScience) to cool the gels. The gels were stained for 30 minutes with SYBR Green II (Roche) and visualized under UV illumination. Recipes for the reagents used for SSCP are shown in Appendix A. The fragments showing variation on the SSCP gels were sequenced for identification of polymorphisms. The primers, restriction enzymes, and PCR conditions used for the SSCP analysis and sequencing of the UCP3 coding region may be found in Appendix A.

Much of the screening efforts were focused on locating variation in the promoter regions of the genes of interest. Direct sequencing was used to examine approximately 2kb of the region 5' to exon 1 of UCP3 (Genbank #AF032871), approximately 1kb of the region 5' to the first exons of FABP2 (Genbank #M18079) and FABP3 (Genbank #U57623 and #U17081), and approximately 500bp of the region 5' to exon 1 of FABP4 (Genbank BAC Clone #AC18616). The primers and PCR conditions for amplification may be found in Appendix A.

Sequencing reactions were set up by combining 4µl of the PCR product, 4µl of 0.8µM primer, and 4µl of the dRhodamine dye terminator mix. The cycling conditions for the sequencing reactions were as follows: 25 cycles of 96^{o}C for 10 seconds, 50^{o}C for 5 seconds, and 60^{o}C for 4 minutes followed by a 4^{o}C hold. Resulting sequence was analyzed using the Sequencher 3.1.2 software.

B. GENOTYPING

The individuals chosen for this study are participants of the San Luis Valley Diabetes Study (SLVDS). The purpose of the SLVDS is to investigate genetic and environmental risk factors for diabetes and cardiovascular disease in Hispanic and non-Hispanic white subjects living in the San Luis Valley of Colorado (Hamman et al. 1989). For this study, 764 individuals (321 Hispanics/443 Non-Hispanic whites) from a control group of participants of the SLVDS that were non-diabetic upon recruitment were genotyped for the variants identified in the UCP genes and the FABP genes.

Genotyping was carried out by first amplifying genomic DNA for each polymorphic site using the primers and PCR conditions outlined in Appendix B. The genotypes were detected through restriction enzyme digestion, restriction enzyme digestion with an engineered cut site, direct observation of fragment size differences, direct sequencing, or fluorescence polarization (outlined below). The methods of genotype detection for each polymorphic site are outlined in Appendix B. The products of restriction enzyme digestion were separated on 2% agarose gels and visualized under UV illumination. Polymorphic sites genotyped by direct sequencing were set up according to the sequencing protocol outlined in Section III.A.

Fluorescence polarization (FP) is a method of genotype detection that employs primer extension with dideoxyribonuceoside triphosphates (ddNTP) labeled with fluorescent tags (Chen et al. 1999). For this procedure, a detection primer is designed to lie immediately upstream from the polymorphism. Each ddNTP is labeled with a different fluorescent dye. A single base extension reaction incorporates the tagged

ddNTP corresponding to the allele at the position 3' of the detection primer. FP is used to determine which ddNTP was incorporated during the single base extension reaction. This is accomplished by observing the behavior of an unincorporated verses an incoporated fluorescently labeled ddNTP. The unincorporated fluorescent molecule is very small, so it rotates and tumbles quickly emitting light in many different planes after excitation (depolarization). On the other hand, the incorporated molecule is linked to a larger molecule, so its motion is much slower and the emitted light remains polarized (Chen et al., 1999). Sample genotyping is performed by looking for the presence or absence of polarization using the LjL Analyst instrument (LjL Biosystems). Each sample is read twice to assay for each of the possible alleles at the polymorhic site.

Prior to reading the FP, three steps are followed to prepare the samples for the assay: amplification of the fragment containing the polymorphism, purification of the PCR product, and the single base extension reaction. In this study, a promoter variant in FABP4 was assayed using FP. The amplification and detection primers are shown in Table 41 of Appendix A. The procedure for assaying samples is outlined in Appendix B. The samples were read using the LjL Analyst and the genotypes were assigned using the AlleleCaller software (LjL Biosystems; procedure adapted from LjL Biosystems SNP Genotyping with an HEFP-Based Assay Application Notes).

C. DATA ANALYSIS

1. Preliminary Analyses of Genotypic Data

All statistical analyses were performed using the SPSS statistical software package version 10.1 for Windows. Allele frequencies for each polymorphic site were calculated by gene counting for the overall cohort and split by ethnicity. Fit to the expectations of Hardy-Weinberg equilibrium was tested using $\chi 2$ tests. The polymorphisms in the FABP2 promoter, with the exception of the –834bp site, were combined into one site named FABP2p-ID for the purposes of analysis since they were all in complete linkage disequilibrium. For all other sites, bivariate correlations and $\chi 2$ tests were computed between each pair of polymorphic sites to estimate linkage disequilibrium. From these analyses, it was determined that four pairs of polymorphisms were highly correlated (correlation coefficient >0.800): UCP1-2 and UCP1-5, UCP3-3a and UCP3p-55, FABP2-2 and FABP2p-834, and FABP4-2a and FABP4p-376. Therefore, the polymorphic site from each pair most likely to be functional was chosen for regression modeling (eg. a promoter variant was chosen over an intronic variant). The sites chosen for further study were as follows: UCP1-2, UCP3p-55, FABP2p-834, and FABP4p-376. Later in the analysis, linkage disequilibrium, D', between each pair of loci residing on the same chromosome was estimated (Devlin et al. 1995).

A portion of the data analysis was performed using the data split by sex and ethnicity. Splitting the data set resulted in four subgroups: non-Hispanic females (n=223), non-Hispanic males (n=211), Hispanic females (n=172), and Hispanic males

(n=142). When the data set was split four ways, the frequencies of the rare homozygote groups from polymorphisms with lower allele frequencies were reduced considerably. Thus, it was necessary to combine the rare homozygotes with the heterozygotes in those analyses. If rare homozygote groups of ten or fewer were observed in any of the four sex/ethnicity subgroups, they were combined with the heterozygotes. The polymorphisms requiring such combination were: UCP1-2, UCP1-5, UCP3-3a, FABP2-2, FABP4-2a, FABP4-2b, UCP3p-55, FABP3p-313, and FABP4p-376. The UCP3 exon 3b site was removed from further analysis due to extremely low frequency of the rare allele.

2. Description of Variables

Outcome variables for the study were chosen based on biological models. The original outcome variables were fat mass, as determined by DEXA, fasting free fatty acid levels, serum triglyceride levels, and insulin resistance. The effect of genetic variation on adiposity is interesting due to the involvement of the UCPs and FABPs in energy metabolism and was assayed using fat mass, measured by dual energy x-ray absorptiometry (DEXA) in grams. Due to the involvement of the UCPs and FABPs in glucose and lipid metabolism, variation in these genes may modify plasma levels of free fatty acids (μmol/L) and triglycerides (mg/dl). Insulin resistance is an interesting variable for study due to the role of the insulin/glucose pathway in energy metabolism and the increase in lipid metabolism related to impaired glucose metabolism. Insulin resistance was represented by HOMA IR, a value derived from fasting glucose and insulin levels (Matthews et al. 1985):

$$\text{HOMA IR} = \frac{(\text{Fasting Insulin} * \text{Fasting Glucose})}{22.5}$$

In addition to genotype data, the following variables were used as possible predictor values in the analysis: total cholesterol, systolic blood pressure, diastolic blood pressure, lean mass, percent body fat, total caloric intake, dietary fat intake, physical activity, sex, age, smoking status, sex, ethnicity, and skin reflectance. Total cholesterol was measured from plasma in mg/dl after a 12 hour fast. Systolic and diastolic blood pressure values were obtained from an average of two blood pressure readings (units: mm Hg). Lean mass was calculated as total body mass minus fat mass from DEXA in grams. Total caloric intake and dietary fat intake were measured in calories and grams, respectively, and obtained from 24-hour recall. Physical activity was measured as total physical activity over one week in mets (kcals/kg/hr). Smoking status was categorized as: non-smoker or ever smoked. Ethnicity was derived from Hispanic origin and categorized as Hispanic or non-Hispanic white. Skin reflectance was used as an estimate of the degree of admixture between Native American and European populations. Skin reflectance was measured by light reflectance using a portable spectrophotometer (Gardner et al. 1984).

3. Descriptive Statistics

Frequencies were calculated for the categorical variables (genotypes, sex, smoking status, and ethnicity) and graphed in histograms. Various measures were computed for the continuous variables including the mean, standard deviation,

skewness, kurtosis, and range. Histograms were graphed to show the frequency distributions of the continuous variables. Any outcome variable with a skewness and kurtosis greater than one was transformed using the natural log. Extreme outliers for any outcome or predictor variable were identified using the descriptive statistics and histograms and removed from the data set. The individuals were classified as extreme outliers based on biologically implausible measurements, which may have been a result of data entry or measurement error. The group of outliers consisted of the following ID numbers: 252, 749, 3077, 3137, 3169, 3194, 3243, 3348, 3467, 3592, 3645, 3757, 3759, 3776, and 3953. The removal of those individuals did not have a significant impact on the descriptive statistics of the other variables.

4. Preliminary Analysis of Outcome and Predictor Variables

Univariate analyses were performed to test for associations between predictor and individual outcome variables. Continuous variables were tested against the outcome variables using linear regression. Categorical variables were tested against the outcome variables using analysis of variance (ANOVA). For the analysis of the genotype variables versus outcome and predictor variables, the data set was split by sex and ethnicity.

The univariate analyses were followed by calculation of correlations between each pair of predictor variables. For the continuous variables, bivariate correlations were displayed in a correlation table. ANOVA was used to look for association between continuous and categorical variables. Correlations between categorical variables were calculated by chi-square analysis.

5. Reselection of Outcome Variables

During computation of predictor correlations, significant potential genetic contribution to the covariates may be revealed by correlations between genotype variables and covariates. This suggests a relationship between genotype and predictor that may be better explored by reclassifying the predictor variable as an outcome variable. In this case, the predictor variable total cholesterol appeared several times within each of the population subgroups to be significantly associated with various polymorphic sites. Thus, cholesterol was added to the data analysis as an outcome variable. The final list of outcome variables was as follows: fat mass, fasting free fatty acids, triglycerides, cholesterol, and HOMA IR.

6. Regression Modeling

For the purpose of regression analyses, the genotype groups were recoded into dummy variables. Variants with three genotype groups were recoded into two variables as shown here with “A” representing the common allele and “a” representing the rare allele:

	AA	**Aa**	**aa**
Variable 1	1	0	0
Variable 2	0	1	0

Variants with two genotype groups were recoded into one dummy variable with the common homozygotes represented by “1” and all others represented by “0”. This

coding scheme allowed for the consideration of each genotype group separately in the context of the regression analyses.

Three different approaches were taken in exploring the genetic contribution to variation in the outcome variables. In the first approach, referred to as the "sex/ethnicity-split" analysis the data set was split by sex and ethnicity. Each outcome variable was analyzed separately for each of the sex/ethnicity subgroups. There were no adjustments made on the outcome variables for this analysis approach.

The second approach to the analysis, referred to as the "sex-split" analysis, was to split the data set by sex and account for ethnic differences by adjusting for skin reflectance. Skin reflectance was used as a measure of ethnicity to adjust for the degree of admixture between Native American and European populations. Since the number of Hispanic males was relatively low (n=143), genotype groups resulting from interactions have the potential to be small and uninformative. In order to maximize the power to detect interesting relationships, this approach to regression model construction was taken. For these analyses, the outcome variables were adjusted for age, smoking status, physical activity, and skin reflectance. Adjustments on each outcome variable were made by entering all four covariates in a linear regression model and saving the unstandardized residuals. Each covariate was added to the model regardless of the size of effect on outcome in order to ensure correction for the entire environmental influence. Adjusted values were computed for each outcome by adding the overall outcome mean to the residual values.

The general method to regression model construction was similar for the first two analysis approaches. Analysis of variance was used to test single locus effects on each

outcome. Single loci with the largest effects ($p \leq 0.05$) were chosen for further study. Those single loci were paired with all other single loci for two-way ANOVA analyses. From the two-way ANOVA, pairs of loci with strong interaction effects ($p \leq 0.1$) were chosen for inclusion in regression models of the corresponding adjusted outcome variables. Linear regression models were constructed for each of the outcome variables to explore possible interactions among loci. Initial models were constructed using the interesting single loci and two-way interactions with corresponding main effects identified in the ANOVA. To obtain the most parsimonious models, backward and stepwise selection methods were used with exclusion and inclusion criteria set such that the "final" models included only terms with a p-value less than 0.05. In the case that the final models for the backward and stepwise methods did not agree, the model with the higher adjusted R^2 was chosen.

The third analysis approach, referred to as the "tissue-specific" analysis was designed to explore the effects of genetic variation on outcome by considering groups of genes expressed in specific tissues separately. The tissues considered in this analysis plan were skeletal muscle, adipose tissue, and the small intestine. For these analyses, variation in the PPARs was included to consider interactions among the three gene families within the tissues where they are expressed. Polymorphisms in the PPAR genes were identified and genotyped by Susan Moffett (Moffett, 2002). The outcome variables considered in these analyses included fat mass, lean mass, cholesterol, triglycerides, free fatty acids, and HOMA IR. Each outcome variable was adjusted for

age, smoking status, physical activity, and skin reflectance, as described above. The cohort was split by sex, but not by ethnicity.

Initially, linear regression models were constructed separately for each tissue type by entering the single loci and all two-way interactions from genes specific to each tissue type. The skeletal muscle models included polymorphisms in the UCP3, FABP3, and PPARα genes. Polymorphisms in UCP1, UCP2, FABP4, and PPARγ were included in the adipose tissue models. The intestine models included variation in UCP2, FABP2, and PPARβ. Backward and stepwise selection methods were used with exclusion and inclusion criteria set such that the final models included only terms with a p-value less than 0.05. In the case that the final models for the backward and stepwise methods did not agree, the model with the higher adjusted R^2 was chosen. In a second round of linear regression modeling, the final models for each tissue type were entered into one regression model. Backward and stepwise selection methods were then used, in the same manner as above, to obtain the most parsimonious models. Theoretically, this second step identified the combined contribution of variation in genes of each tissue type to the outcome variables. The resulting regression models were referred to as the combined models.

D. PROMOTER ACTIVITY ASSAYS

Gene expression studies were carried out on the series of insertion/deletion polymorphisms in the 5' region of FABP2 and the insertion/deletion polymorphism in the 5’ region of FABP3 to look for functional consequences of the variation. These polymorphisms appeared interesting due to their location, approximately 150bp and 493bp upstream from exon 1, respectively, and the potential effects of such extensive sequence alterations on promoter function.

The Dual-Luciferase Reporter Assay System (Promega) was used to determine the effect of the insertion/deletion polymorphisms in the 5’ regions of FABP2 and FABP3 on promoter activity. This system combines an experimental reporter with an internal control reporter. This cotransfected control provides a baseline response to adjust for variability in transfection efficiency or cell viability within the experiment. In this reporter system, the experimental reporter contains the gene for firefly luciferase and the control reporter contains the gene for the *Renilla* (sea pansy) luciferase. The activities of firefly and *Renilla* luciferases are measured sequentially from a single sample by adding the proper substrates to initiate a luminescent signal. The firefly luciferase reporter is measured first by adding Luciferase Assay Reagent II (LAR II). After quantifying the firefly luminescence, the addition of the Stop & Glo Reagent quenches the firefly luciferase signal and initiates the *Renilla* luciferase reaction (Promega Technical Manual #040).

The experiment was carried out by first amplifying the promoter sequences of both homozygous inserted and homozygous deleted individuals, using a high-fidelity

DNA polymerase. The primers were designed to incorporate restriction enzyme sites compatible with those of the reporter vector. The PCR products were gel purified and digested with the appropriate restriction enzymes. The resulting fragments were ligated into the luciferase reporter vector. Competent *E. coli* cells were transformed with the plasmids. The recombinant plasmid DNA were purified by miniprep and confirmed with sequencing. Finally, host cells were transfected with the plasmid DNA, and promoter function was determined by measuring activity of the firefly luciferase corrected by the *Renilla* luciferase measurements (Promega Technical Manual #040).

1. Preparation of Insert for Ligation

The promoter sequences of both homozygous inserted and homozygous deleted individuals were amplified using *Pfu* (Stratagene), a high-fidelity DNA polymerase. The primers were designed to incorporate restriction enzyme sites compatible with those of the reporter vector by adding tags to the 5' end. Restriction enzyme sites that form sticky ends upon digestion were incorporated in the tags. In this case, an *Mlu*I site was incorporated at the 5' ends of the fragments and an *Xho*I site was incorporated at the 3' ends of the fragments to ensure insertion of the fragment into the vector in the correct orientation. The following primers were used:

FABP2-*MluI*-F: $^{5'}$-GGCCA$^{\downarrow}$CGCGT-CTAGAGCTTCTTTCCTGACCCT-$^{3'}$
FABP2-*XhoI*-R: $^{5'}$-GGGCC$^{\downarrow}$TCGAG-GATTTCAGTTGAGTCAGCCTCT-$^{3'}$

FABP3-*MluI*-F: $^{5'}$-GGCCA$^{\downarrow}$CGCGT-AGCCCTCAGCATGCAATAAATAG-$^{3'}$
FABP3-*XhoI*-R:$^{5'}$-GGGCC$^{\downarrow}$TCGAG-GAAATTCTTGCTGTCCACTAGCTT-$^{3'}$

Four inserts were constructed for the experiment: FABP2-62, FABP2-3733, FABP3-62, and FABP3-3061. The PCR cycling conditions are outlined in Appendix B with annealing temperatures of 62^{o}C for the FABP2 insert and 56^{o}C for the FABP3 insert. Each PCR reaction contained: 5.0µl of 10X *Pfu* buffer, 8.0µl of 1.25mM dNTP mix, 0.5µl of 20µM forward primer, 0.5µl of 20µM reverse primer, 34.0µl dH_2O, 1.0µl *Pfu*, and 1.0µl of DNA. The PCR products were gel purified using the "QIAEX II Agarose Gel Extraction Protocol" (Quiagen). The resulting pellets were resuspended in distilled water to a concentration of ~100µg/ml.

The purified PCR products were digested with ~4 units each of the appropriate enzymes. Each reaction mix contained: 0.2µl *Xho*I, 0.4µl *Mlu*I, 0.2µl 100X BSA, 2.0µl 10X NEB3 (New England Biolabs), 7.2µl dH_2O, and 10.0µl of the purified sample for a final reaction volume of 20.0µl. The digests were allowed to incubate at 37^{o}C overnight. Following digestion, the samples were incubated at 65^{o}C for 15 minutes to inactivate the restriction enzymes.

2. Preparation of Vector for Ligation

The luciferase reporter vector, pGL3-Basic (Promega) was chosen as the cloning vehicle. The pGL3-Basic Vector, shown in Figure 2, contains the luciferase gene, but lacks eukaryotic promoter and enhancer sequences. This vector also contains the β-lactamase gene, which confers ampicillin resistance in *E.coli* cells (Promega Technical Manual #TM033).

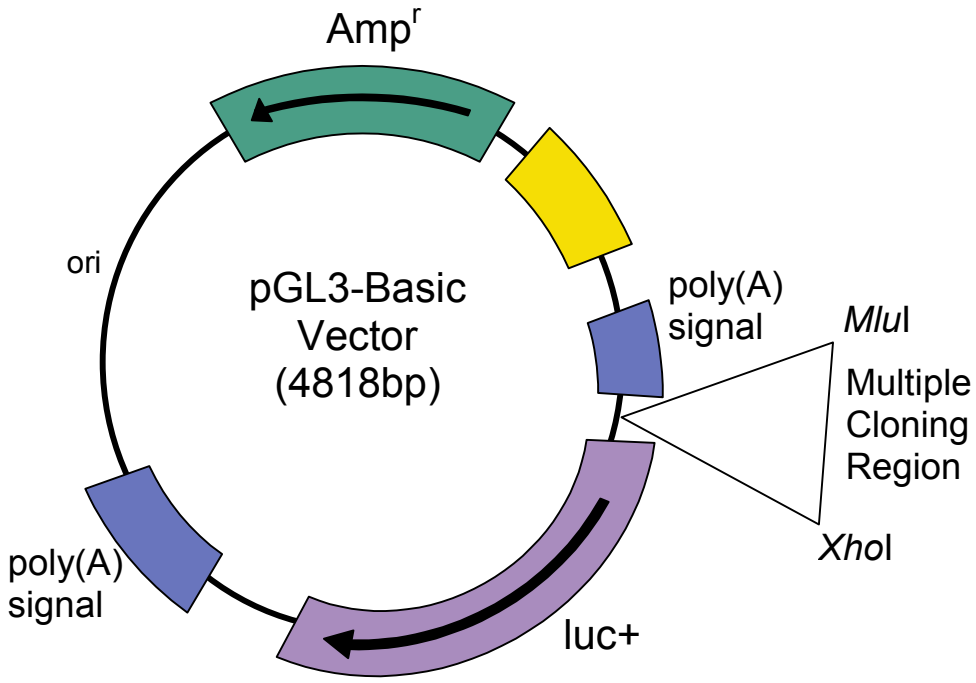

Figure 2: Arrangement of the Luciferase Reporter Vector, pGL3-Basic

To prepare the vector for ligation of the inserts, 4µg of plasmid DNA was digested with 2X-3X excess restriction enzyme in a 40µl reaction. The reaction mix contained: 0.5µl *Xho*I, 1.0µl *Mlu*I, 0.4µl 100X BSA, 4.0µl 10X NEB3 (New England Biolabs), 30.1µl dH_2O, and 4.0µl of the pGL3-Basic vector. An overnight digestion at 37^oC was followed by a 15-minute incubation at 65^oC to inactivate the restriction enzyme.

The digested plasmid was dephosphorylated with shrimp alkaline phosphatase (SAP) in order to inhibit recircularizaton of the plasmid DNA. To the 40µl sample, 10µl of 10X SAP buffer, 2µl of SAP (Roche), and 48µl of dH_2O were added for a final

reaction volume of 100µl. The reaction was incubated at 37°C for 2 hours. Following dephosphorylation, the sample was incubated at 65°C for 15 minutes to inactivate the SAP. The plasmid was purified with phenol:chloroform and extracted with ethanol precipitation, using the protocol outlined in Appendix H.

3. Ligation

Each of the four experimental promoter fragments was ligated into the pGL3-Basic luciferase reporter vector separately. The ligation reaction mixtures included: 2µl digested vector, 2µl insert, 2µl 10X ligation buffer, 1µl T4 DNA ligase (Gibco BRL), and 13µl dH_2O for a final reaction volume of 20µl. A control reaction was set up with vector only. The reactions were incubated overnight at 16°C. Proper ligation was confirmed by restriction enzyme digestion of the resulting products using *Xho*I and *Mlu*I.

4. Transformation of Competent *E. coli* Cells

The four experimental constructs, consisting of the pGL3-Basic vector and each experimental insert, were transformed into JM109 competent *E. coli* cells (Promega) using a heat shock protocol. 10µl of the ligation mixture was added to 50µl of JM109 competent cells. The mixture was incubated on ice for 45 minutes. The cells were heat shocked by incubation at 42°C for 2 minutes and placed back on ice. 200µl of LB broth (see Appendix H for recipe) was added, and the cells were incubated at 37°C for 1 hour. Finally, 100µl of the transformed cells were plated on LB agar plates containing

ampicillin (LB Amp; see Appendix H for recipe) with a cell spreader and incubated at 37^{o}C overnight.

Transformed colonies were identified by PCR using various primer sets within and spanning the inserts. Isolated colonies were picked from the agar plates and the cells were digested with Proteinase K (ProK; Gibco BRL). For one 96-well tray, 2ml of TE was mixed with 5µl ProK. 15µl of the ProK mixture was aliquoted into each well. Colonies were picked with sterile toothpicks. Each colony was placed in the ProK solution in the 96-well tray. Then, LB Amp plates with grids drawn on the back were stabbed with the same toothpick, and the coordinates of the colony on the agar plate and in the 96-well tray were recorded. The LB Amp plates were incubated at 37^{o}C overnight. The 96-well trays were incubated at 55^{o}C for 15 minutes followed by incubation at 80^{o}C for 15 minutes to inactivate the enzyme.

To identify transformed colonies, PCR reactions were set up using the product from the ProK digest including the following: 14.7µl dH_2O, 2.5µl 10X Buffer, 1.3µl DMSO, 0.8µl MgCl2, 4µl dNTP, 0.25µl primer F, 0.25µl primer R, 0.2µl *Taq* polymerase, and 1µl of the ProK digest for a final volume of 25µl. The transformation status of each colony was determined based on fragment size of the PCR products. Transformation was confirmed by direct sequencing of the PCR products. The transformed colonies were replated on LB Amp plates, streaking for isolation.

5. Purification of Recombinant Plasmid DNA

The Wizard Plus Minipreps DNA Purification System (Promega) was used to purify the recombinant plasmid DNA from the JM109 cells. To obtain material for

purification, 5ml aliquots of LB broth were inoculated with colonies and incubated at 37^{o}C overnight. This overnight culture was centrifuged at 10,000×g for 10 minutes, and the supernatant was discarded. The pellets were used to perform the Wizard Plus Minipreps DNA Purification procedure using a vacuum manifold. The resulting purified plasmid DNA was sequenced to confirm the presence of the desired inserts.

6. Cell Culture

Three cell lines were used for the transfection assays: two types of human colonic adenocarcinoma cell lines, HT-29 and Caco-2, and a human fibroblast cell line, HT-1080. Each cell line was obtained from the American Type Culture Collection. HT-29 cells were grown in McCoy's medium with 10% fetal bovine serum, 1.5mM L-glutamine, and 1% penicillin/streptomycin (Gibco BRL). Caco-2 cells were grown in minimum essential media supplemented with 20% fetal bovine serum, 1% penicillin/streptomycin, 2mM L-glutamine, 1.5 g/L sodium bicarbonate, 0.1 mM non-essential amino acids, and 1.0 mM sodium pyruvate. HT-1080 cells were maintained in minimum essential media supplemented with 10% fetal bovine serum, 2mM L-glutamine, 1% penicillin/streptomycin, and 0.1mM non-essential amino acids (Gibco BRL). The cells were grown in T-25 cm^2 plastic flasks at 37^{o}C in a 5% CO_2 environment. Cells were plated in 6-well plates for the transfection assays.

a) Thawing of Cryopreserved Cells

A cryotube of each cell type was removed from storage and thawed quickly in a 37^{o}C water bath. The cells were added to 5 ml of their respective growth media in T-25 cm^{2} plastic flasks. The cells were cultured for 12 to 24 hours before the growth media was replaced with fresh media to remove the cryopreservative from the cultures.

b) Passaging Cells

The cell lines were grown in T-25 cm^{2} plastic flasks to ~80-90% confluency before passaging. To split the cells, the media was removed and discarded from the culture. 2ml of wash solution (Phosphate Buffered Saline; PBS) was added to the side of the flask opposite the cells. The cell sheet was rinsed by carefully rocking the flask, and the wash solution was discarded. 2ml of Trypsin/EDTA (Gibco BRL) was added to the flask, and the cells were incubated at 37^{o}C. The culture flasks were checked for dissociation of the cell sheet at one-minute intervals. The flasks were tapped to expedite removal of cells difficult to remove. Growth media was added to bring the final volume of each new flask up to 5ml. For example, a culture flask split 1:4 required the addition of 18ml of growth media. The media was pipetted repeatedly over the surface of the flask containing the cells, and 5ml of the cell suspension was quickly aliquotted into each new flask.

c) Cryopreservation of Cells

As cell lines became established, it was necessary to freeze down aliquots of cells for storage. To freeze cells down, flasks of cells were trypsinized and placed in a glycerol/growth media mixture in cryotubes.

The growth media was removed from the culture flasks and discarded. 2ml of wash solution (PBS) was added to the side of the flask opposite the cells. The cell sheet was rinsed by rocking the flask carefully, and the wash solution was discarded. 2ml of trypsin/EDTA was added, and the cells were incubated at 37^{o}C. The culture flasks were checked for dissociation of the cell sheet at one-minute intervals. The flasks were tapped to expedite removal of cells difficult to remove. 2ml of media was added to inactivate the trypsin/EDTA, and the media was pipetted repeatedly over the surface of the flask containing the cells. The cell suspension was transferred into a 15ml conical tube and centrifuged for 5 minutes at 1200 rpm. The supernatant was removed and 1ml of growth media containing 10% DMSO was added to the cell pellet. The mixture was transferred to a cryotube and placed in the –20^{o}C freezer to begin a slow freeze-down. Finally, the cryotube was transferred to liquid nitrogen for storage.

7. Host Cell Transfection

The transfection experiments were set up using each of the four recombinant plasmids containing the experimental promoter fragments and the Renilla vector, pRL-TK. The pRL-TK Vector, shown in Figure 3, contains the herpes simplex virus thymidine kinase (HSV-TK) promoter region upstream of the Renilla luciferase gene.

The HSV-TK promoter provides low to moderate levels of expression in cotransfected mammalian cells (Promega Technical Manual #TB240). Two control vectors were also used: the pGL3-Basic Vector without a promoter insert (Figure 2) and the pGL3-Control Vector. The pGL3-Control Vector, shown in Figure 4, contains the SV-40 promoter and enhancer sequences upstream of the firefly luciferase gene. This vector provides strong expression of the luciferase gene, serving as an internal standard for expression studies of recombinant constructs (Promega Technical Manual #TM033). LipofectAMINE Plus (Gibco BRL), a liposomal transfection vehicle was used to deliver the plasmid DNA into the cells.

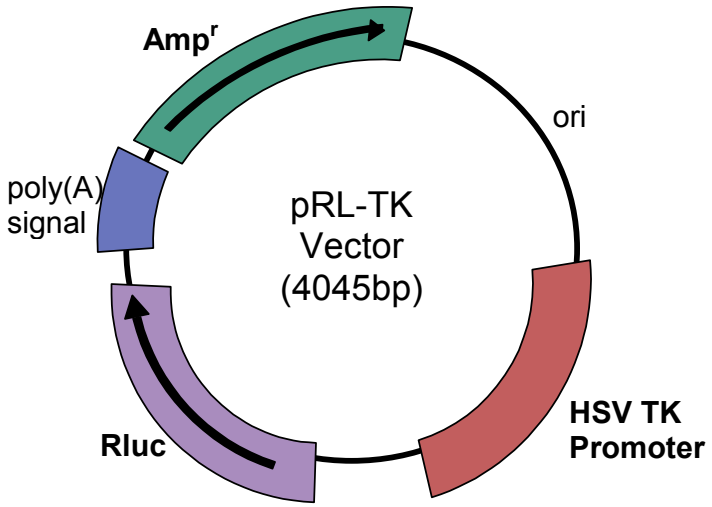

Figure 3: Arrangement of pRL-TK, the Co-transfected Internal Control Plasmid

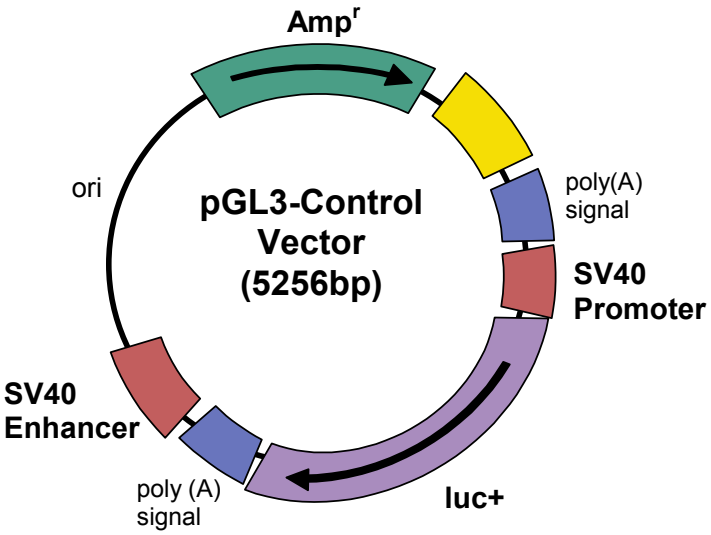

Figure 4: Arrangement of the pGL3-Control Plasmid

One control experiment was performed prior to transfection of the experimental plasmids to determine the transfection efficiency of each cell line. In this experiment, cells of both types were transfected with each of the following: pGL3-Control only, pRL-TK only, and both pGL3-Control and pRL-TK. The conditions of the control experiment are shown in Table 71 of Appendix H and the protocol is outlined below. Duplicate samples were done to show reproducibility.

In the actual experiments, the HT-29 intestinal cell line was transfected with the FABP2 experimental plasmids and the HT-1080 fibroblast cell line was transfected with the FABP3 experimental constructs. The Caco-2 cell line replaced the HT-29 cell line due to low transfection efficiency. The experimental conditions are shown in Table 72 of Appendix H and the protocol is outlined below. For each experiment, the

experimental samples were transfected in duplicate or triplicate. The transfection experiments were also independently repeated to show reproducability.

The day before transfection, the cells were trypsinized and plated in 6-well culture plates so that they were 60-80% confluent the day of transfection. 3µl of LipofectAMINE per µg of plasmid DNA was diluted in 50µl serum-free media, mixed, and incubated at room temperature. In a separate tube, the plasmid DNA was pre-complexed with the PLUS Reagent by first diluting the plasmid DNA in 50µl serum-free media. Then, 3µl of PLUS Reagent per µg of plasmid DNA was added and mixed. The DNA was allowed to complex with the PLUS Reagent for 15 minutes at room temperature. The pre-complexed DNA mix was added to the diluted LipofectAMINE, mixed, and incubated at room temperature for 15 minutes. During the incubation, the cells were prepared for transfection by rinsing with 1ml of PBS per well. Then, enough serum-free media was added to the cells to bring the final transfection volume to 1ml. The DNA-PLUS-LipofectAMINE Reagent complexes were added to each well containing the fresh media. The cells were incubated at 37^{o}C for 3 hours. Finally, 1ml of culture media containing 2X of serum was added and the cells were incubated at 37^{o}C for 24-48 hours before performing assays (Procedure adapted from LipofectAMINE PLUS Reagent protocol: Life Technologies Form No. 18057N).

8. Luciferase Assays

The luciferase assays were performed using the Dual-Luciferase Reporter Assay System. A schematic of the procedure is shown in Figure 5. To prepare for the

luciferase assays, the cells were lysed using the passive lysis buffer (PLB) provided in the kit. To prepare for lysis, the growth medium was removed from the cultured cells, and 1ml of PBS was added to wash the cells. The rinse solution was removed, and 1 ml of PLB was added to each well. The culture plates were placed on an orbital shaker and rocked at room temperature for 15 minutes. The lysate was transferred to 1.5ml microcentrifuge tubes and placed in the –20^{o}C freezer until the luciferase assays were performed.

The luciferase assays were performed using the Turner Designs Model TD-20/20 Luminometer. The luminometer was programmed to perform a 2-second premeasurement delay, followed by a 10-second measurement period for each reporter assay. To perform the assay, 20µl of cell lysate was transferred into luminometer tubes. 100µl of the Luciferase Assay Reagent II (LAR II) reagent was added and mixed by pipetting 2 or 3 times. The tube was placed in the luminometer and reading of the firefly luciferase activity was initiated. 100µl of Stop & Glo Reagent was dispensed immediately into the sample and mixed by vortexing. The tube was replaced in the luminometer and reading of the *Renilla* luciferase activity was initiated. Samples were done in duplicate, and the average of the two readings was used. Differences between the two recombinant plasmids were determined by comparing their relative firefly luciferase activities corrected by the *Renilla* luciferase activity (Procedure adapted from Promega Technical Manual No. 040).

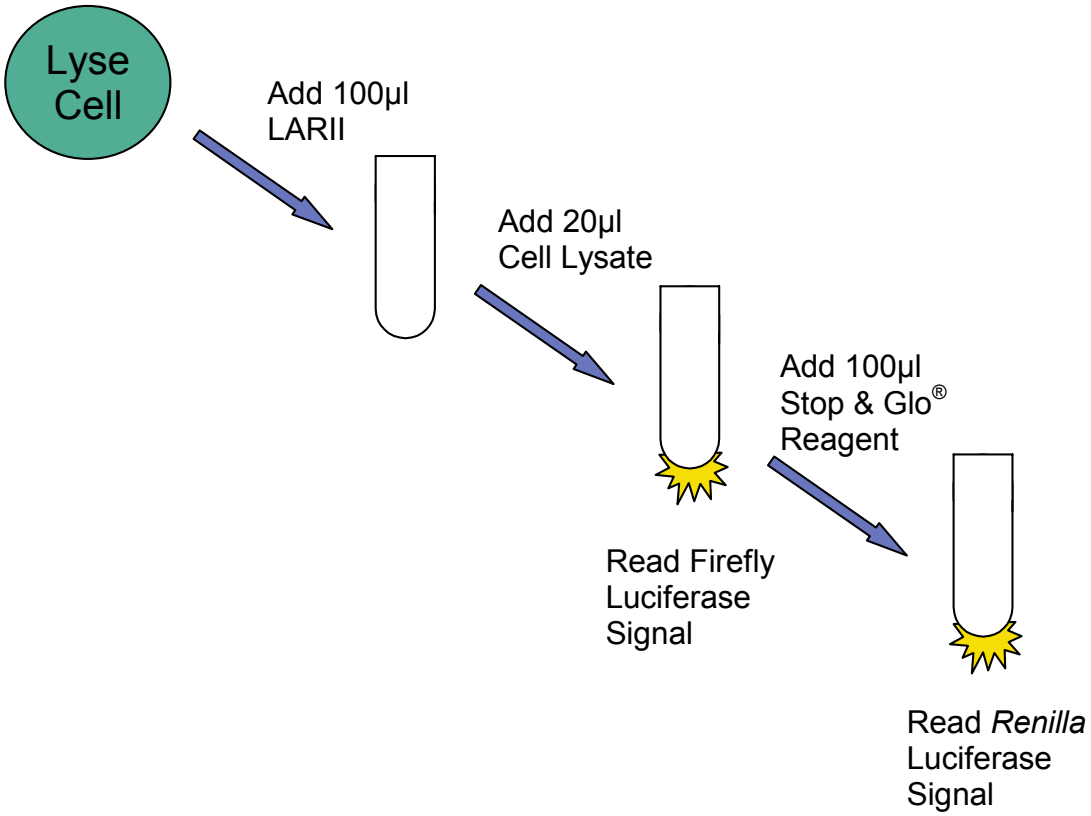

Figure 5: Dual Luciferase Reporter Assay System

IV. RESULTS

A. SCREENING FOR VARIATION

In this study, mutation screening focused on the coding region of UCP3 and the region 5' of the initiation codons of UCP3, FABP2, FABP3, and FABP4. These screening efforts revealed three polymorphisms in the coding region of UCP3 and fourteen variants in the promoter regions of UCP3, FABP2, FABP3, and FABP4. Additional information on variation in the UCP and FABP gene families was obtained from prior screening efforts described in the literature. Overall, eight variants from the coding regions, two variants from intronic sequence, and ten variants from promoter sequence have been chosen for examination in this study.

1. Uncoupling protein-1

The polymorphic sites in UCP1 were chosen from the literature. Urhammer et al. (1997a) reported two variants of interest located in exons 2 (UCP1-2) and 5 (UCP1-5) of UCP1. The variant in exon 2 consists of a G to A substitution in codon 64 (nucleotide 3035, Genbank #X51952), which results in an alanine to threonine amino acid change. The exon 5 variant is located in codon 229 (nucleotide 69, Genbank #X51954), where an A to T substitution results in a methionine to leucine amino acid change. UCP1-2 and UCP1-5 genotypes were assigned following digestion of engineered restriction enzyme sites using *Hha*I and *Hind*III, respectively.

2. Uncoupling Protein-2

Two polymorphic sites in UCP2 were chosen from the literature for genotyping. Urhammer et al. (1997b) reported a C to T substitution in exon 4 of UCP2 (UCP2-4), which results in an alanine to valine amino acid change in codon 55 (nucleotide 164, Genbank #U76367). UCP2-4 genotypes were assigned following digestion of an engineered restriction enzyme site using *Eae*I. A 45-base pair insertion/deletion polymorphism in the 3' untranslated region of exon 8 (UCP2-8) was reported by Otabe et al. (1998). UCP2-8 genotypes were assigned based on fragment size differences when separated on a 2% agarose gel.

3. Uncoupling Protein-3

Single-stranded conformational polymorphism analysis (SSCP) and direct sequencing were used to screen the seven exons of UCP3, resulting in localization of three polymorphic sites within the coding region. Two of these sites are located in exon 3. The first, shown in Figure 6, is a T to C substitution in codon 99 (UCP3-3a; nucleotide 271, Genbank #AF012198), which conserves the amino acid tyrosine. The second polymorphism in exon 3 is shown in Figure 7 and consists of a G to A substitution in codon 102 (UCP3-3b; nucleotide 278, Genbank #AF012198), causing a valine to isoleucine amino acid change. The third polymorphic site in UCP3 resides in exon 5, where a T to C substitution in codon 210 (UCP3-5; nucleotide 189, Genbank

#AF012200) conserves the amino acid tyrosine. The SSCP gel picture showing variation in exon 5 is shown in Figure 8, and the chromatograms identifying the UCP3-5 variant are shown in Figure 9. All three UCP3 polymorphisms have been described in the literature: codon 99 (Urhammer et al. 1998), codon 102 (Argyropoulos et al. 1998), and codon 210 (Otabe et al. 1999). UCP3-3a and UCP3-5 genotypes were assigned following restriction enzyme digestion of engineered sites using *Drd*I and *Rsa*I, respectively. UCP3-3b genotypes were assigned following restriction enzyme digestion using *Asp*I.

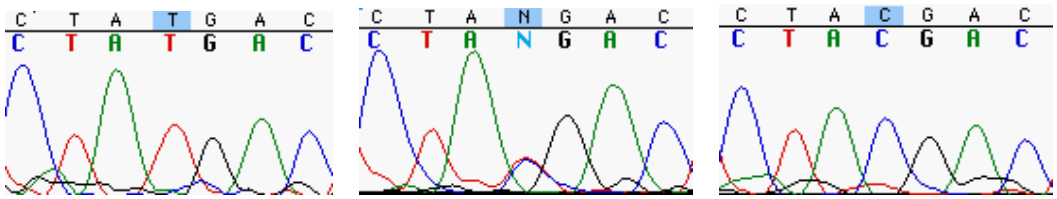

Figure 6: Chromatograms showing a T to C substitution in exon 3 of UCP3 (UCP3-3a)

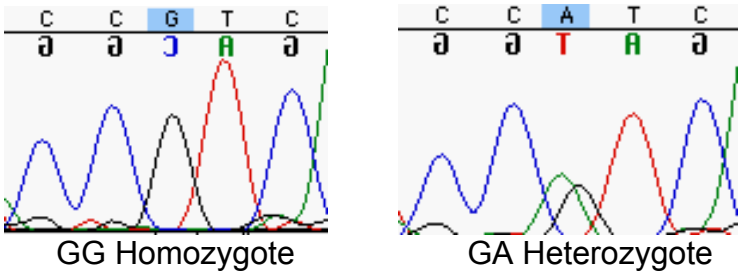

Figure 7: Chromatograms showing a G to A substitution in exon 3 of UCP3 (UCP3-3b)

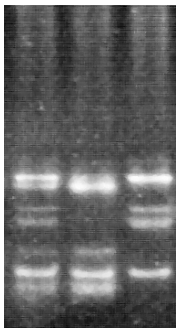

CT CC TT

Figure 8: SSCP gel picture showing variation in UCP3 exon 5

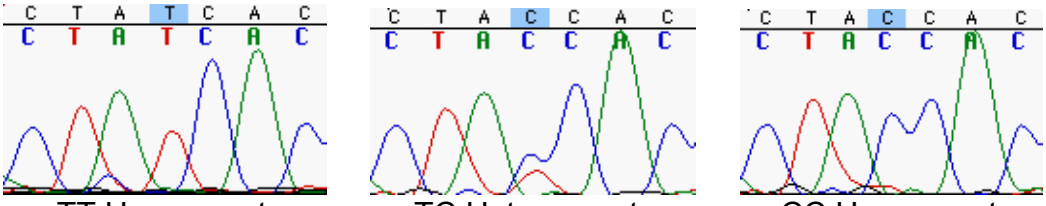

TT Homozygote TC Heterozygote CC Homozygote

Figure 9: Chromatograms showing a T to C substitution in exon 5 of UCP3 (UCP3-5)

Approximately 2kb of the region 5' to exon 1 of UCP3 were screened for variation by direct sequencing (Genbank #AF032871). Two polymorphic sites were localized upstream from exon 1: a C to T substitution at -55 bp (UCP3p-55), shown in Figure 10, and a C to T substitution at -1095 bp. The -55 variant is confirmed in the literature by

Schrauwen et al. (1999a). UCP3p-55 genotypes were assigned following digestion of an engineered restriction enzyme site using AvaI.

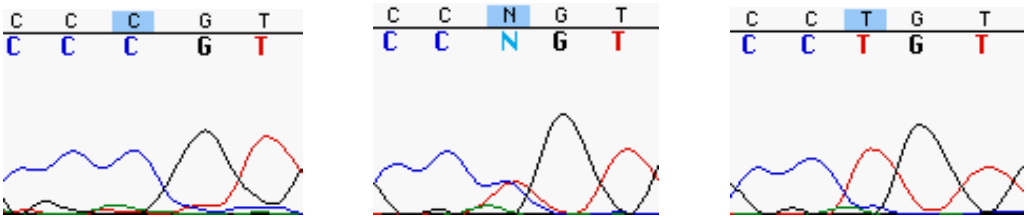

Figure 10: Chromatograms showing a C to T substitution 55 bp upstream of the UCP3 initiation codon (UCP3p-55)

4. Fatty Acid Binding Protein-2

One polymorphic site in FABP2 was chosen from the literature for genotyping. Baier et al. (1995) reported a G to A substitution in codon 54 (nucleotide 163, Genbank #NM_000134) of exon 2 (FABP2-2), which results in an alanine to threonine amino acid change. FABP2-2 genotypes were assigned following restriction enzyme digestion using *Hha*I.

Approximately 1kb of the region 5' of the initiation codon of FABP2 was screened for variation by direct sequencing (Genbank #M18079). Five point mutations were located in this region: a T to C substitution at -883 bp, a C to T substitution at -834 bp (Figure 11), a G to T substitution at -778 bp (Figure 12), a T to C substitution at -701 bp, and a G to A substitution at -260 bp (Figure 13). Three insertion/deletion

polymorphisms were also localized upstream of exon 1: the insertion/deletion of a T at -169 bp (Figure 14), the insertion/deletion of a GAA at -166 bp (Figure 14), and the insertion/deletion of an AGTAG at -136 bp (Figure 15). Genotypes at the –834 variant (FABP2p-834) were assigned following digestion of an engineered restriction enzyme site using *Ban*II. Direct sequencing of 50 individuals from the SLVDS confirmed that the insertion/deletion polymorphisms were in complete linkage disequilibrium with one another as well as with the -260 bp and -778 bp point mutations. Therefore, genotypes at these point mutations were inferred from the genotypes of the insertion/deletion variants, which were assigned based on fragment size differences when separated on a 3% agarose gel. These polymorphims were combined into one variant named "FABP2p-ID" for the purposes of data analysis.

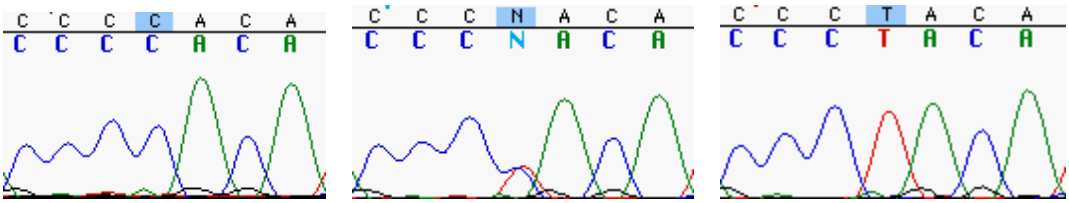

Figure 11: Chromatograms showing a C to T substitution 834 bp upstream of the FABP2 initiation codon (FABP2p-834)

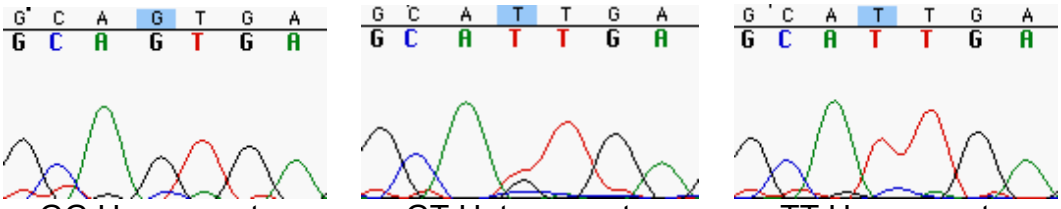

Figure 12: Chromatograms showing a G to T substitution 778 bp upstream of the FABP2 initiation codon (FABP2p-ID)

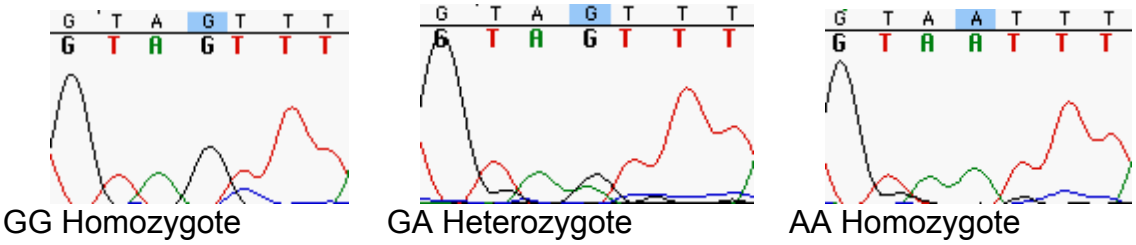

Figure 13: Chromatograms showing a G to A substitution 260 bp upstream of the FABP2 initiation codon (FABP2p-ID)

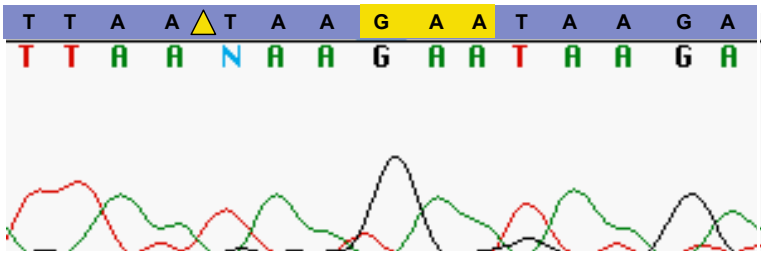

T Deletion Homozygote; GAA Insertion Homozygote

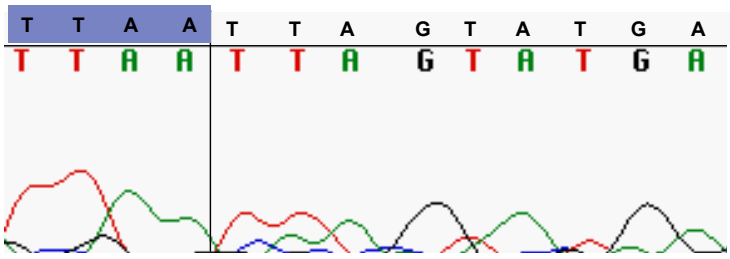

T Insertion/Deletion Heterozygote; GAA Insertion/Deletion Heterozygote

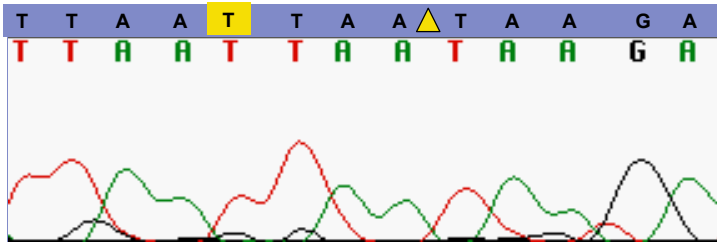

T Insertion Homozygote; GAA Deletion Homozygote

Figure 14: Chromatograms showing a T insertion/deletion and a GAA insertion/deletion 169 bp and 166 bp, respectively, upstream of the FABP2 initiation codon (FABP2p-ID)

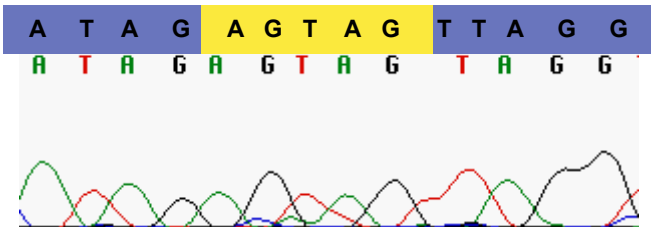

AGTAG Insertion Homozygote

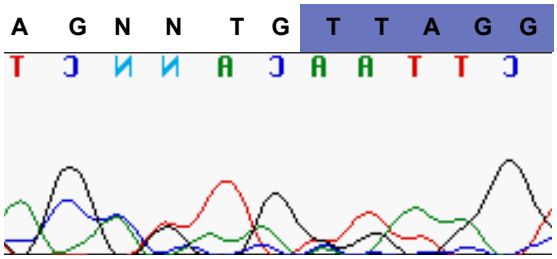

AGTAG Insertion/Deletion Heterozygote

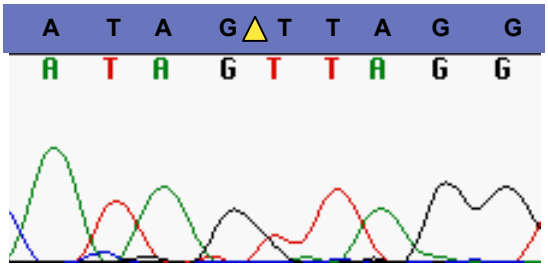

AGTAG Deletion Homozygote

Figure 15: Chromatograms showing an AGTAG insertion/deletion 136 bp upstream of the FABP2 initiation codon (FABP2p-ID)

5. Fatty Acid Binding Protein-3

Direct sequencing was used to screen approximately 1kb of the region 5' to exon 1 of FABP3 (Genbank #U57623 and #U17081). Two polymorphic sites were localized to this region: a C to T substitution at -313 bp (FABP3p-313) shown in Figure 16 and the insertion/deletion of a CTC at -496 bp (FABP3p-ID) shown in Figure 17. Both of these sites were genotyped by direct sequencing.

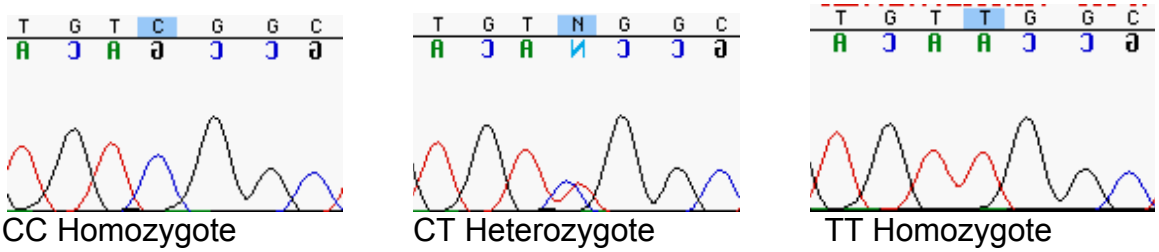

Figure 16: Chromatograms showing a C to T substitution 313 bp upstream of the FABP3 initiation codon (FABP3p-313)

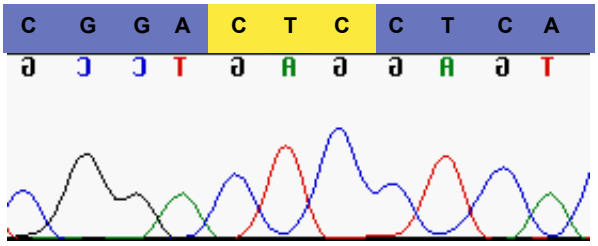

CTC Insertion Homozygote

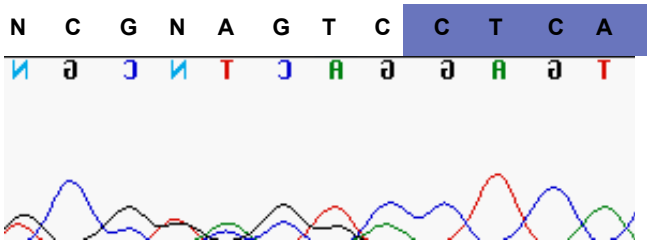

CTC Insertion/Deletion Heterozygote

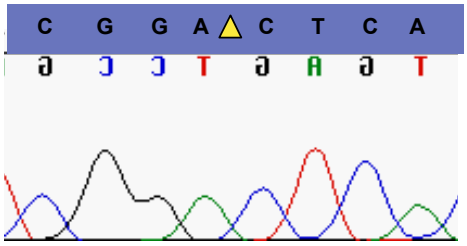

CTC Deletion Homozygote

Figure 17: Chromatograms showing a CTC insertion/deletion 493 bp upstream of the FABP3 initiation codon (FABP3p-ID)

6. Fatty Acid Binding Protein-4

Two polymorphic sites were located in intron 2 of FABP4 through direct sequencing (unpublished data-Ferrell Lab: E. Lawrence). The first site was a T to G substitution 224 bp downstream from exon 2 (FABP4-2a). FABP4-2a genotypes were assigned following restriction enzyme digestion using *Afl*III. The second was a G insertion/deletion polymorphism 412 bp downstream from exon 2 (FABP4-2b). FABP4-2b genotypes were assigned following restriction enzyme digestion using *Pvu*II.

Approximately 500bp of the region 5' of the first exon of FABP4 was screened for variation by direct sequencing (Genbank BAC Clone #AC018616). Two point mutations were located in this region: an A to C substitution at –376 bp and an A to C substitution 2 bp upstream at –378 bp, shown in Figure 18. These polymorphisms are in high linkage disequilibrium. FABP4p-376 genotypes were assigned using fluorescence polarization.

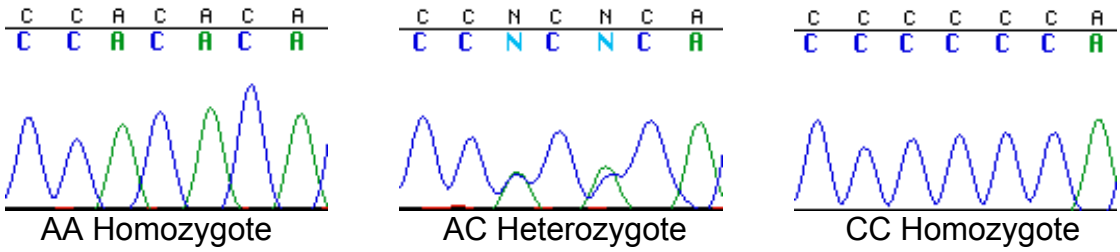

Figure 18: Chromatograms showing an A to C substitution 376 bp upstream of the FABP4 initiation codon (FABP4p-376)

B. GENOTYPING

764 individuals from the non-diabetic (at baseline) control cohort of the SLVDS (321 Hispanics/443 Non-Hispanic whites) were genotyped for variation in the uncoupling protein and fatty acid binding protein gene families. Overall, genotyping was completed for twenty polymorphic sites located in the coding, intronic, and promoter regions of the UCP and FABP genes. Table 2 shows the genotype frequencies for each variant in the entire study cohort and split by ethnicity. Fit to Hardy-Weinberg equilibrium was tested using χ^2 analysis. The bold frequencies denote the sites that show statistically significant deviation from Hardy-Weinberg equilibrium at the 0.05 level. Table 3 shows the allele frequencies for each polymorphic site in the entire study cohort and in each ethnic group. Table 44 in Appendix C shows the allele frequencies for the polymorphic sites in the PPAR and RXR gene families genotyped by Susan Moffett (Moffett, 2002).

Table 2: Genotype Frequencies and Fit to Hardy-Weinberg Equilibrium

		Overall		Non-Hispanics		Hispanics	
		Frequency	p-value	Frequency	p-value	Frequency	p-value
UCP1-2	**GG**	0.810	0.974	0.834	0.642	0.775	0.809
	GA	0.179		0.154		0.215	
	AA	0.011		0.012		0.010	
UCP1-5	**AA**	0.810	0.999	0.827	0.951	0.785	0.916
	AT	0.180		0.163		0.205	
	TT	0.010		0.010		0.010	
UCP2-4	**CC**	**0.265**	**0.001**	0.281	0.101	**0.244**	**0.004**
	CT	**0.564**		0.545		**0.591**	
	TT	**0.171**		0.174		**0.166**	
UCP2-8	**DD**	0.439	0.877	0.445	0.346	**0.429**	**0.033**
	DI	0.454		0.420		**0.500**	
	II	0.108		0.135		**0.071**	
UCP3-3a	**TT**	0.550	0.407	0.524	0.519	0.586	0.725
	TC	0.396		0.415		0.369	
	CC	0.054		0.062		0.045	
UCP3-3b	**GG**	0.991	0.992	0.995	0.999	0.984	0.990
	GA	0.009		0.005		0.016	
UCP3-5	**TT**	0.297	0.999	0.298	0.690	0.295	0.544
	TC	0.497		0.477		0.525	
	CC	0.207		0.226		0.180	
FABP2-2	**GG**	0.512	0.994	0.540	0.966	0.472	0.976
	GA	0.406		0.386		0.434	
	AA	0.082		0.074		0.094	
FABP4-2a	**TT**	0.744	0.086	0.682	0.354	0.831	0.559
	TG	0.225		0.275		0.155	
	GG	0.031		0.043		0.014	
FABP4-2b	**II**	0.773	0.986	0.826	0.963	0.699	0.934
	ID	0.211		0.164		0.278	
	DD	0.015		0.010		0.023	

Table 2: continued

		Overall		Non-Hispanics		Hispanics	
		Frequency	p-value	Frequency	p-value	Frequency	p-value
UCP3p-55	CC	0.613	0.995	0.582	0.912	0.658	0.813
	CT	0.339		0.367		0.299	
	TT	0.048		0.051		0.043	
FABP2p-834	CC	0.512	0.417	0.539	0.551	0.474	0.796
	CT	0.393		0.376		0.417	
	TT	0.095		0.085		0.109	
FABP2p-778	GG	0.349	1.000	0.342	0.927	0.360	0.877
	GT	0.484		0.478		0.492	
	TT	0.167		0.180		0.149	
FABP2p-260	GG	0.349	1.000	0.342	0.927	0.360	0.877
	GA	0.484		0.478		0.492	
	AA	0.167		0.180		0.149	
FABP2p-169	DD	0.349	1.000	0.342	0.927	0.360	0.877
	DI	0.484		0.478		0.492	
	II	0.167		0.180		0.149	
FABP2p-166	II	0.349	1.000	0.342	0.927	0.360	0.877
	ID	0.484		0.478		0.492	
	DD	0.167		0.180		0.149	
FABP2p-136	II	0.349	1.000	0.342	0.927	0.360	0.877
	ID	0.484		0.478		0.492	
	DD	0.167		0.180		0.149	
FABP3p-493	DD	**0.317**	**0.013**	**0.325**	**0.009**	0.306	0.602
	DI	**0.538**		**0.551**		0.520	
	II	**0.145**		**0.124**		0.174	
FABP3p-313	CC	0.602	0.867	0.625	0.685	0.569	0.325
	CT	0.343		0.340		0.349	
	TT	0.055		0.035		0.082	
FABP4p-376	AA	0.745	0.055	0.703	0.080	0.801	0.909
	AC	0.224		0.252		0.185	
	CC	0.032		0.045		0.014	

Table 3: Allele Frequencies

Polymorphic Site	Allele	Overall Frequency	Frequency	
			Non-Hispanics	Hispanics
UCP1 Exon 2	G (Ala)	0.899	0.911	0.883
	A (Thr)	0.101	0.089	0.117
UCP1 Exon 5	A (Met)	0.900	0.909	0.887
	T (Leu)	0.100	0.091	0.113
UCP2 Exon 4	C (Ala)	0.547	0.553	0.539
	T (Val)	0.453	0.447	0.461
UCP2 Exon 8	Del	0.665	0.656	0.679
	Ins	0.335	0.344	0.321
UCP3 Exon 3a	T	0.748	0.731	0.771
	C	0.252	0.269	0.229
UCP3 Exon 3b	G (Val)	0.995	0.998	0.989
	A (Ile)	0.005	0.002	0.011
UCP3 Exon 5	T	0.545	0.536	0.557
	C	0.455	0.464	0.443
FABP2 Exon 2	G (Ala)	0.715	0.733	0.689
	A (Thr)	0.285	0.267	0.311
FABP4 Intron 2a	T	0.856	0.819	0.909
	G	0.144	0.181	0.091
FABP4 Intron 2b	Ins	0.879	0.908	0.838
	Del	0.121	0.092	0.162
UCP3 Promoter (-55bp)	C	0.783	0.765	0.808
	T	0.217	0.235	0.192
FABP2 Promoter (-834bp)	C	0.709	0.727	0.683
	T	0.291	0.273	0.317
FABP2 Promoter (-778bp)	G	0.591	0.581	0.606
	T	0.409	0.419	0.394
FABP2 Promoter (-260bp)	G	0.591	0.581	0.607
	A	0.409	0.419	0.393
FABP2 Promoter (-169bp)	Del	0.591	0.581	0.607
	Ins	0.409	0.419	0.393
FABP2 Promoter (-166bp)	Ins	0.591	0.581	0.607
	Del	0.409	0.419	0.393
FABP2 Promoter (-136bp)	Ins	0.591	0.581	0.607
	Del	0.409	0.419	0.393
FABP3 Promoter (-493bp)	Del	0.586	0.600	0.566
	Ins	0.414	0.400	0.434
FABP3 Promoter (-313bp)	C	0.774	0.795	0.743
	T	0.226	0.205	0.257
FABP4 Promoter (-376bp)	A	0.856	0.829	0.894
	C	0.144	0.171	0.106

C. DATA ANALYSIS

1. Preliminary Analyses of Genotypic Data

Genotype frequencies and allele frequencies for each polymorphic site are shown in Tables 2 and 3, respectively. Pairwise linkage disequilibrium, D', was estimated for each pair of loci residing on the same chromosome. The D' value for UCP1-2 and UCP1-5 was 0.860. Table 4 shows D' values between each pair of loci in UCP2 and UCP3, which are located within 8 kb of one another on chromosome 11q13. D' values between the polymorphic sites in FABP2 are shown in Table 5. D' between FABP3p-ID and FABP3p-313 was 0.974. D' values between the FABP4 variants are shown in Table 6.

Table 4: Linkage Disequilibrium Between UCP2 & UCP3 Polymorphic Sites

	UCP2-4	UCP2-8	UCP3p-55	UCP3-3a	UCP3-5
UCP2-4	-	0.735	0.328	0.259	0.683
UCP2-8	0.735	-	0.347	0.396	0.514
UCP3p-55	0.328	0.347	-	0.978	0.838
UCP3-3a	0.259	0.396	0.978	-	0.740
UCP3-5	0.683	0.514	0.838	0.740	-

Table 5: Linkage Disequilibrium Between FABP2 Polymorphic Sites

	FABP2p-834	FABP2p-ID	FABP2-2
FABP2p-834	-	0.884	0.954
FABP2p-ID	0.884	-	0.904
FABP2-2	0.954	0.904	-

Table 6: Linkage Disequilibrium Between FABP4 Polymorphic Sites

	FABP4p-376	FABP4-2a	FABP4-2b
FABP4p-376	-	0.967	0.979
FABP4-2a	0.967	-	0.991
FABP4-2b	0.979	0.991	-

2. Descriptive Statistics

Descriptive statistics of the phenotypic data collected on the study participants are shown in Tables 7 and 8. Bar charts of the phenotype counts for each categorical variable are shown in Figures 73-75 in Appendix D. Frequency distributions for each continuous variable are displayed in histograms shown in Figure 76 of Appendix D. The study population was comprised of slightly more females than males, with frequencies of 52.8% and 47.2%, respectively. There was also a higher rate of participation for Non-Hispanics (58%) than for Hispanics (42%). The average age of the participants was 63 years. The cohort was slightly overweight, with an average BMI of 27 kg/m^2 ("healthy" BMI range: 18.5-25 kg/m^2; World Health Organization, 1997). Average fasting glucose for the cohort was 100 mg/dl, which falls within the normal range

("healthy" fasting glucose <110 mg/dl; American Diabetes Association, 2002). The average fasting cholesterol level for the cohort was 201 mg/dl, which is borderline healthy ("healthy" cholesterol <200 mg/dl; National Cholesterol Education Program, 2001). On average, the fasting triglyceride level for the cohort was 178 mg/dl, which falls in the "borderline high" range of 150-199 mg/dl (National Cholesterol Education Program, 2001). The average diet consisted of 1931 calories, with 35% of caloric intake derived from fat (~76 grams). Since the distributions for two of the outcome variables, fasting triglyceride levels and HOMA IR values, were highly skewed, they were transformed using the natural log.

Table 7: Categorical Variable Frequencies

		N	Percentage
Sex	Males	353	47.2%
	Females	395	52.8%
Ethnicity	Non-Hispanics	434	58.0%
	Hispanics	314	42.0%
Smoking Status	Non-Smoker	359	49.2%
	Ever Smoked	371	50.8%

Table 8: Descriptive Statistics of Continuous Variables

	N	Mean	Std. Deviation	Skewness Statistic	Kurtosis Statistic
Fat Mass (grams - DEXA)	699	26197	9284	0.460	0.452
Free Fatty Acids (µmol/L)	747	599	238	0.658	0.342
Triglycerides (mg/dl)	747	178	92	**1.799**	**4.490**
ln(Triglycerides)	747	5.07	0.46	0.277	0.189
Cholesterol (mg/dl)	747	201	36	0.360	0.677
HOMA IR [(ins*gluc)/22.5]	747	17	13	**2.444**	**7.560**
ln(HOMA R)	747	2.65	0.60	0.504	0.152
Total Calories	715	1931	845	0.983	1.580
Fat Intake (grams)	714	76	42	1.282	2.700
Fasting Glucose (mg/dl)	747	100	22	3.615	18.738
Fasting Insulin (mg/dl)	747	11	6.6	2.022	5.327
Body Mass Index (kg/m^2)	748	27	4.9	0.756	1.402
Lean Mass (grams - DEXA)	699	44642	10835	0.432	-0.860
% Body Fat	699	35	9.6	-0.110	-0.543
Systolic Reading (mm Hg)	747	127	18	1.003	1.730
Diastolic Reading (mm Hg)	747	74	9	0.321	0.764
Physical Activity (kcal/kg/hr)	727	283	62	1.941	3.959
Skin reflectance (%)	746	33	3.8	-0.396	0.147
Age (years)	748	63	12	-0.174	-0.760

Table 9 shows the mean for each continuous variable in each ethnic group. ANOVA was used to test for statistical differences in means between the two ethnic groups. The non-Hispanic cohort was slightly older than the Hispanic group ($p=0.039$). The Hispanic cohort had higher levels of fasting free fatty acids ($p<0.001$) and triglycerides ($p=0.002$) with lower insulin sensitivity ($p<0.001$). Despite higher total caloric ($p=0.001$) and fat intake ($p=0.015$) in the non-Hispanic cohort, there was no statistically significant difference in fat mass between the two ethnic groups; however, the non-Hispanic cohort did show statistically significant increases in lean mass ($p<0.001$).

Table 9: Continuous Variable Means Split by Ethnicity

	Non-Hispanics		Hispanics		p-value
	N	Mean (SD)	N	Mean (SD)	
Fat Mass (grams)	408	26539 (9164)	291	25717 (9445)	0.249
Free Fatty Acids (µmol/L)	433	**568 (223)**	314	**641 (252)**	**<0.001**
Triglycerides (mg/dl)	433	**169 (87)**	314	**190 (97)**	**0.002**
ln(Triglycerides)	433	**5.02 (0.45)**	314	**5.13 (0.46)**	**0.001**
Cholesterol (mg/dl)	433	201 (37)	314	201 (35)	0.867
HOMA IR [(ins*gluc)/22.5]	433	**15.51 (11.30)**	314	**19.85 (14.73)**	**<0.001**
ln(HOMA IR)	433	**2.56 (0.57)**	314	**2.78 (0.62)**	**<0.001**
Total Calories	422	**2014 (826)**	293	**1810 (860)**	**0.001**
Fat Intake (grams)	422	**79 (41)**	292	**71 (43)**	**0.015**
Lean Mass (grams)	408	**46460 (11347)**	291	**42094 (9522)**	**<0.001**
Physical Activity (kcal/kg/hr)	426	284 (61)	301	281 (63)	0.567
Skin Reflectance (%)	432	**34.27 (2.99)**	314	**30.43 (3.75)**	**<0.001**
Age (years)	433	**64 (11)**	313	**62 (12)**	**0.039**

3. Preliminary Analyses of Outcome and Predictor Variables

Tables 10 to 14 show the means of each outcome variable for each genotype, split by sex and ethnicity. ANOVA was used to test for statistically significant differences in outcome means between genotype groups for each polymorphic site. The values shown in bold represent the statistically significant single-locus effects on the outcome variables. Relationships between the outcome variables and the remaining predictor variables are represented in a correlation matrix shown in Table 45 of Appendix D.

Table 10: Means for Fat Mass vs UCPs and FABPs in SLVDS Split by Ethnicity and Sex

Fat Mass (kg)	Non-Hispanic Males				Non-Hispanic Females				Hispanic Males				Hispanic Females			
	11	12	22	p-value	11	12	22	p-value	11	12	22	p-value	11	12	22	p-value
UCP1-2	*24.7*	*21.9*		*.075*	28.5	28.9		.843	21.6	21.4		.918	*28.3*	*31.7*		*.055*
UCP1-5	24.6	22.3		.162	28.9	28.3		.735	21.6	22.0		.798	28.6	31.0		.203
UCP2-4	24.2	24.3	24.1	.987	28.5	29.4	27.2	.504	20.6	22.3	21.1	.507	29.2	28.4	30.1	.729
UCP2-8	*24.9*	*23.0*	*26.9*	*.074*	28.5	29.0	29.1	.925	21.1	22.5	19.3	.408	29.1	29.0	29.3	.991
UCP3-3a	24.1	24.4		.759	28.7	28.7		.983	21.9	21.1		.560	29.7	28.2		.344
UCP3-5	24.8	24.5	23.4	.651	**32.0**	**26.3**	**28.2**	**.002**	21.4	21.7	21.7	.986	29.1	28.9	29.8	.926
FABP2-2	24.7	23.7		.347	27.8	29.5		.230	**23.1**	**20.4**		**.039**	29.5	29.1		.812
FABP4-2a	23.5	25.4		.116	28.2	30.1		.256	21.8	21.1		.713	29.3	28.9		.871
FABP4-2b	24.4	23.4		.528	28.9	27.8		.553	21.0	23.2		.129	29.0	30.1		.532
UCP3p-55	24.0	24.6		.600	28.4	29.3		.510	21.7	21.2		.756	29.8	29.0		.624
FABP2p-ID	*24.3*	*23.4*	*26.8*	*.077*	27.8	28.3	31.4	.188	21.9	21.5	21.5	.963	29.3	29.3	31.0	.750
FABP2p-834	24.8	23.4	24.7	.464	27.7	29.2	32.7	.180	22.5	21.0	19.1	.251	29.6	29.9	28.2	.783
FABP3p-ID	24.8	24.1	24.6	.854	28.4	29.0	26.9	.630	20.4	22.5	20.8	.329	30.1	29.0	29.4	.815
FABP3p-313	24.9	23.4		.176	29.1	27.3		.234	21.7	21.5		.854	29.0	29.9		.560
FABP4p-376	*23.5*	*25.9*		*.088*	27.8	29.6		.304	21.8	20.4		.567	29.2	30.1		.645

Table 11: Means for Fasting FFA vs UCPs and FABPs in SLVDS Split by Ethnicity and Sex

Fasting FFA (µmol/L)	Non-Hispanic Males				Non-Hispanic Females				Hispanic Males				Hispanic Females			
	11	12	22	p-value	11	12	22	p-value	11	12	22	p-value	11	12	22	p-value
UCP1-2	505	471		.359	638	590		.246	559	531		.596	*684*	*769*		*.054*
UCP1-5	501	495		.861	630	597		.407	564	543		.690	**674**	**774**		**.030**
UCP2-4	495	498	526	.751	653	628	598	.470	**489**	**602**	**482**	**.016**	*686*	*696*	*793*	*.158*
UCP2-8	497	502	501	.980	*634*	*647*	*564*	*.194*	570	552	572	.900	724	687	719	.639
UCP3-3a	496	506		.700	633	638		.872	556	559		.932	695	725		.426
UCP3-5	519	495	493	.739	**685**	**584**	**633**	**.022**	559	564	526	.763	724	682	757	.332
FABP2-2	503	499		.867	628	637		.755	556	559		.943	719	695		.540
FABP4-2a	510	483		.339	628	659		.387	562	511		.359	701	729		.598
FABP4-2b	499	509		.780	639	617		.604	548	569		.638	716	684		.454
UCP3p-55	496	509		.644	627	636		.767	554	579		.561	708	698		.802
FABP2p-ID	490	510	486	.713	646	634	601	.640	589	544	568	.607	707	686	759	.482
FABP2p-834	497	512	449	.429	620	638	681	.588	539	567	590	.675	715	698	670	.766
FABP3p-ID	*454*	*512*	*526*	*.094*	606	632	698	.225	536	555	601	.571	734	695	669	.503
FABP3p-313	482	512		.272	641	623		.599	556	557		.978	690	717		.493
FABP4p-376	508	477		.220	*623*	*653*		*.089*	557	501		.220	697	726		.602

Table 12: Means for Triglycerides vs UCPs and FABPs in SLVDS Split by Ethnicity and Sex

Tri-glycerides (mg/dl)	Non-Hispanic Males				Non-Hispanic Females				Hispanic Males				Hispanic Females			
	11	12	22	p-value	11	12	22	p-value	11	12	22	p-value	11	12	22	p-value
UCP1-2	173	186		.970	162	155		.523	194	164		.259	**184**	**217**		**.039**
UCP1-5	171	199		.150	162	151		.257	190	182		.899	**183**	**224**		**.019**
UCP2-4	167	181	166	.625	**147**	**173**	**158**	**.047**	189	184	194	.757	*203*	*196*	*162*	*.101*
UCP2-8	176	175	159	.570	157	167	160	.487	197	183	154	.460	*209*	*180*	*162*	*.051*
UCP3-3a	*186*	*160*		*.062*	**151**	**176**		**.041**	177	200		.256	189	197		.520
UCP3-5	167	180	174	.887	**175**	**161**	**143**	**.027**	178	200	175	.491	190	194	205	.654
FABP2-2	178	170		.410	168	159		.202	188	189		.801	193	195		.963
FABP4-2a	170	185		.214	160	170		.368	189	187		.680	192	204		.467
FABP4-2b	173	182		.543	167	143		.156	184	202		.260	189	205		.510
UCP3p-55	**190**	**153**		**.006**	**150**	**176**		**.032**	*176*	*212*		*.105*	192	197		.833
FABP2p-ID	*193*	*160*	*184*	*.071*	159	160	167	.974	191	190	170	.843	195	193	191	.978
FABP2p-834	181	165	181	.319	166	158	163	.348	186	192	169	.984	196	191	192	.746
FABP3p-ID	164	183	172	.396	150	172	151	.094	180	187	209	.523	208	185	189	.627
FABP3p-313	169	183		.223	162	165		.535	**172**	**211**		**.016**	197	188		.757
FABP4p-376	172	186		.302	158	172		.249	189	181		.812	192	199		.600

Table 13: Means for Cholesterol vs UCPs and FABPs in SLVDS Split by Ethnicity and Sex

Cholesterol (mg/dl)	Non-Hispanic Males				Non-Hispanic Females				Hispanic Males				Hispanic Females			
	11	12	22	p-value	11	12	22	p-value	11	12	22	p-value	11	12	22	p-value
UCP1-2	197	194		.733	206	202		.505	194	194		.984	206	204		.738
UCP1-5	197	199		.785	205	201		.465	193	194		.995	206	207		.917
UCP2-4	198	199	188	.327	205	206	209	.824	192	193	199	.716	207	206	207	.982
UCP2-8	200	195	189	.393	206	208	200	.588	**192**	**192**	**228**	**.018**	208	206	193	.367
UCP3-3a	197	195		.721	205	206		.949	194	195		.854	205	207		.620
UCP3-5	194	198	197	.760	209	206	199	.373	197	195	187	.473	**216**	**202**	**201**	**.050**
FABP2-2	*201*	*191*		*.072*	206	206		.950	194	194		.913	205	207		.613
FABP4-2a	195	200		.329	204	208		.493	*191*	*204*		*.103*	206	201		.521
FABP4-2b	196	199		.651	205	210		.463	195	189		.427	207	202		.408
UCP3p-55	199	194		.379	208	201		.182	194	195		.922	203	207		.399
FABP2p-ID	202	195	193	.328	**212**	**199**	**210**	**.047**	196	194	195	.954	207	204	204	.875
FABP2p-834	199	194	194	.582	206	203	217	.364	194	191	205	.413	205	203	212	.589
FABP3p-ID	193	199	201	.514	*198*	*210*	*210*	*.098*	190	194	197	.733	206	207	198	.423
FABP3p-313	**193**	**203**		**.050**	207	205		.676	*190*	*199*		*.101*	*209*	*201*		*.153*
FABP4p-376	195	201		.463	204	208		.614	*193*	*202*		*.145*	206	203		.712

Table 14: Means for HOMA IR vs UCPs and FABPs in SLVDS Split by Ethnicity and Sex

HOMA IR	Non-Hispanic Males				Non-Hispanic Females				Hispanic Males				Hispanic Females			
	11	12	22	p-value	11	12	22	p-value	11	12	22	p-value	11	12	22	p-value
UCP1-2	15.9	18.1		.914	14.7	16.0		.752	20.4	18.5		.885	*18.9*	*22.0*		*.170*
UCP1-5	15.8	18.6		.766	15.1	15.4		.788	20.5	18.7		.830	*19.1*	*22.8*		*.159*
UCP2-4	16.2	16.4	15.3	.854	14.1	15.6	14.6	.570	16.9	21.4	19.6	.445	21.0	18.3	20.4	.680
UCP2-8	*16.7*	*15.6*	*17.9*	*.149*	15.4	15.1	13.2	.753	19.3	20.8	17.0	.651	20.5	18.2	24.4	.268
UCP3-3a	15.9	16.8		.994	**12.9**	**16.9**		**.022**	20.6	18.4		.517	19.6	20.0		.515
UCP3-5	15.9	16.6	16.0	.901	**16.1**	**14.7**	**12.3**	**.046**	17.9	21.1	20.1	.442	22.5	17.9	22.2	.494
FABP2-2	16.1	16.5		.456	14.3	15.4		.832	21.1	19.2		.458	*22.0*	*18.0*		*.092*
FABP4-2a	16.1	16.2		.392	14.6	15.0		.627	20.4	19.3		.970	20.3	18.0		.838
FABP4-2b	16.3	15.3		.573	15.1	12.5		.447	20.4	20.0		.515	*18.9*	*22.3*		*.077*
UCP3p-55	16.0	16.9		.939	**12.9**	**17.7**		**.010**	19.4	20.3		.591	20.6	19.6		.756
FABP2p-ID	*16.7*	*15.2*	*18.6*	*.188*	15.9	14.0	15.9	.484	22.7	17.8	19.5	.193	21.9	19.6	16.4	.304
FABP2p-834	16.2	16.1	18.0	.737	14.0	16.0	13.7	.983	19.8	19.1	22.9	.627	*21.9*	*19.6*	*13.7*	*.072*
FABP3p-ID	15.8	16.0	18.0	.401	14.1	14.6	14.4	.622	19.9	20.8	18.0	.789	20.3	20.5	18.6	.592
FABP3p-313	16.3	16.0		.574	14.6	14.2		.927	20.6	19.4		.920	*18.8*	*21.5*		*.141*
FABP4p-376	16.2	16.8		.362	14.8	15.2		.339	20.2	17.6		.774	20.0	19.1		.763

4. Regression Modeling – Split by Sex and Ethnicity

The results of the preliminary analyses of outcome and predictor variables suggested the presence of interesting sex- and ethnic-specific influences of genetic variation on outcome variables. Thus, for the initial analyses, the data was split by sex and ethnicity. ANOVA was used to test for single locus effects on each outcome (Tables 10-14) for each sex/ethnic subgroup separately. Two-way ANOVA was used to identify pairs of loci with strong interaction effects. Linear regression models were constructed for each outcome variable to explore multi-locus effects and interactions. To find the most parsimonious models, backward and stepwise selection methods were used with exclusion and inclusion criteria set such that the "final" models included only terms with a p-value less than 0.05. The final models for fat mass in each of the female cohorts and triglycerides in each of the male cohorts are described below. The final models for the remaining outcome variables for each of the sex/ethnic subgroups may be found in Tables 46 to 58 in Appendix E.

a) Fat Mass in Non-Hispanic Females

Table 10 shows the results of ANOVA for each of the single loci versus mean fat mass. The UCP3-5 variant was significantly associated with fat mass ($p=0.002$) in the non-Hispanic female cohort. Homozygosity for the UCP3-5 T allele corresponded to ~5 kg higher fat mass compared to carriers of at least one C allele (Figure 19). Alone, the UCP3-5 variant explained ~6.2% of the variation in fat mass in the non-Hispanic females.

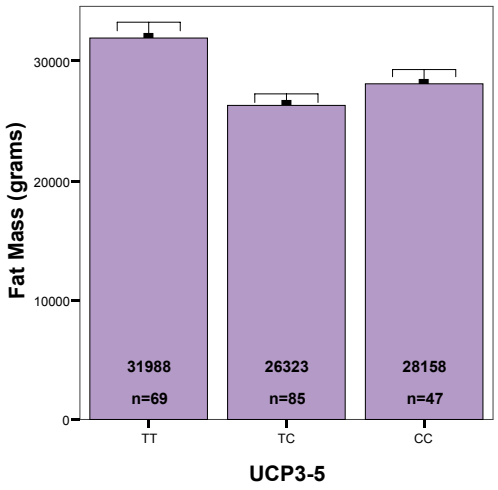

Figure 19: Fat Mass vs. UCP3-5 in Non-Hispanic Females

The final linear regression model for fat mass, shown in Table 15, included interactions between UCP2-4 and UCP3-5 as significant predictors ($p<0.001$). Mean fat mass for individuals of each UCP2-4/UCP3-5 multi-locus genotype group in the non-Hispanic female cohort are shown in Figure 20. Individuals carrying at least one UCP3-5 C allele exhibit an average fat mass of 27 kg (baseline level). Fat mass levels for UCP3-5 T homozygotes are modified by UCP2-4 genotype. On the UCP3-5 T background, UCP2-4 C homozygotes have the highest levels of fat mass (~40 kg). Increasing prevalence of the UCP2-4 T allele reduces fat mass in an additive manner. UCP2-4 heterozygotes, on the UCP3-5 T/T background, show an ~4.8 kg reduction in fat mass, while UCP2-4 T homozygosity results in an ~8.3 kg further reduction in fat

mass, retaining baseline levels (~27 kg). The addition of interactive effects of the UCP2-4 variant substantially increased the R^2 to 13.5%.

Table 15: Non-Hispanic Females – Final Regression Model for Fat Mass

	β	p-value	R^{2*}
Constant	29713	<0.001	0.135
UCP2-4 (CC) * UCP3-5 (TT)	13238	0.001	
UCP2-4 (CT) * UCP3-5 (TT)	8369	<0.001	

*p<0.001

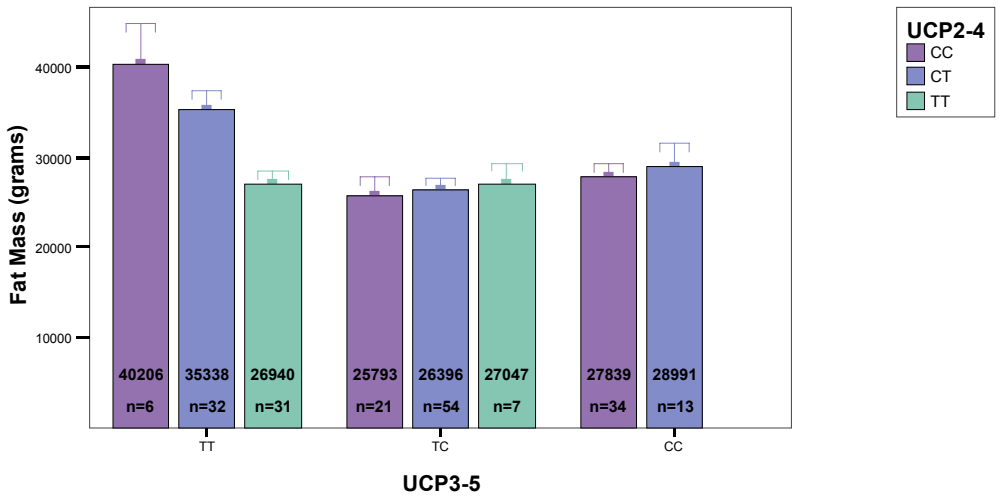

Figure 20: Fat Mass vs. UCP2-4/UCP3-5 Multi-Locus Genotypes in Non-Hispanic Females

b) Fat Mass in Hispanic Females

ANOVA results for fat mass versus each of the single loci in Hispanic females are shown in Table 10. The UCP1-2 variant was marginally associated with fat mass in the Hispanic female cohort (p=0.055), with presence of the A allele contributing to ~3.4 kg higher mean fat mass than G homozygotes (Figure 21).

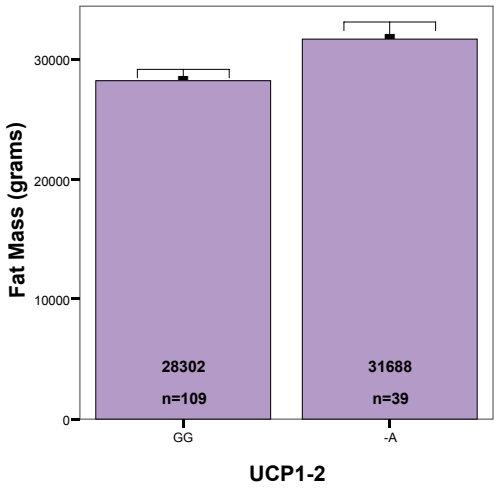

Figure 21: Fat Mass vs. UCP1-2 in Hispanic Females

Table 16 shows the final model for fat mass in Hispanic females. This model included UCP1-2, UCP3-5, and an interaction between those sites as significant predictors of fat mass (p<0.001), explaining ~12.2% of the variation in that trait. Mean fat mass for individuals of each UCP1-2/UCP3-5 multi-locus genotype group in the Hispanic female cohort are shown in Figure 22. Higher fat mass levels associated with

the UCP1-2 A allele are elevated further when in combination with the UCP3-5 T/T genotype, showing an average 12.4 kg increase over all other genotype combinations. Presence of the UCP3-5 C allele reduces fat mass by ~7-14 kg; however, UCP3-5 heterozygotes show a larger average reduction in fat mass than C homozygotes. Homozygosity for the G allele at UCP1-2 contributes to an average 3.4 kg reduction in fat mass in comparison to carriers of at least one A allele. However, within the UCP1-2 G/G group, UCP3-5 heterozygotes showed an average 3.4 kg increase in fat mass over the homozygous groups.

Table 16: Hispanic Females – Final Regression Model for Fat Mass

	β	p-value	R^{2*}
Constant	37317	<0.001	0.122
UCP1-2 (GG)	-10874	<0.001	
UCP3-5 (TC)	-9978	0.001	
UCP1-2 (GG) * UCP3-5 (TC)	13395	<0.001	

*p<0.001

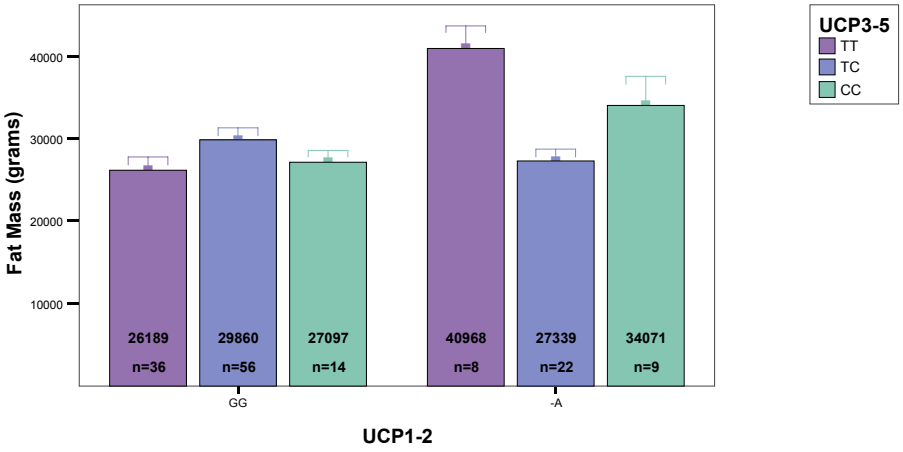

Figure 22: Fat Mass vs. UCP1-2/UCP3-5 Multi-Locus Genotypes in Hispanic Females

c) Triglycerides in Non-Hispanic Males

Table 12 shows the results of ANOVA for each of the single loci versus mean triglycerides. The UCP3p-55 variant was significantly associated with triglycerides (p=0.002) in the non-Hispanic male cohort. The UCP3p-55 T allele corresponded to ~37 mg/dl lower triglyceride levels (Figure 23). Alone, the UCP3p-55 variant explained ~3.6% of the variation in triglyceride levels in the non-Hispanic males. The FABP2p-ID variant was marginally associated with triglyceride levels (p=0.071) in the non-Hispanic male cohort. Mean triglyceride levels in FABP2p-ID heterozygous individuals, shown in Figure 24, were reduced by ~20-30 mg/dl in comparison to the homozygote groups.

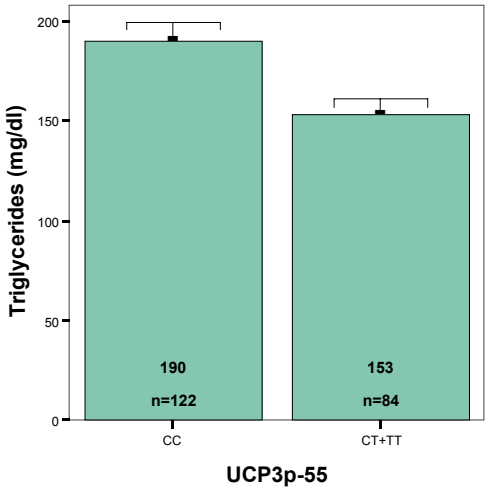

Figure 23: Triglycerides vs. UCP3p-55 in Non-Hispanic Males

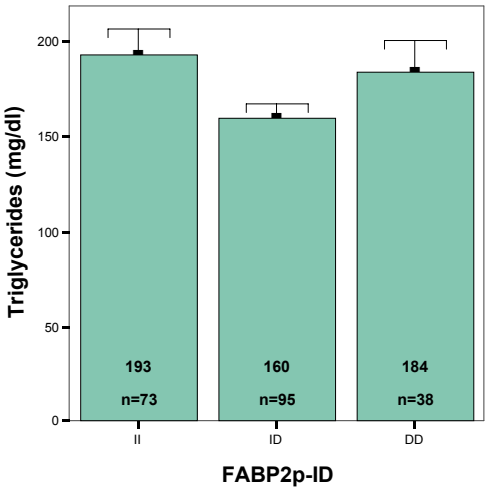

Figure 24: Triglycerides vs. FABP2p-ID in Non-Hispanic Males

The final model for ln(Triglycerides) in the non-Hispanic males ($p<0.001$) is shown in Table 17. The significant predictors of triglyceride levels involve interactions among UCP3 variants and the insertion/deletion polymorphisms in the 5' regions of FABP2 and FABP3. This model explains ~10.1% of the variation in triglycerides. Mean triglycerides for individuals of each UCP3p-55/FABP3p-ID multi-locus genotype group in the non-Hispanic males are shown in Figure 25. The model shows that the FABP3p-ID heterozygotes on the UCP3p-55 C/C background have elevated triglycerides compared to all other genotype groups. In the non-Hispanic males, shown in the graph, this increase is ~ 48 mg/dl. The graph also shows that FABP3p-ID D homozygotes on the UCP3p-55 C/C background and FABP3p-ID I homozygotes in the presence of the UCP3p-55 I allele exhibit intermediate levels of triglycerides. Figure 26 shows the UCP3-5/FABP2p-ID multi-locus genotypes versus triglycerides. On the FABP2p-ID heterozygote background, the UCP3-5 T allele confers an average 41 mg/dl reduction in triglycerides in comparison to all other genotype combinations.

Table 17: Non-Hispanic Males – Final Regression Model for ln(Triglycerides)

	β	p-value	R^{2*}
Constant	4.962	<0.001	0.101
UCP3-5 (TC)	0.148	0.046	
UCP3-5 (TC) * FABP2p-ID (ID)	-0.288	0.001	
UCP3p-55 (CC) * FABP3p-ID (ID)	0.246	<0.001	

*p<0.001

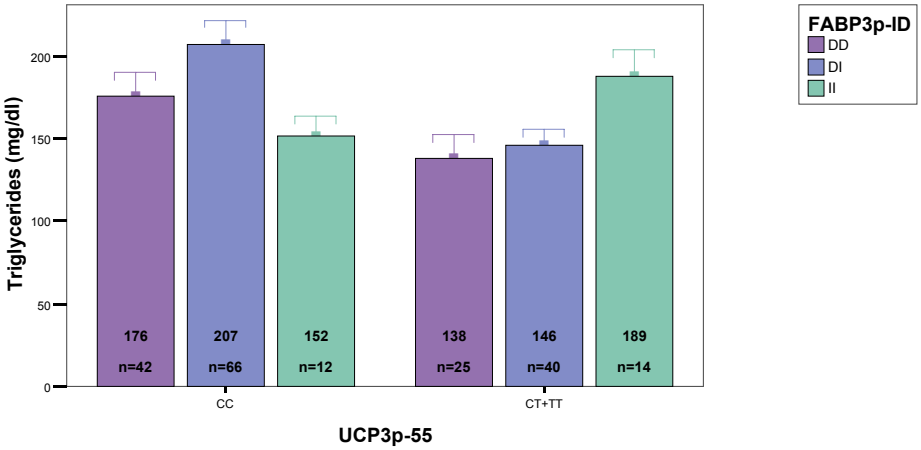

Figure 25: Triglcyerides vs. UCP3p-55/FABP3p-ID Multi-Locus Genotypes in Non-Hispanic Males

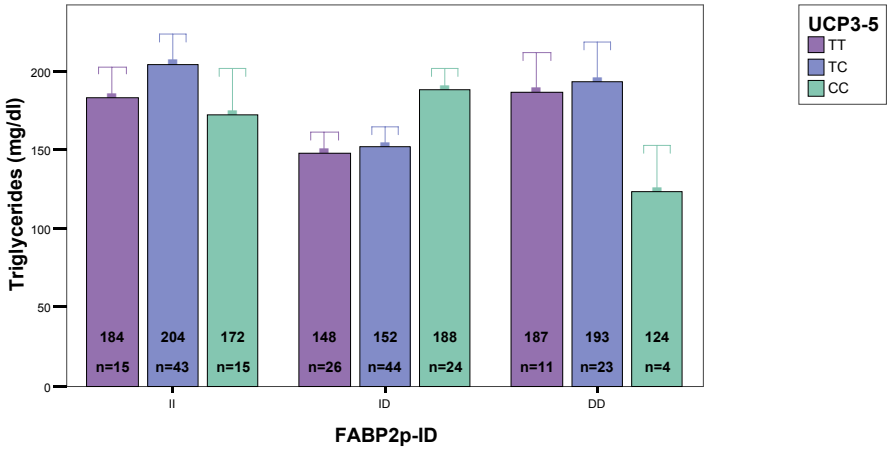

Figure 26: Triglycerides vs. UCP3-5/FABP2p-ID Multi-Locus Genotypes in Non-Hispanic Males

d) Triglycerides in Hispanic Males

ANOVA for triglycerides versus each of the single loci in Hispanic males is shown in Table 12. The FABP3p-313 variant was associated with triglyceride levels in the Hispanic male cohort (p=0.016). The FABP3p-313 T allele contributed to an ~39 mg/dl increase in triglycerides (Figure 27). A similar effect on triglycerides was observed in the UCP3p-55 variant (Figure 28); however, this effect was not statistically significant (p=0.105).

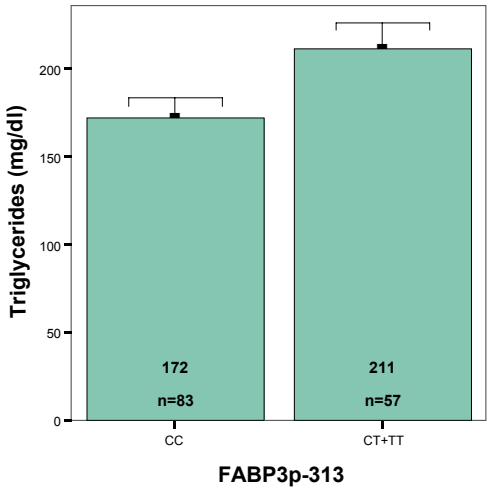

Figure 27: Triglycerides vs. FABP3p-313 in Hispanic Males

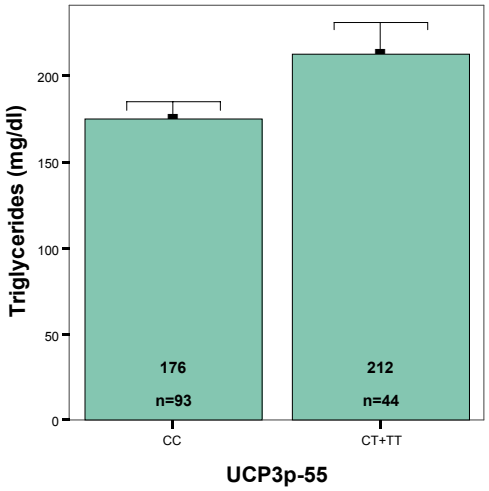

Figure 28: Triglycerides vs. UCP3p-55 in Hispanic Males

Table 18 shows the final model for log transformed triglycerides in Hispanic males. This model included both FABP3p-313 and UCP3-5 in an interaction as the significant predictor of ln(Triglycerides) (p=0.010), explaining ~4.9% of the variation in triglyceride levels in Hispanic males. Mean triglycerides for individuals of each FABP3p-313/UCP3-5 multi-locus genotype group in the Hispanic males are shown in Figure 29. The lowest level of mean triglycerides results from the combination of homozygosity for the FABP3p-313 C allele and the UCP3-5 T allele. Presence of the UCP3-5 C allele on the FABP3p-313 background produces an average 43 mg/dl increase in triglyceride levels. In the presence of the FABP3p-313 T allele, UCP3-5 genotype seems to have the opposite effect on mean triglyceride levels. UCP3-5 T

homozygotes show the highest levels of triglycerides, while increasing presence of the UCP3-5 C allele results in a dose dependent reduction.

Table 18: Hispanic Males – Final Regression Model for ln(Triglycerides)

	β	p-value	R^{2*}
Constant	5.161	<0.001	0.049
UCP3-5 (TT) * FABP3p-313 (CC)	-0.291	0.010	

*p=0.010

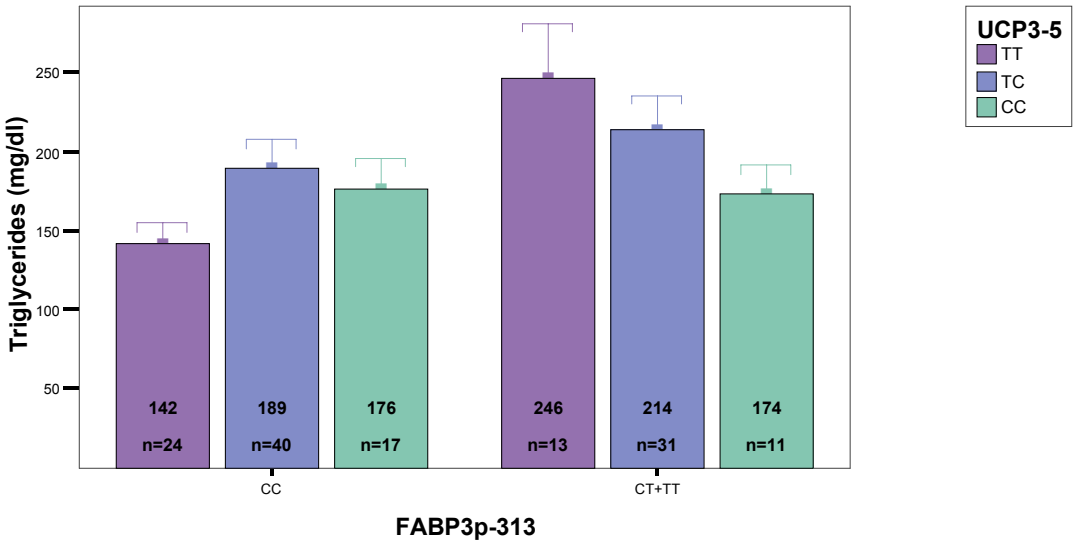

Figure 29: Triglycerides vs. FABP3p-313/UCP3-5 Multi-Locus Genotypes in Hispanic Males

5. Regression Modeling – Split by Sex

Since the Hispanic male cohort was relatively small (n=143), a second approach was taken to the analysis. In an attempt to consider the Hispanic males as part of a larger cohort, the entire data set was split by sex, and the outcome variables were adjusted for skin reflectance to account for ethnic differences. The outcome variables were also adjusted for age, physical activity, and smoking status, using linear regression. As in the previous analysis, ANOVA was used to test for single locus effects on each adjusted outcome for females and males separately. Two-way ANOVA were used to identify pairs of loci with strong interaction effects. Multi-locus effects and interactions were explored for each adjusted outcome variable using linear regression. To find the most parsimonious models, backward and stepwise selection methods were used with exclusion and inclusion criteria set such that the "final" models included only terms with a p-value less than 0.05. The final models for fat mass in the female cohort and triglycerides in the male cohort are described below. The final models for the remaining adjusted outcome variables for females and males may be found in Tables 59 to 66 in Appendix F.

a) Adjusted Fat Mass in SLVDS Females

ANOVA for each of the single loci versus mean adjusted fat mass in the female cohort revealed a significant association between the UCP3-5 variant and adjusted fat mass (p=0.008). Figure 30 shows that the UCP3-5 C allele corresponds to ~3.4 kg lower fat mass. Alone, the UCP3-5 variant explained ~2.8% of the variation in adjusted fat mass in the SLVDS females.

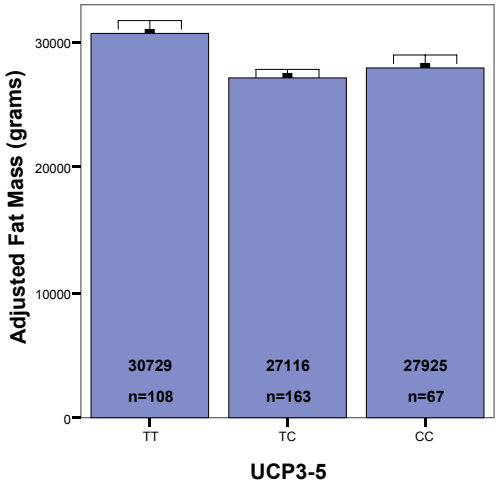

Figure 30: Adjusted Fat Mass vs. UCP3-5 in SLVDS Females

The final model for adjusted fat mass in females is shown in Table 19. This model includes three sets of interactions terms: UCP1-2 x FABP4p-376, UCP3-5 x FABP2p-834, and UCP3-5 x FABP3p-313. These terms combine to explain ~5.4% of the variation in adjusted fat mass. In the female cohort, homozygosity for both the UCP1-2 G allele and the FABP4p-376 A produces an average 2 kg decrease in mean fat mass (Figure 31). The effects of the FABP2p-834 variant on fat mass in UCP3-5 heterozygotes are shown in Figure 32. On UCP3-5 T/C background, there is a roughly dose dependent increase in adjusted fat mass with increasing presence of the FABP2p-834 T allele. Presence of one FABP2p-834 T allele results in an ~3 kg over FABP2p-834 C homozygotes (~26 kg), while FABP2p-834 T homozygosity leads to an additional

~2 kg increase. Adjusted fat mass for UCP3-5 T homozygotes is modified by FABP3p-313 genotype as shown in Figure 33. On the FABP3p-313 C/C background, UCP3-5 T homozygotes show an average 4.8 kg increase in fat mass over carriers of the C allele, slightly increasing the disparity between the TT homozygotes and carriers of the C allele (compare to Figure 30). In the presence of the FABP3p-313 T allele, UCP3-5 C homozygotes retain baseline levels (~2.8 kg) of adjusted fat mass.

Table 19: Females – Final Regression Model for Adjusted Fat Mass

	β	p-value	R^{2*}
Constant	29713	<0.001	0.054
UCP1-2 (GG) * FABP4p-376 (AA)	-2177	0.042	
UCP3-5 (TC) * FABP2p-834 (CC)	-2774	0.029	
UCP3-5 (TT) * FABP3p-313 (CC)	2701	0.043	

*p=0.001

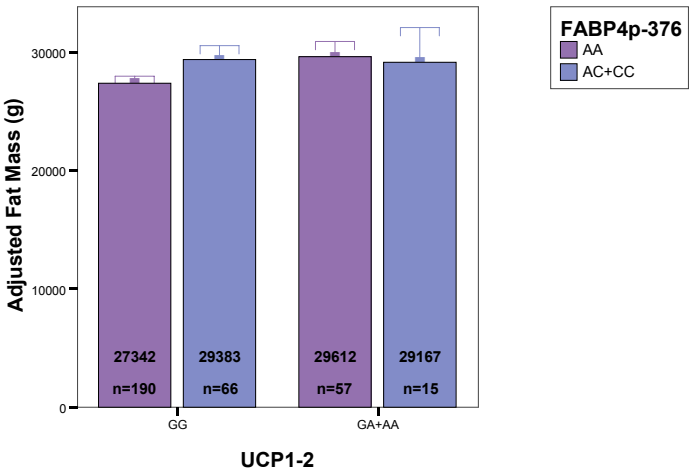

Figure 31: Adjusted Fat Mass vs. UCP1-2/FABP4p-376 Multi-Locus Genotypes in SLVDS Females

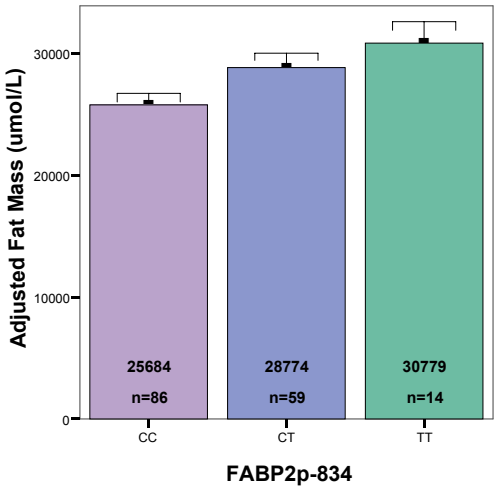

Figure 32: Adjusted Fat Mass vs. FABP2p-834 Genotypes on the UCP3-5 C/T Background in SLVDS Females

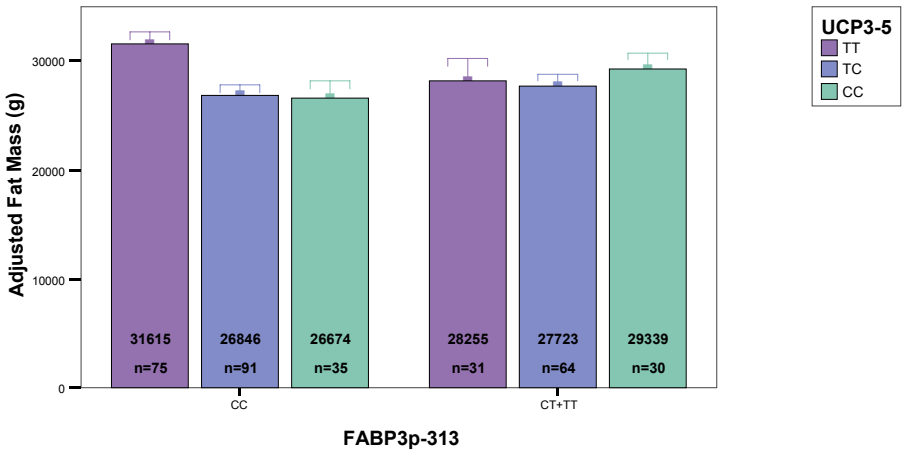

Figure 33: Adjusted Fat Mass vs. UCP3-5/FABP3p-313 Multi-Locus Genotypes in SLVDS Females

b) Adjusted Triglycerides in SLVDS Males

ANOVA was performed for adjusted triglycerides versus each of the single loci in the SLVDS males. A significant association was identified between adjusted triglycerides and the FABP3p-313 variant (p=0.029). The FABP3p-313 T allele contributes to ~22 mg/dl higher triglycerides (Figure 34). A similar, but non-significant, relationship was also observed between triglycerides and the FABP4-2b variant (p=0.297). Presence of the FABP4-2b D allele results in an ~14 mg/dl increase in triglyceride levels (Figure 35).

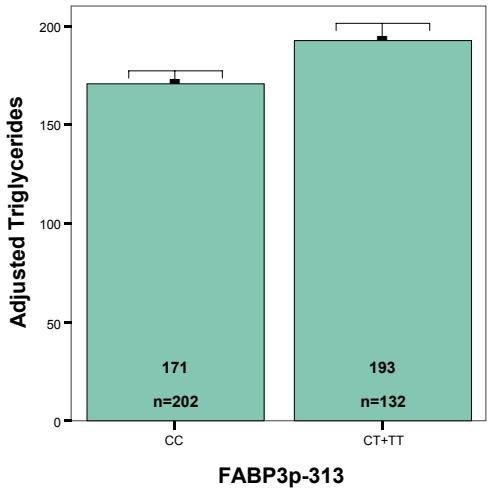

Figure 34: Adjusted Triglycerides vs. FABP3p-313 in SLVDS Males

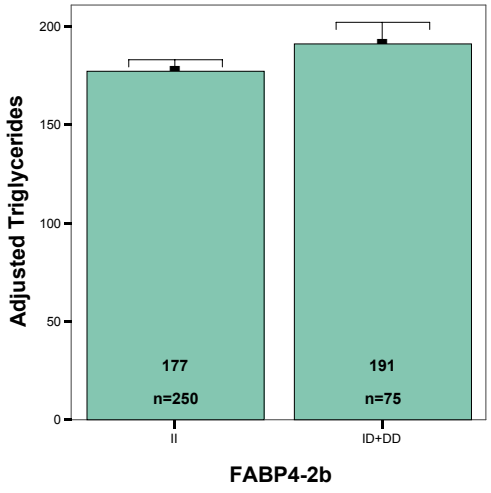

Figure 35: Adjusted Triglycerides vs. FABP4-2b in SLVDS Males

Table 20 shows the final model for adjusted ln(Triglycerides) in males. This model included FABP3p-313, FABP4-2b, and an interaction between those sites as significant predictors of fat mass (p=0.020), explaining ~3.1% of the variation in that trait. Mean adjusted triglycerides for individuals of each FABP4-2b/FABP3p-313 multi-locus genotype group are shown in Figure 36. On the FABP4-2b I/I backgroud, the FABP3p-313 genotype has no affect on adjusted triglyceride levels. However, the presence of the FABP4-2b D allele dramatically influences the effect of FABP3p-313 genotype on adjusted triglycerides. In carriers of the FABP4-2b D allele, the FABP3p-313 T allele is associated with an ~72 mg/dl increase in adjusted triglycerides, a 50 mg/dl increase in the disparity between the FABP3p-313 C homozygotes and carriers of the T allele (compare Figures 34 and 36).

Table 20: Males – Final Regression Model for Adjusted ln(Triglycerides)

	β	p-value	R^{2*}
Constant	5.281	<0.001	0.031
FABP4-2b (II)	-0.210	0.024	
FABP3p-313 (CC)	-0.311	0.005	
FABP4-2b (II) * FABP3p-313 (CC)	0.272	0.035	

*p=0.020

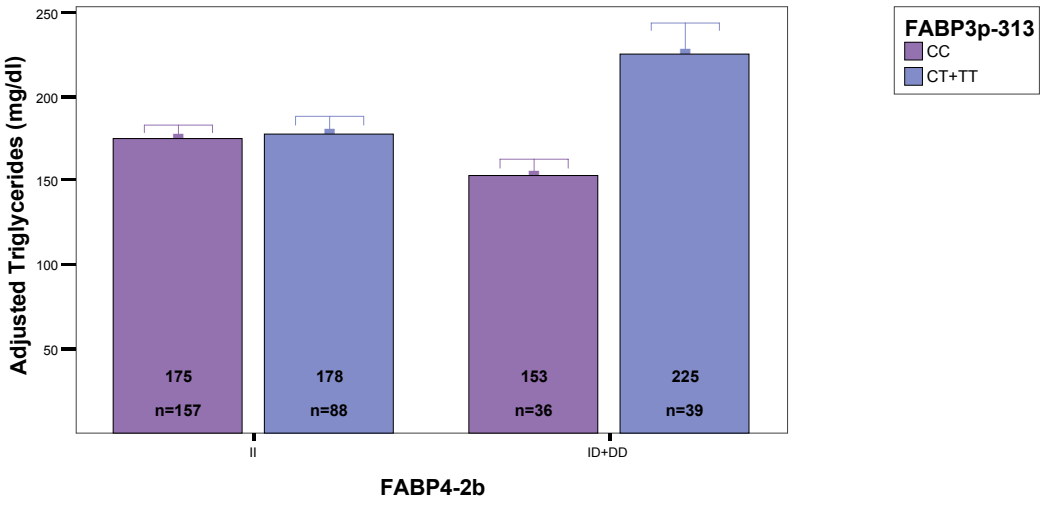

Figure 36: Adjusted Triglycerides vs. FABP4-2b/FABP3p-313 Multi-Locus Genotypes in SLVDS Males

6. Effects of "Muscle Genes" on Triglycerides and HOMA IR in Non-Hispanic Females

The single locus analyses revealed a number of interesting associations between the UCP3 variants and outcome variables in the non-Hispanic female cohort. HOMA IR and triglyceride levels were particularly interesting because they were influenced by UCP3 variants in a similar fashion. The UCP3p-55 variant was significantly associated with HOMA IR (p=0.010) and triglyceride levels (p=0.032). Presence of the UCP3p-55 T allele resulted in an ~5 unit increase in HOMA IR (Figure 37) and an ~22 mg/dl increase in triglycerides (Figure 38) compared to UCP3p-55 C homozygotes. The UCP3-5 polymorphism is also associated with HOMA IR (p=0.046) and triglycerides (p=0.027). Figure 39 shows that the presence of the UCP3-5 T allele corresponds to an ~3.5 unit increase in HOMA IR index. The effect of UCP3-5 genotype on triglyceride levels, shown in Figure 40, follows a dose dependent increase in triglycerides with increasing presence of the T allele. The triglcyeride levels in UCP3-5 T homozygotes were ~32 mg/dl higher than the C homozygotes.

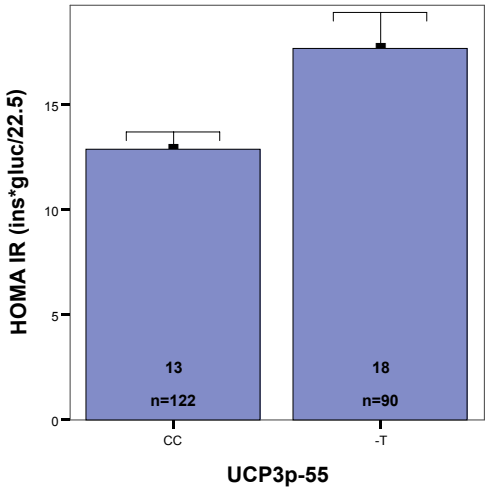

Figure 37: HOMA IR vs. UCP3p-55 in non-Hispanic Females

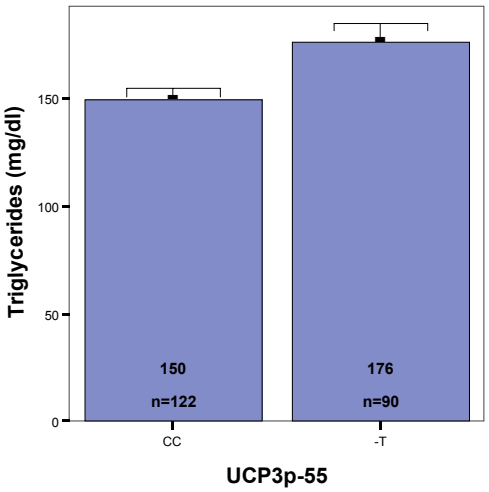

Figure 38: Triglycerides vs. UCP3p-55 in non-Hispanic Females

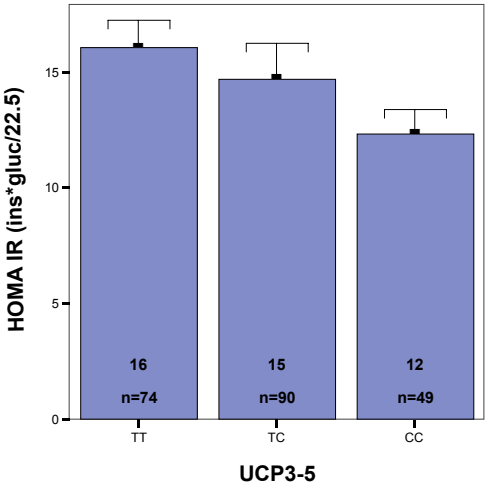

Figure 39: HOMA IR vs. UCP3-5 in non-Hispanic Females

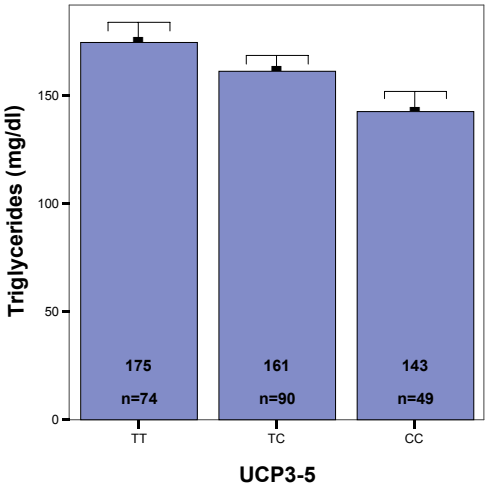

Figure 40: Triglycerides vs. UCP3-5 in non-Hispanic Females

Linear regression models were constructed for ln(HOMA IR) and ln(triglycerides) to explore multi-locus effects and interactions, including all genotyped UCP and FABP variants. The final model for ln(HOMA IR) is shown in Table 21. This model included interaction terms between the UCP3 variants and a polymorphism in the 5' region of FABP3, explaining approximately 5.6% of the variation in HOMA IR. Mean HOMA IR for individuals of each UCP3-5/UCP3p-55 multi-locus genotype group in non-Hispanic female individuals homozygous for the FABP3p-313 C allele are shown in Figure 41. In the presence of the UCP3p-55 T allele, the UCP3-5 T homozygotes show the highest average HOMA IR index (~19 units). Increasing presence of the UCP3-5 C allele results in a dose dependent reduction in HOMA IR index; however, the UCP3-5 C/C group, which has a HOMA IR index of ~6 units, only contains one individual. UCP3-5 genotype has no effect on HOMA IR in UCP3p-55 C homozygotes.

Table 21: Non-Hispanic Females – Final Regression Model for ln(HOMA IR)

	β	p-value	R^{2*}
Constant	2.470	<0.001	0.056
UCP3-5 (TT) * FABP3p-313 (CC)	0.257	0.007	
UCP3p-55 (CC)*FABP3p-313 (CC)	-0.169	0.042	

*p=0.003

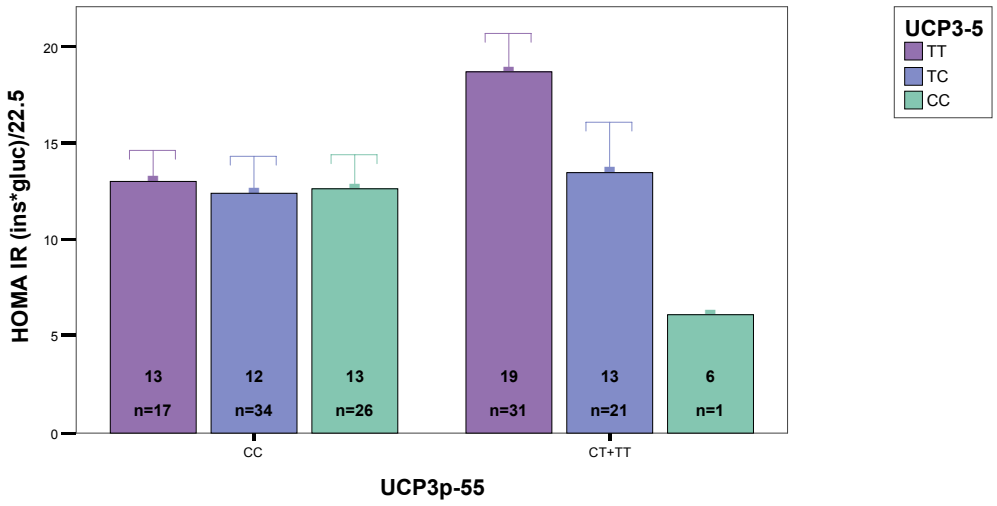

Figure 41: HOMA IR vs. UCP3-5/UCP3p-55 Multi-Locus Genotypes on the FABP3p-313 C/C Background in Non-Hispanic Females

The final model for ln(triglycerides), shown in Table 22, included a UCP2-4 main effect term and an interaction between UCP3p-55 and FABP3p-ID as significant predictors. This model explains ~7.1% of the variation in triglyceride levels in the non-Hispanic females. Figure 42 shows average triglyceride levels for non-Hispanic females homozygous for the FABP3p-313 C allele in each UCP3-5/UCP3p-55 multi-locus genotype group. In the presence of the UCP3p-55 T allele, the UCP2-4 T homozygotes show the highest average plasma triglycerides (~201 mg/dl). Increasing presence of the UCP2-4 C allele results in a dose dependent reduction in triglycerides. UCP2-4 genotype has no effect on triglyceride levels in UCP3p-55 C homozygotes.

Table 22: Non-Hispanic Females – Final Regression Model for ln(Triglycerides)

	β	p-value	R^{2*}
Constant	4.972	<0.001	0.071
UCP2-4 (CT)	0.238	<0.001	
UCP3p-55 (CC) * FABP3p-ID (DD)	-0.120	0.018	

*p=0.001

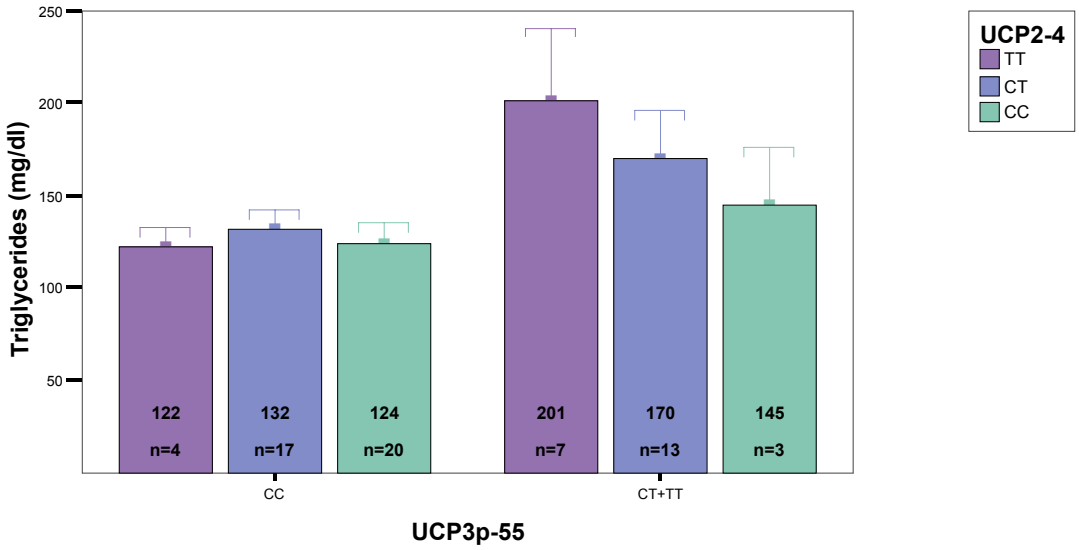

Figure 42: Triglycerides vs. UCP2-4/UCP3p-55 Multi-Locus Genotypes on the FABP3p-ID D/D Background in Non-Hispanic Females

7. Effects of the UCP2/UCP3 Region on Dietary Intake in SLVDS Females

Preliminary results from the adjusted analyses suggested that variation in UCP2 and UCP3 affects total caloric and fat intake in the female cohort. Thus, the relationship between the UCP2/UCP3 region and dietary intake was explored using linear regression. Table 23 shows the genotype counts and allele frequencies for each of the polymorphic sites. There was no statistically significant deviation from Hardy-Weinberg equilibrium for any of the three polymorphisms. For the analysis, individuals of UCP3p-55 genotypes C/T and T/T were pooled due to the small number of T/T individuals (There was no statistically significant difference in mean total caloric intake or fat intake between the UCP3p-55 C/T and T/T genotype groups.). Linkage disequilibrium (LD), measured as D', between the UCP2-4 variant and the UCP3-5 variant was 0.737, while D' between the UCP3-5 and UCP3p-55 variants was 0.814. The D' value for the UCP2-4 and UCP3p-55 variants was 0.338.

Table 23: Genotype Counts and Allele Frequencies

		Genotype Counts	T	C
UCP3-5	TT	125	0.565	0.435
	TC	176		
	CC	76		
UCP3p-55	CC	225	0.229	0.771
	CT	127		
	TT	22		
UCP2-4	CC	110	0.447	0.553
	CT	200		
	TT	70		

Table 24 shows the results of analysis of variance for each of the individual sites versus mean adjusted total caloric intake and adjusted fat intake. The UCP3-5 variant was significantly associated with both total caloric intake (p=0.030) and fat intake (p=0.024), with the C allele corresponding to increased intake. The UCP3p-55 polymorphism showed significant association with total caloric intake (p=0.025) and marginal correlation with fat intake (p=0.063), with the T allele corresponding to increased intake. The UCP2-4 variant was not associated with either outcome variable when considered alone.

Table 24: ANOVA of Single Loci Effects on Outcome w/Means

		Mean Adjusted Caloric Intake	p-value (R^2)	Mean Adjusted Fat Intake (grams)	p-value (R^2)
UCP3-5	**TT**	1559	**0.030** (0.020)	60	**0.024** (0.021)
	TC	1769		70	
	CC	1749		71	
UCP3p-55	**CC**	1640	**0.025** (0.014)	65	0.063 (0.010)
	CT+TT	1807		72	
UCP2-4	**CC**	1665	0.674 (0.002)	65	0.808 (0.001)
	CT	1728		68	
	TT	1660		68	

Linear regression models were constructed to explore multi-locus effects and interactions. The results of those analyses are shown in Table 25 to 28. Two models are shown for each outcome variable. Tables 25 and 27 show the final models using backward selection for total caloric intake and fat intake, respectively, which was set to remove all terms with a p-value greater than 0.05. Tables 26 and 28 show the models with the largest adjusted R-squared value for total caloric intake and fat intake, respectively, and are referred to as the "best fit" models. It should be noted, however, that these are only the best fitting models among those tested by the backward selection procedure, and cannot be considered globally optimal.

Table 25: Regression Model for Total Caloric Intake (Final Model)

	β	p-value	R^{2*}
Constant	1957	<0.001	0.053
UCP3-5 (TT)	-276	0.001	
UCP3p-55 (CC)	-271	0.001	

*p<0.001

Table 26: Regression Model for Total Caloric Intake ("Best Fit" Model)

	β	p-value	R^{2*}
Constant	2345	<0.001	0.079
UCP3-5 (TT)	-646	0.001	
UCP3p-55 (CC)	-666	0.001	
UCP2-4 (CC) * UCP3-5 (TC)	-605	0.003	
UCP2-4 (CT) * UCP3-5 (TC)	-422	0.022	
UCP3-5 (TT) * UCP3p-55 (CC)	344	0.136	
UCP3-5 (TC) * UCP3p-55 (CC)	460	0.023	

*p<0.001

Table 27: Regression Model for Fat Intake (Final Model)

	β	p-value	R^{2*}
Constant	111	<0.001	0.097
UCP3-5 (TT)	-45	<0.001	
UCP3p-55 (CC)	-42	<0.001	
UCP2-4 (CC) * UCP3-5 (TC)	-45	<0.001	
UCP2-4 (CT) * UCP3-5 (TC)	-35	<0.001	
UCP3-5 (TT) * UCP3p-55 (CC)	29	0.014	
UCP3-5 (TC) * UCP3p-55 (CC)	32	0.002	

*p<0.001

Table 28: Regression Model for Fat Intake ("Best Fit" Model)

	β	p-value	R^{2*}
Constant	111	<0.001	0.101
UCP3-5 (TT)	-49	<0.001	
UCP3p-55 (CC)	-42	<0.001	
UCP2-4 (CC) * UCP3-5 (TC)	-45	<0.001	
UCP2-4 (CT) * UCP3-5 (TC)	-35	<0.001	
UCP2-4 (CT) * UCP3-5 (TT)	8	0.224	
UCP3-5 (TT) * UCP3p-55 (CC)	29	0.014	
UCP3-5 (TC) * UCP3p-55 (CC)	32	0.002	

*p<0.001

The final model for total caloric intake (Table 25) included both UCP3-5 and UCP3p-55 as significant predictors (p<0.001), explaining approximately 5.3% of the variation in total caloric intake. The model shows that individuals homozygous for the T allele at UCP3-5 or the C allele at UCP3p-55 experience a reduction of approximately 270 calories in total intake compared to the baseline, while homozygosity for both alleles doubles that reduction. Figure 43 shows the average total caloric intake for SLVDS females in each UCP3-5/UCP3p-55 multi-locus genotype group.

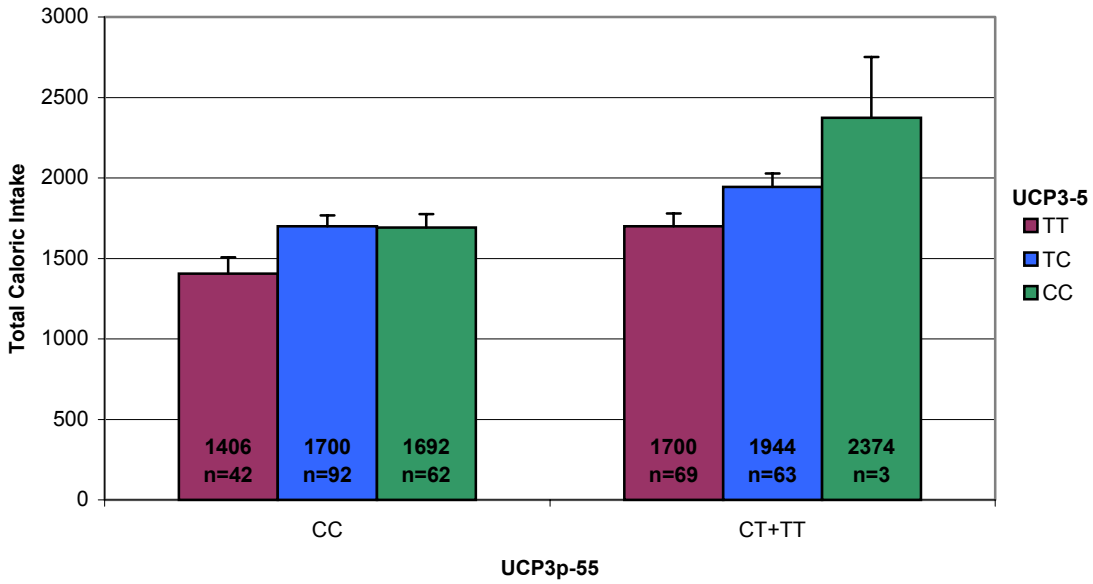

Figure 43: Total Caloric Intake as a Function of UCP3-5 and UCP3p-55 Genotype

Table 26 shows the model for total caloric intake with the largest adjusted R-square value. In this model, UCP3-5 and UCP3p-55 genotypes have similar effects on total caloric intake to those described in the final model above; however, interactions between the UCP2-4 and UCP3-5 sites modify those effects. In particular, the C allele of UCP2-4 seems to reduce total caloric intake in a dose dependent manner when on the UCP3-5 heterozygote background. In addition, heterozygosity at UCP3-5 modifies the effect of the C homozygosity at UCP3p-55 by slightly increasing total caloric intake. This model explains approximately 7.9% of the variation in total caloric intake and includes the effect of the UCP2-4 polymorphism ($p<0.001$). Figure 44 shows the actual average caloric intake for each multi-locus genotype group, including all three of the polymorphic sites.

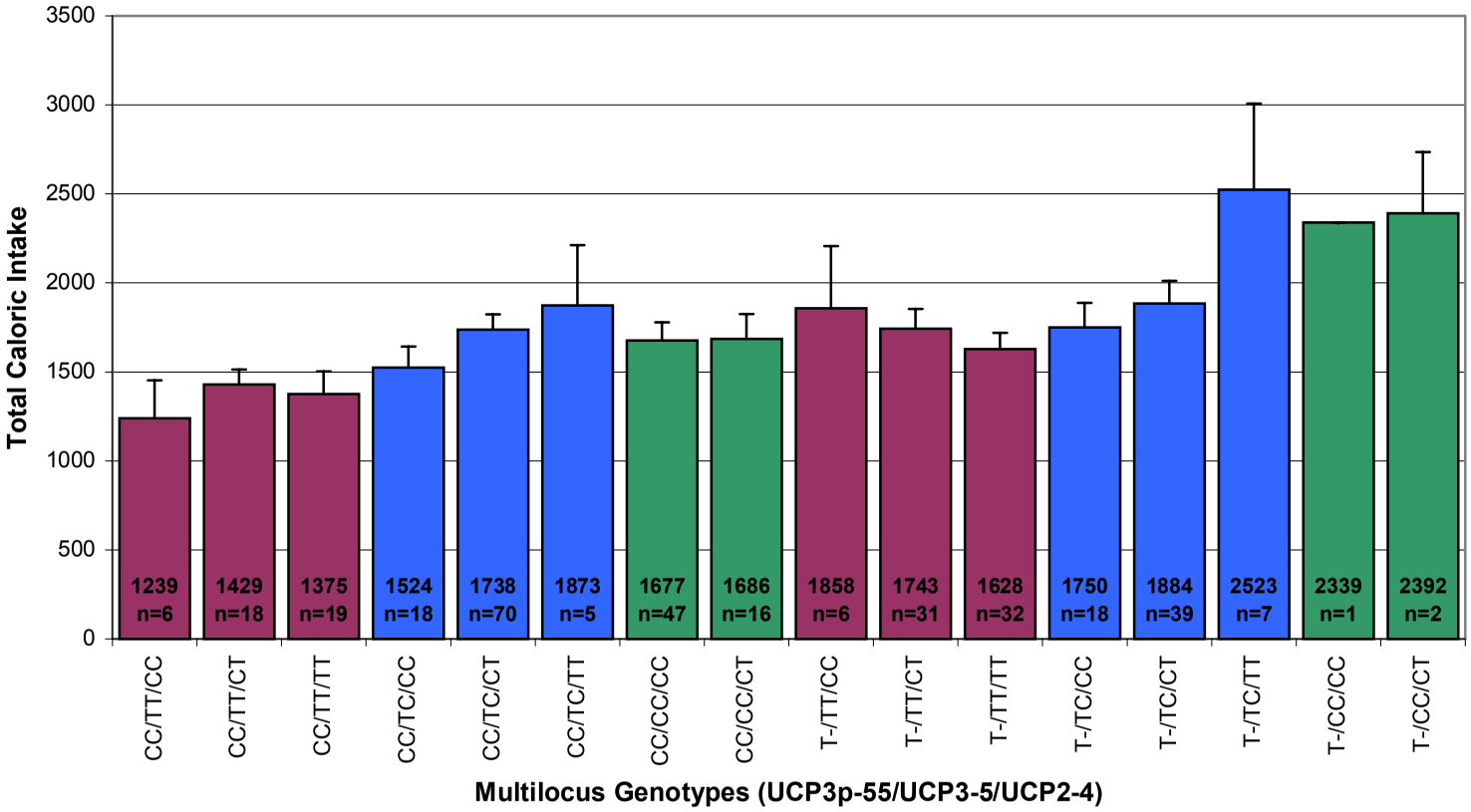

Figure 44: Total Caloric Intake vs. UCP3p-55/UCP3-5/UCP2-4 Multi-Locus Genotypes

The final model for fat intake is shown in Table 27. This model includes the same terms seen in the “best fit” model for total caloric intake (see Table 26). The major genotypic effect on fat intake seems to result from UCP3-5 and UCP3p-55, similar to total caloric intake. The presence of the UCP3-5 T/T genotype or the UCP3p-55 C/C genotype results in an ~43 gram reduction in fat intake, while the presence of both genotypes doubles that reduction. Figure 45 shows average fat intake for multi-locus genotype groups involving the two UCP3 sites in the SLVDS females. The regression model shows that interaction between UCP2-4 and UCP3-5 results in modification of the effect of the UCP3-5 T/C genotype on fat intake, while UCP3-5 heterozygosity modifies the effect of the C/C genotype at UCP3p-55. This model accounts for approximately 9.7% of the variation in ingested fat ($p<0.001$). The fat intake means for the three-locus genotype groups in the SLVDS females are shown in Figure 46.

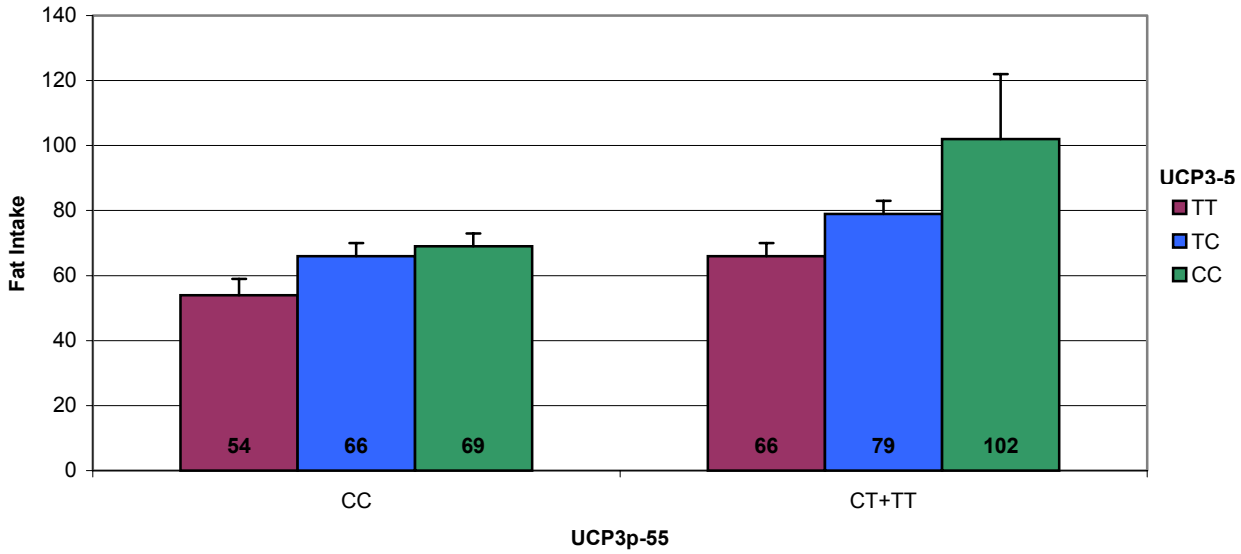

Figure 45: Fat Intake as a Function of UCP3-5 and UCP3p-55 Genotype

Table 28 shows the "best fit" model for fat intake. This model is identical to the final model for fat intake (see Table 27) with the addition of another interaction term, which defines a small effect of UCP2-4 heterozygosity on the T/T genotype at UCP3-5. This model explains 10.1% of the variation in fat intake ($p<0.001$), a slight increase over the final model.

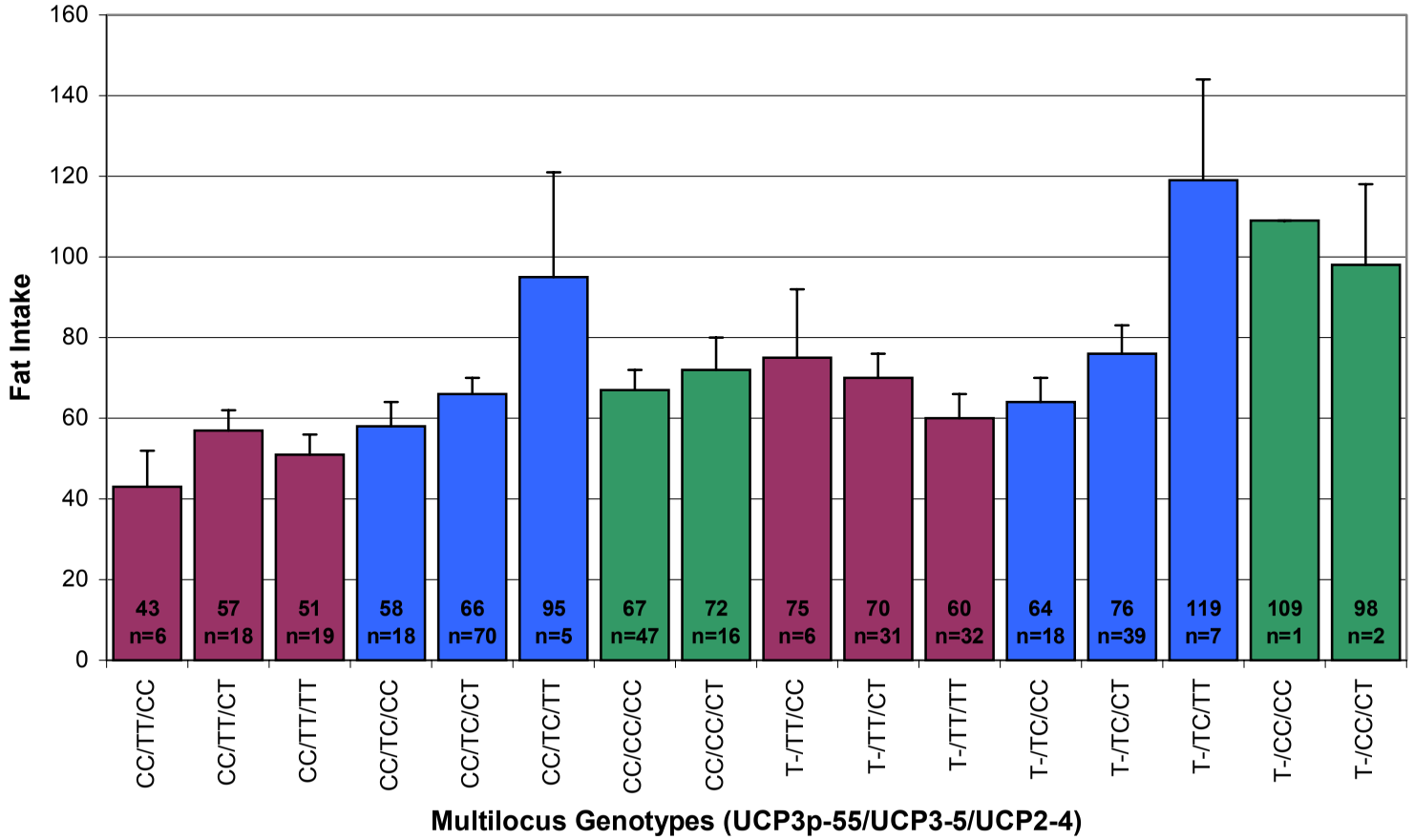

Figure 46: Fat Intake vs. UCP3p-55/UCP3-5/UCP2-4 Multi-Locus Genotypes

8. Tissue-Specific Regression Modeling

A third analysis approach was created to explore correlations between outcome variables and interactions among the genes expressed in specific tissue types. Three tissues were considered in this analysis plan: skeletal muscle, adipose tissue, and the small intestine. The skeletal muscle models considered polymorphisms in UCP3, FABP3, and PPARα. Polymorphisms in UCP1, UCP2, FABP4, and PPARγ were included in the adipose tissue models. The intestine models included variation in UCP2, FABP2, and PPARβ. The outcome variables considered in these analyses were fat mass, lean mass, cholesterol, triglycerides, free fatty acids (FFA), and HOMA IR. Each outcome variable was adjusted for age, smoking status, physical activity, and skin reflectance. The cohort was split by sex. Identification and genotyping of the PPAR polymorphisms was performed by Susan Moffett and reported in her dissertation (Moffett, 2002). Linear regression models were constructed for each adjusted outcome variable to explore the possible interactions among loci specific to each tissue type. This approach to regression modeling differs from the earlier approaches in that the initial models were constructed with polymorphisms and all possible interactions from genes expressed in each tissue. To find the most parsimonious models, backward and stepwise selection methods were used with exclusion and inclusion criteria set such that the "final" models included only terms with a p-value less than 0.05. In the case that the final models for the backward and stepwise methods did not agree, the model with the higher adjusted R^2 was chosen. The final models for each tissue were combined in a second round of linear regression modeling to determine the contribution of variation in genes of each tissue type to the outcome variables. The final models for adjusted FFA,

triglycerides, and cholesterol in each tissue type and in the combined models for both the male and female cohorts are described below. The final models for adjusted fat mass and lean mass may be found in Tables 67 to 70 in Appendix G.

a) Adjusted Free Fatty Acids in Males

The final models for each tissue-specific analysis of adjusted FFA in males are shown in Table 29. In skeletal muscle, there were no significant predictors of adjusted FFA. The adipose tissue model involved interaction among all of the UCP genes expressed in that tissue with a contribution from FABP4 to explain ~7.4% of the variation in adjusted FFA. All three gene families contributed to the intestine model, explaining ~6.5% of the variation in adjusted FFA. The overall combined model for adjusted FFA in males was identical to the adipose model.

Table 29: Regression Model Summaries of Tissue-Specific Analyses for Adjusted Free Fatty Acids in Males

Tissue	Genotype Terms	p-value	R^2
Muscle	No Model		
Adipose	UCP1-2 UCP2-4 UCP2-8 UCP1-2*UCP2-8 UCP2-4*FABP4-2b UCP2-8*FABP4-2b	0.003	0.074
Intestine	UCP2-4 FABP2p-834 PPARb6*FABP2p-834 UCP2-4*UCP2-8 UCP2-8*FABP2p-834 UCP2-8*FABP2p-ID	0.006	0.065
Combined Model	UCP1-2 UCP2-4 UCP2-8 UCP1-2*UCP2-8 UCP2-4*FABP4-2b UCP2-8*FABP4-2b	0.003	0.074

The combined regression model for the tissue-specific analyses of adjusted FFA in males is shown in Table 30. This model accounts for ~7.4% of the variation in adjusted FFA in males and is composed only of the genes expressed in the adipose tissue. Mean adjusted FFA for individuals of each UCP2-8/FABP4-2b multi-locus genotype group in the male cohort are shown in Figure 47. On the FABP4-2b I/I background, the UCP2-8 D homozygote is associated with an ~40 µmol/L reduction in adjusted FFA compared to the UCP2-8 I homozygote. For a closer look at the UCP2-8 D/D genotype, Figure 48 shows the effects of the FABP4-2b/UCP1-2 multi-locus genotype on adjusted FFA in individuals homozygous for the UCP2-8 D allele. Presence of either of the less common alleles (FABP4-2b D allele or UCP1-2 A allele)

increases adjusted FFA by ~75 µmol/L over the II/GG individuals, while presence of both of the less common alleles results in an ~158 µmol/L increase in adjusted FFA over the II/GG individuals. The bar chart suggests that the increase in adjusted FFA is dose dependent; however, the ID+DD/GA+AA group only contains three individuals. The effects of the UCP2-4/FABP4-2b multi-locus genotypes on FFA are shown in Figure 49. On the FABP4-2b I/I background, UCP2-4 heterozygotes show an ~40 µmol/L increase in adjusted FFA over the homozygous groups.

Table 30: Final Regression Model for Combined Tissue Analyses of Adjusted Free Fatty Acids in Males

	β	p-value	R^{2*}
Constant	456	<0.001	
UCP1-2 (GG)	102	0.014	
UCP2-4 (CC)	-145	0.020	
UCP2-8 (DD)	279	0.001	
UCP1-2 (GG) * UCP2-8 (DD)	-189	0.010	0.074
UCP2-4 (CC) * FABP4-2b (II)	207	0.011	
UCP2-4 (CT) * FABP4-2b (II)	99	0.017	
UCP2-8 (DD) * FABP4-2b (II)	-229	0.001	
UCP2-8 (DI) * FABP4-2b (II)	-94	0.035	

*p=0.004

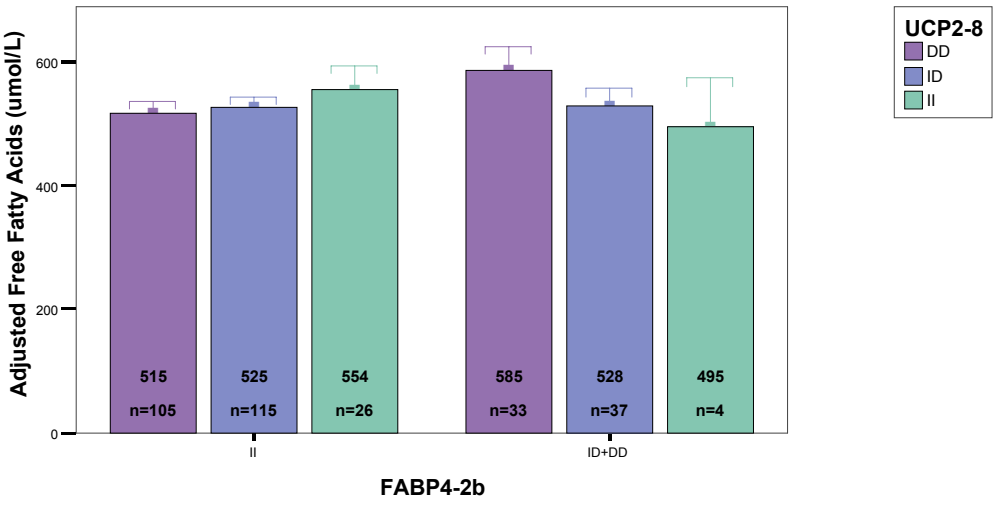

Figure 47: Adjusted Free Fatty Acids vs. UCP2-8/FABP4-2b Multi-Locus Genotypes in Males

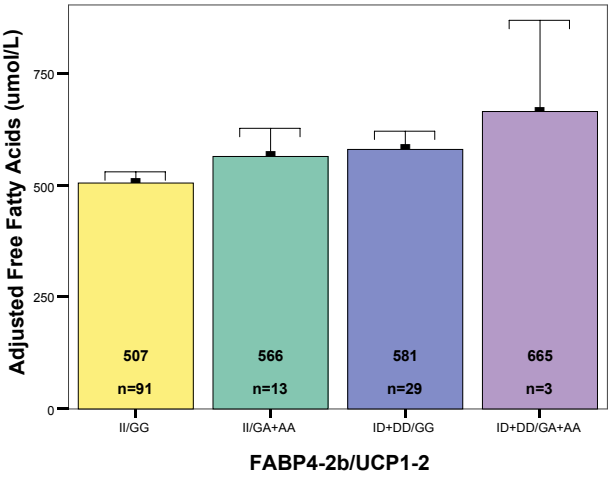

Figure 48: Adjusted Free Fatty Acids vs. FABP4-2b/UCP1-2 Multi-Locus Genotypes on the UCP2-8 D/D Background in Males

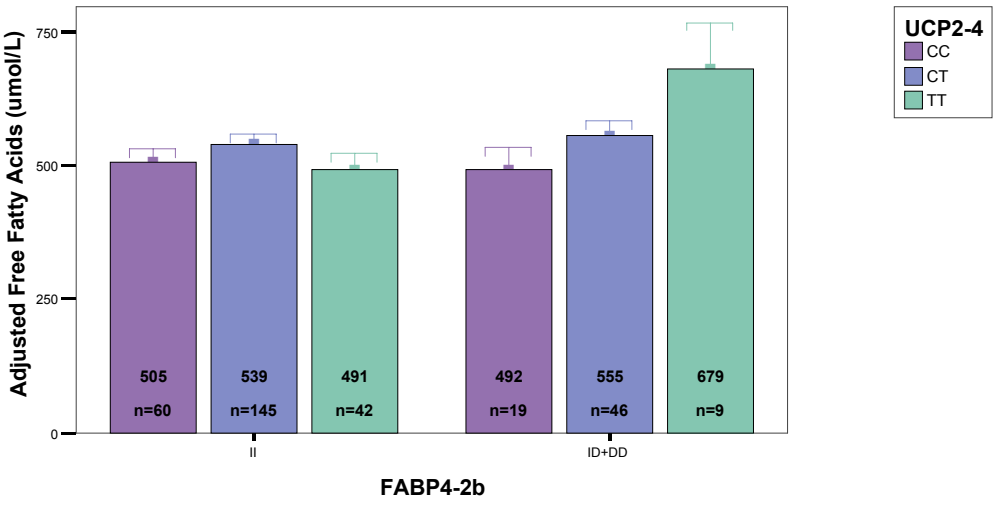

Figure 49: Adjusted Free Fatty Acids vs. UCP2-4/FABP4-2b Multi-Locus Genotypes in Males

b) Adjusted Triglycerides in Males

The results of tissue-specific analyses for adjusted ln(triglycerides) in males are shown in Table 31. The skeletal muscle model explains ~3.3% of the variation in adjusted triglycerides in males using terms from UCP3 and FABP3. The adipose tissue model is complex, including several interaction terms between the UCP2 and FABP4 variants and explaining ~6.5% of the variation in adjusted triglycerides. The intestine model includes an interaction between UCP2 and FABP2, which explains ~2.0% of the variation in adjusted triglycerides. The combined model is a mixture of the adipose tissue and intestine models.

Table 31: Regression Model Summaries of Tissue-Specific Analyses for Adjusted ln(Triglycerides) in Males

Tissue	Genotype Terms	p-value	R^2
Muscle	FABP3p-313 UCP3-5*UCP3p-55	0.005	0.033
Adipose	FABP4-2b UCP2-4*FABP4-2b UCP2-4*FABP4p-376 UCP2-8*FABP4-2b UCP2-8*FABP4p-376	0.005	0.065
Intestine	UCP2-4*FABP2p-ID	0.012	0.020
Combined Model	UCP2-4 FABP4-2b UCP2-4*FABP2p-ID UCP2-4*FABP4-2b UCP2-4*FABP4p-376 UCP2-8*FABP4-2b UCP2-8*FABP4p-376	0.003	0.075

The final regression model for the combined tissue analyses of adjusted ln(triglycerides) in males is shown in Table 32. This model accounts for ~7.5% of the variation in adjusted triglycerides in males. The contribution from the intestine genes to the combined adjusted triglyceride model in the SLVDS males is shown in Figure 50. This graph shows an average 38 mg/dl increase in adjusted triglycerides for individuals with the FABP2p-ID I/I genotype and the UCP2-4 C/T genotype over all other genotype combinations.

Table 32: Final Regression Model for Combined Tissue Analyses of Adjusted Triglycerides in Males

	β	p-value	R^{2*}
Constant	5.342	<0.001	0.075
UCP2-4 (CT)	-0.412	0.002	
FABP4-2b (II)	-0.408	0.002	
UCP2-4 (CC)*FABP4-2b (II)	0.473	0.003	
UCP2-4 (CT)*FABP4-2b (II)	0.524	0.001	
UCP2-4 (CC)*FABP4p-376 (AA)	-0.389	0.006	
UCP2-8 (DD)*FABP4-2b (II)	-0.256	0.013	
UCP2-8 (DD)*FABP4p-376 (AA)	0.233	0.017	
UCP2-4 (CT)*FABP2p-ID (II)	0.151	0.040	

*p=0.003

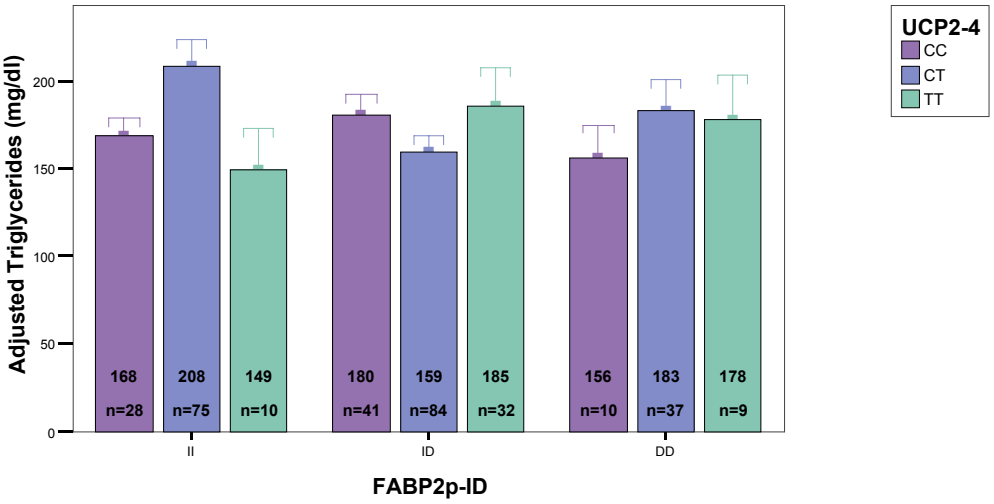

Figure 50: Adjusted Triglycerides vs. UCP2-4/FABP2p-ID Multi-Locus Genotypes in Males

The effects of the adipose-specific genes found in the combined model on mean adjusted triglycerides in the male cohort are shown in Figures 51-54. On the FABP4-2b I/I background, UCP2-4 heterozygotes show an ~23 mg/dl increase in adjusted triglycerides over the homozygous groups (Figure 51). A closer look at the UCP2-4 C/C homozygotes, in Figure 52, reveals an interactive effect on adjusted triglycerides between genotype at FABP4-2b and FABP4p-376. Increasing presence of the rare alleles for either of the sites appears to produce a dose dependent elevation in adjusted triglycerides. Specifically, presence of the FABP4-2b D allele or the FABP4p-376 C allele results in a 20-30 mg/dl increase in adjusted triglycerides over the II/AA genotype group, while presence of both of those alleles corresponds to an ~45 mg/dl increase over the II/AA individuals.

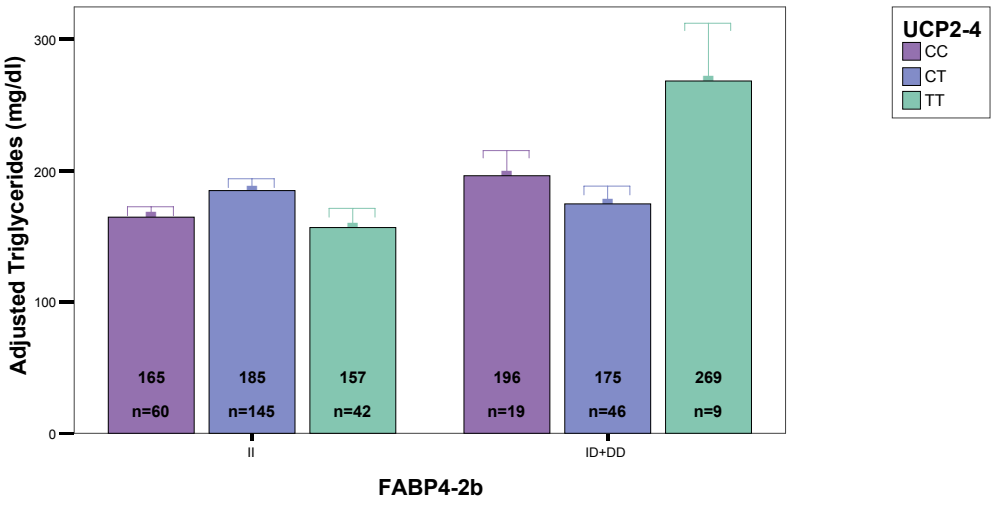

Figure 51: Adjusted Triglycerides vs. UCP2-4/FABP4-2b Multi-Locus Genotypes in Males

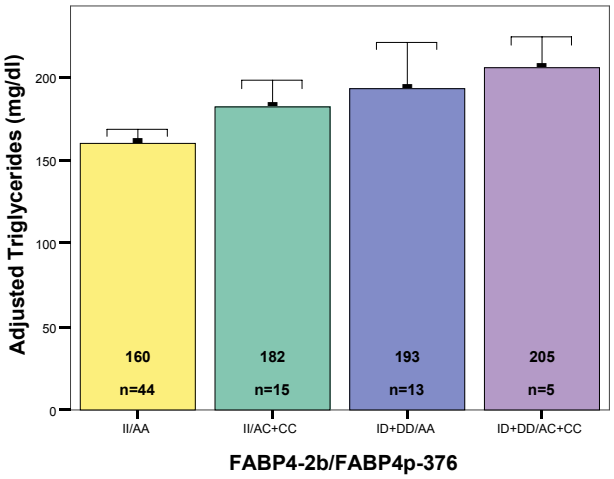

Figure 52: Adjusted Triglycerides vs. FABP4-2b/FABP4p-376 Multi-Locus Genotypes on the UCP2-4 C/C Background in Males

The effects of interactions between UCP2-8, FABP4-2b, and FABP4p-376 on mean adjusted triglycerides in the SLVDS males are shown in Figures 53 and 54. On the FABP4p-376 A/A background, there is a dose dependent decrease in adjusted triglycerides with increasing presence of the UCP2-8 I allele (Figure 53). Within the UCP2-8 D homozygote group, shown in Figure 54, the FABP4-2b genotype shows a dramatic effect on adjusted triglycerides. Presence of the FABP4-2b D allele results in an average 58 mg/dl increase in adjusted triglycerides in comparison to I homozygotes.

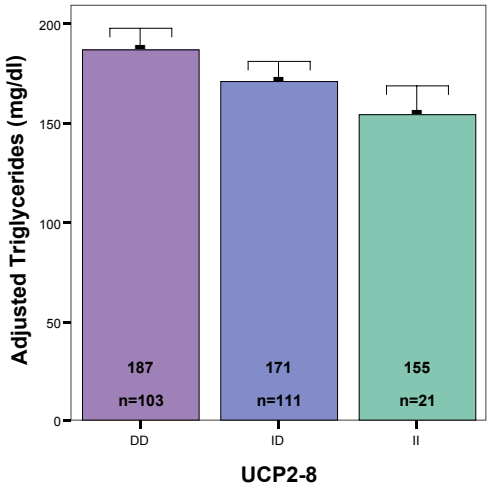

Figure 53: Adjusted Triglycerides vs. UCP2-8 Genotypes on the FABP4p-376 A/A Background in Males

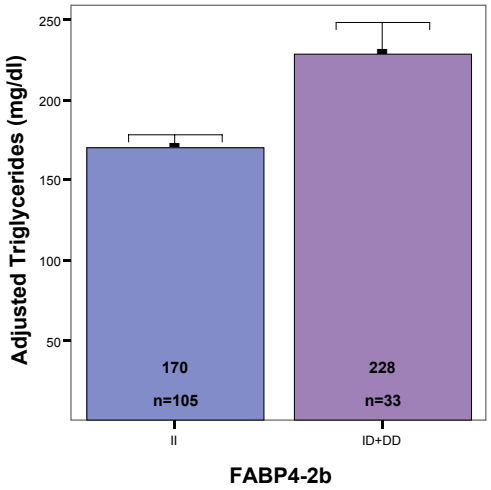

Figure 54: Adjusted Triglycerides vs. FABP4-2b/FABP4p-376 Multi-Locus Genotypes on the UCP2-8 D/D Background in Males

c) Adjusted Cholesterol in Males

The summary of the tissue-specific analyses for adjusted cholesterol in males is shown in Table 33. The skeletal muscle and adipose tissue models were only able to explain ~1.5% of the variation in adjusted cholesterol, while no model was defined for the intestine.

Table 33: Regression Model Summaries of Tissue-Specific Analyses for Adjusted Cholesterol in Males

Tissue	Genotype Terms	p-value	R^2
Muscle	FABP3p-313	0.025	0.015
Adipose	UCP2-8*FABP4p-376	0.031	0.014
Intestine	No Model		
Combined Model	UCP2-8*FABP4p-376	0.034	0.014

d) Adjusted Free Fatty Acids in Females

The results of the tissue-specific analyses for adjusted FFA in females are summarized in Table 34. The skeletal muscle model consists of an interaction between PPARa5 and UCP3-5 and explains ~1.8% of the variation in adjusted FFA. The adipose tissue model contains a complex mixture of terms from UCP1, UCP2, FABP4, and PPARγ that explain ~5.8% of the variation in adjusted FFA. Interactions among the polymorphisms in UCP2 and FABP2 make up the intestine model, which explains ~9.0% of the variation in adjusted FFA. The combined model includes genotype terms from each of the three tissue types.

Table 34: Regression Model Summaries of Tissue-Specific Analyses for Adjusted Free Fatty Acids in Females

Tissue	Genotype Terms	p-value	R^2
Muscle	PPARa5*UCP3-5	0.010	0.018
Adipose	UCP1-2 FABP4-2b PPARg2*UCP2-8 PPARg6*UCP1-2 UCP1-2*UCP2-8 UCP2-4*FABP4-2b	0.008	0.058
Intestine	FABP2p-ID FABP2p-834 UCP2-4*FABP2p-ID UCP2-4*FABP2p-834 UCP2-8*FABP2p-ID UCP2-8*FABP2p-834	0.001	0.090
Combined Model	UCP1-2 FABP2p-ID PPARa5*UCP3-5 UCP1-2*UCP2-8 UCP2-4*FABP2p-ID UCP2-4*FABP2p-834 UCP2-8*FABP2p-ID UCP2-8*FABP2p-834	<0.001	0.113

The combined regression model for the tissue-specific analysis of adjusted FFA is shown in Table 35. This model accounts for ~11.3% of the variation in adjusted FFA. The effects of the skeletal muscle-specific genes on adjusted FFA in the SLVDS females are shown in Figure 55. In individuals with the PPARa5 C/C genotype, UCP3-5 heterozygotes have an ~60 µmol/L reduction in adjusted FFA in comparison to both of the homozygous groups.

Table 35: Final Regression Model for Combined Tissue Analyses of Adjusted Free Fatty Acids in Females

	β	p-value	R^{2*}
Constant	729	<0.001	0.113
PPARa5 (CC) * UCP3-5 (TC)	-89	0.001	
UCP1-2 (GG)	-90	0.010	
UCP1-2 (GG) * UCP2-8 (DD)	114	0.002	
FABP2p-ID (ID)	-99	0.010	
UCP2-4 (CC) * FABP2p-ID (ID)	160	0.004	
UCP2-4 (CC)*FABP2p-834 (CT)	-160	0.002	
UCP2-8 (DI) * FABP2p-ID (II)	161	0.013	
UCP2-8 (DI) * FABP2p-ID (ID)	221	<0.001	
UCP2-8 (DI)*FABP2p-834 (CC)	-147	0.006	

*p<0.001

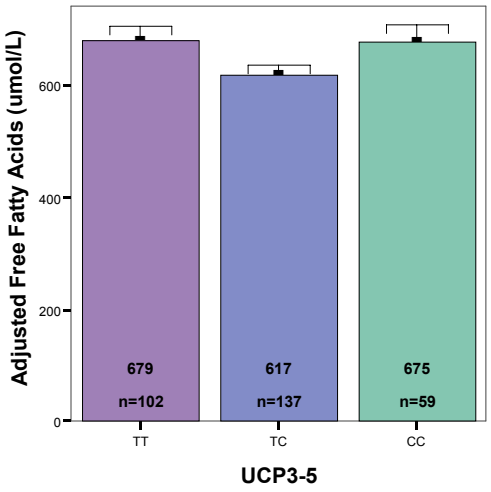

Figure 55: Adjusted Free Fatty Acids vs. UCP3-5 Genotypes on the PPARa5 C/C Background in Females

The adipose-specific contribution to mean adjusted FFA in the SLVDS females is shown in Figure 56. On the UCP1-2 GG background, presence of the UCP2-8 D allele corresponds to an average 103 µmol/L increase in adjusted FFA over the UCP2-8 I homozygous group.

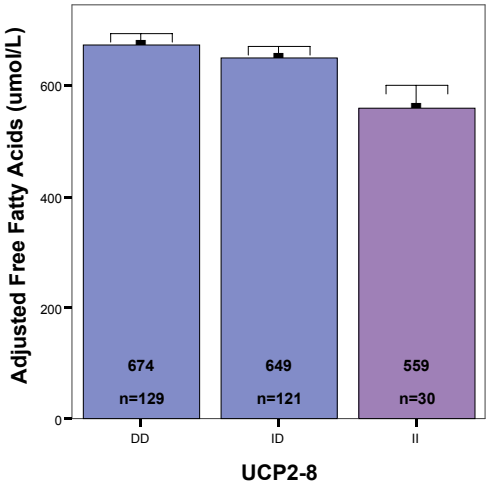

Figure 56: Adjusted Free Fatty Acids vs. UCP2-8 Genotypes on the UCP1-2 G/G Background in Females

Figures 57 and 58 show a portion of the effects of the intestine-specific gene variants on adjusted FFA in the female cohort. On the UCP2-4 C/C background, presence of the FABP2p-834 T allele results in an average 106 µmol/L reduction in adjusted FFA in comparison to the C homozygotes (Figure 57). In UCP2-8 heterozygotes, shown in Figure 58, the FABP2p-834 T allele corresponds to an average

88 µmol/L increase in adjusted FFA in comparison to the C/C group. Genotype at FABP2p-ID also interacts with both UCP2-4 and UCP2-8 to influence adjusted FFA levels in the SLVDS females.

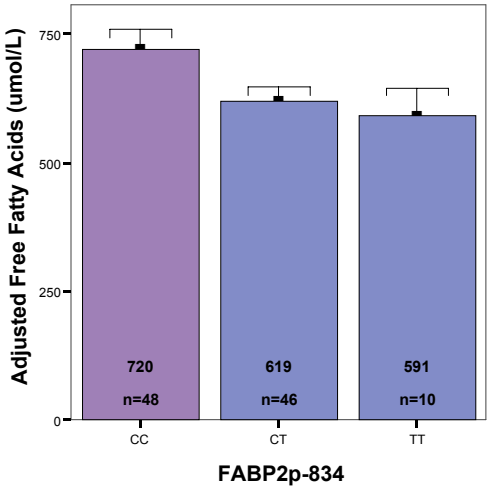

Figure 57: Adjusted Free Fatty Acids vs. FABP2p-834 Genotypes on the UCP2-4 C/C Background in Females

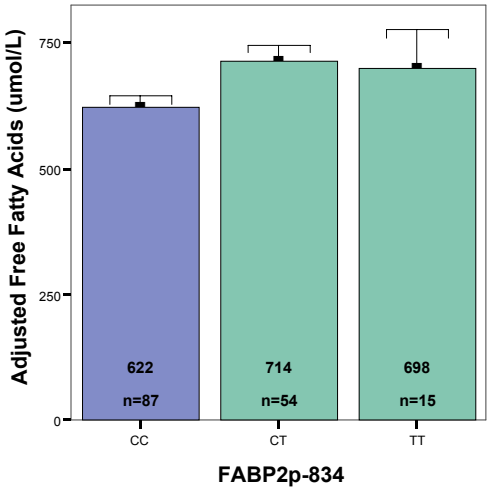

Figure 58: Adjusted Free Fatty Acids vs. FABP2p-834 Genotypes on the UCP2-8 D/I Background in Females

e) Adjusted Triglycerides in Females

The final models for each of the tissue-specific analyses of adjusted ln(triglycerides) in females are shown in Table 36. In skeletal muscle, there were no significant terms remaining to define a regression model for adjusted triglycerides. The adipose tissue model is complex, including several interaction terms between UCP1, UCP2, and PPARg2 variants and explaining ~8.0% of the variation in adjusted triglycerides. The intestine model includes a main effect term from UCP2-4, which accounts for ~2.0% of the variation in adjusted triglycerides. The combined model for adjusted triglycerides in females was identical to the adipose model.

Table 36: Regression Model Summaries of Tissue-Specific Analyses for Adjusted Triglycerides in Females

Tissue	Genotype Terms	p-value	R^2
Muscle	No Model		
Adipose	UCP2-4 PPARg2*UCP2-4 PPARg2*UCP2-8 UCP1-2*UCP2-4 UCP1-2*UCP2-8	<0.001	0.080
Intestine	UCP2-4	0.007	0.020
Combined Model	UCP2-4 PPARg2*UCP2-4 PPARg2*UCP2-8 UCP1-2*UCP2-4 UCP1-2*UCP2-8	<0.001	0.080

The combined regression model for the tissue-specific analyses of adjusted triglycerides in females is shown in Table 37. This model accounts for ~8.0% of the variation in adjusted triglycerides and is composed only of the genes expressed in the adipose tissue. Figure 59 shows the average triglyceride levels for SLVDS females in each UCP2-8/PPARg2 multi-locus genotype group. Presence of the PPARg2 G allele lowers adjusted triglycerides by ~10 mg/dl. Increasing presence of the UCP2-8 I allele results in an ~10 mg/dl decrease in adjusted triglycerides. The additive relationship between the PPARg2 and UCP2-8 variants results in an ~30 mg/dl difference in adjusted triglycerides between the CC/DD individuals (185 mg/dl) and the CG+GG/II (157 mg/dl). This relationship is influenced further by UCP2-4 genotype. Figure 60 shows the effects of the UCP2-8/UCP2-4 multi-locus genotypes on the PPARg2 C/C background.

Table 37: Final Regression Model for Combined Tissue Analyses of Adjusted Triglycerides in Females

	β	p-value	R^{2*}
Constant	4.987	<0.001	0.080
UCP2-4 (CT)	0.233	0.009	
PPARg2 (CC) * UCP2-4 (CT)	-0.209	0.022	
PPARg2 (CC) * UCP2-8 (DI)	0.268	0.002	
UCP1-2 (GG) * UCP2-4 (CC)	-0.188	0.035	
UCP1-2 (GG) * UCP2-8 (DD)	0.222	0.003	
UCP1-2 (GG) * UCP2-8 (DI)	-0.225	0.004	

*p<0.001

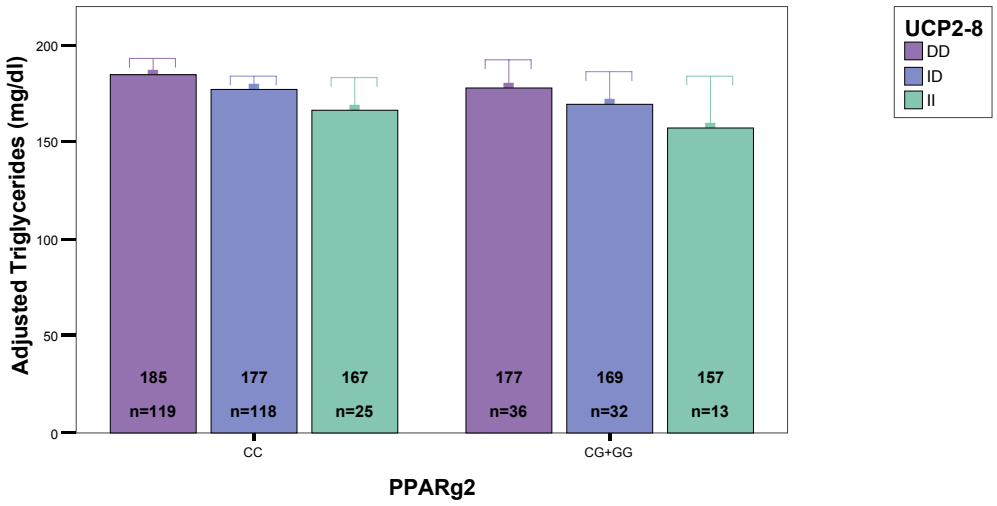

Figure 59: Adjusted Triglycerides vs. UCP2-8/PPARg2 Multi-Locus Genotypes in Females

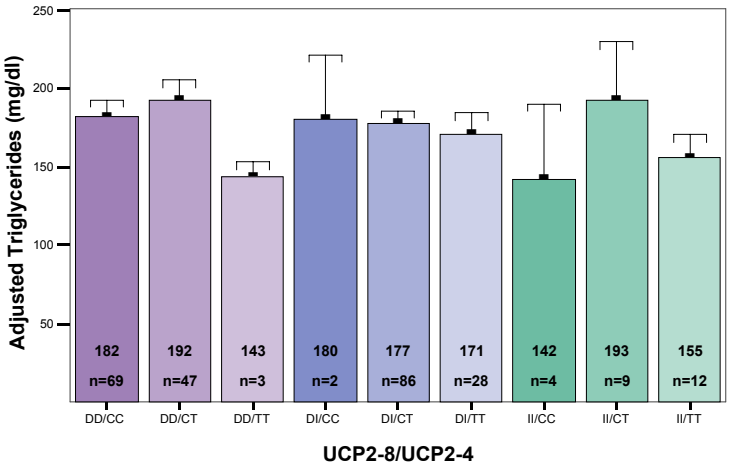

Figure 60: Adjusted Triglycerides vs. UCP2-8/UCP2-4 Multi-Locus Genotypes on the PPARg2 C/C Background in Females

The effects of UCP1-2 genotype on adjusted triglycerides in the female cohort are shown in Figure 61. UCP1-2 G homozygotes show an average 18 mg/dl reduction in adjusted triglycerides in comparison to individuals carrying at least one UCP1-2 A allele. Adjusted triglcyeride levels for UCP1-2 G homozygotes are further modified by genotype at UCP2-4 and UCP2-8 in a similar fashion to PPARg2 C homozygotes (see Figure 60).

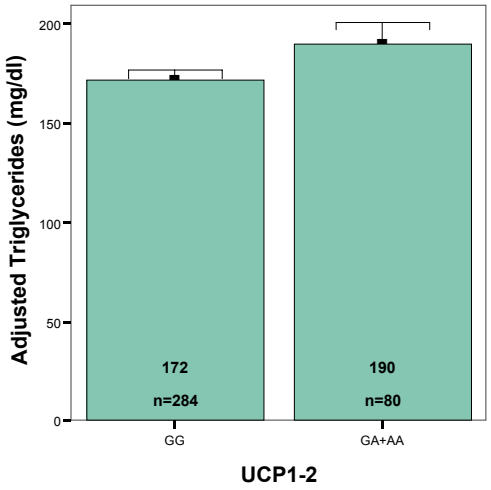

Figure 61: Adjusted Triglycerides vs. UCP1-2 in Females

f) Adjusted Cholesterol in Females

The results of tissue-specific analyses for adjusted cholesterol in females are shown in Table 38. The skeletal muscle model involves interactions between variants in each of the three gene families and accounts for ~3.6% of the variation in adjusted cholesterol. There were no terms remaining to define a regression model for adjusted cholesterol in adipose tissue. For the intestine-specific model, interactions among the UCP2 variants and a variant in FABP2 explain ~3.0% of the variation in adjusted cholesterol. The combined model for adjusted cholesterol is composed of terms from both the muscle-specific and intestine-specific models.

Table 38: Regression Model Summaries of Tissue-Specific Analyses for Adjusted Cholesterol in Females

Tissue	Genotype Terms	p-value	R^2
Muscle	FABP3p-313 PPARa5*UCP3-5 FABP3p-ID*FABP3p-313	0.006	0.036
Adipose	No Model		
Intestine	UCP2-8 UCP2-4*UCP2-8 UCP2-4*FABP2p-834	0.039	0.030
Combined Model	UCP2-8 FABP3p-313 UCP2-4*UCP2-8 UCP2-4*FABP2p-834 FABP3p-ID*FABP3p-313	0.002	0.061

The combined regression model for the tissue-specific analyses of adjusted cholesterol in females is summarized in Table 39. This model explains ~6.1% of the variation in adjusted cholesterol. The actual contribution of skeletal muscle-specific gene variation on adjusted cholesterol in the SLVDS females is shown in Figure 62. On the FABP3p-313 C/C background, adjusted cholesterol is increased in a roughly dose dependent manner with increasing presence of the I allele, resulting in an average 29 mg/dl increase in FABP3p-ID I homozygotes over the FABP3p-ID D homozygotes. The presence of the FABP3p-313 allele appears to mute the effect of UCP3p-ID genotype on adjusted cholesterol, so those individuals retain baseline cholesterol levels.

Table 39: Final Regression Model for Combined Tissue Analyses of Adjusted Cholesterol in Females

	β	p-value	R^{2*}
Constant	203	<0.001	0.061
UCP2-8 (DD)	24	0.002	
UCP2-4 (CT) * UCP2-8 (DD)	-30	0.001	
UCP2-4 (CC)*FABP2p-834 (CC)	-23	0.009	
UCP2-4 (CC)*FABP2p-834 (CT)	-27	0.003	
FABP3p-313 (CC)	12	0.011	
FABP3p-ID (DD)*FABP3p-313 (CC)	-14	0.005	

*p=0.002

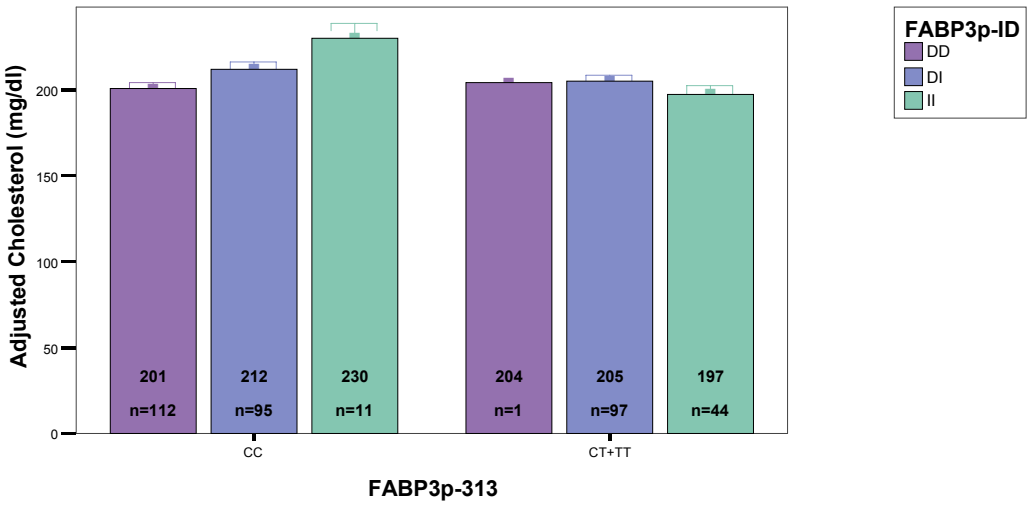

Figure 62: Adjusted Cholesterol vs. FABP3p-313/FABP3p-ID Multi-Locus Genotypes in Females

The intestine-specific contributions to adjusted cholesterol in the SLVDS females are shown in Figures 63 and 64. In UCP2-4 C/C individuals, the presence of the FABP2p-834 C allele results in an average 26 mg/dl reduction in adjusted cholesterol in comparison to the T homozygous group (Figure 63). The regression model predicts an ~24 mg/dl increase in adjusted cholesterol in UCP2-8 D homozygotes over the UCP2-8 D/I and I/I individuals. In the SLVDS females, shown in Figure 64, presence of the UCP2-4 C allele counteracts the UCP2-8 DD-mediated increase in adjusted cholesterol, retaining baseline levels of adjusted cholesterol.

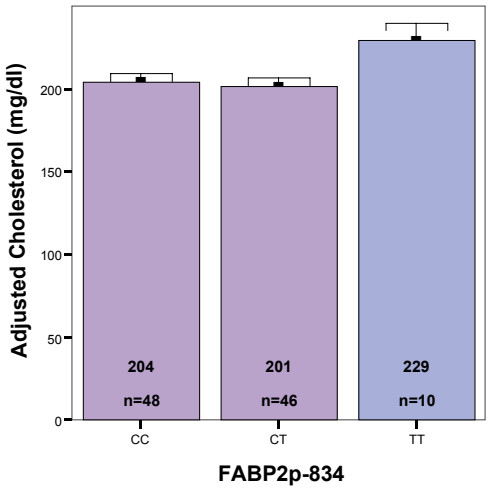

Figure 63: Adjusted Cholesterol vs. FABP2p-834 Genotypes on the UCP2-4 C/C Background in Females

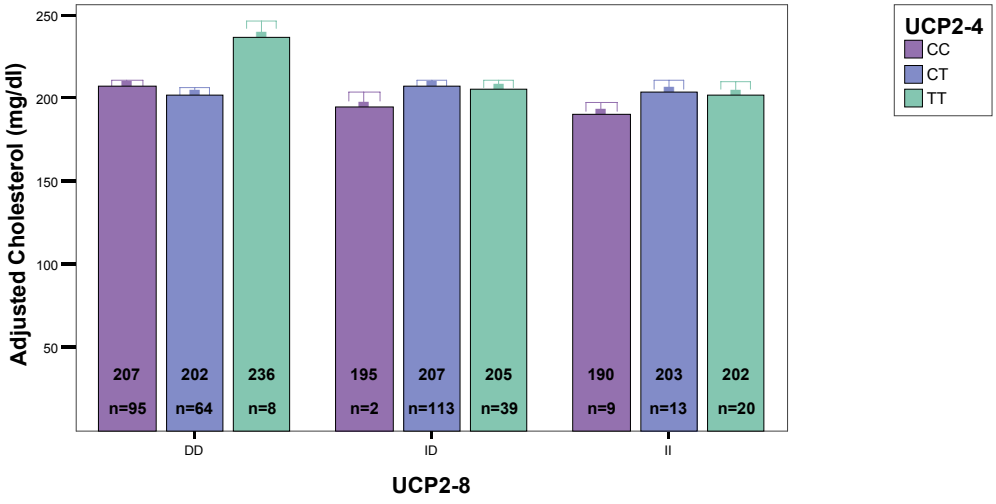

Figure 64: Adjusted Cholesterol vs. UCP2-4/UCP2-8 Multi-Locus Genotypes in Females

D. PROMOTER ACTIVITY ASSAYS

Direct sequencing of the 5' regions of FABP2 and FABP3 in twelve control samples revealed a number of interesting polymorphisms. Figure 65 shows the 5' region of FABP2, which contains a series of insertion/deletion polymorphims at –136 bp (AGTAG Ins/Del), -166 bp (GAA Ins/Del), and –169 bp (T Del/Ins) that are in complete linkage disequilibrium (LD) with one another. The insertion/deletion series is also in complete LD with the G/A polymorphisms at –260 bp and –471 bp and the G/T variant at –778bp. The 5' region of FABP3, shown in Figure 66, contains a C/T polymorphism at –313 bp and an insertion/deletion variant at –493 bp (CTC Del/Ins). LD between the –313 bp and –493 bp polymorphisms in FABP3 is 0.977.

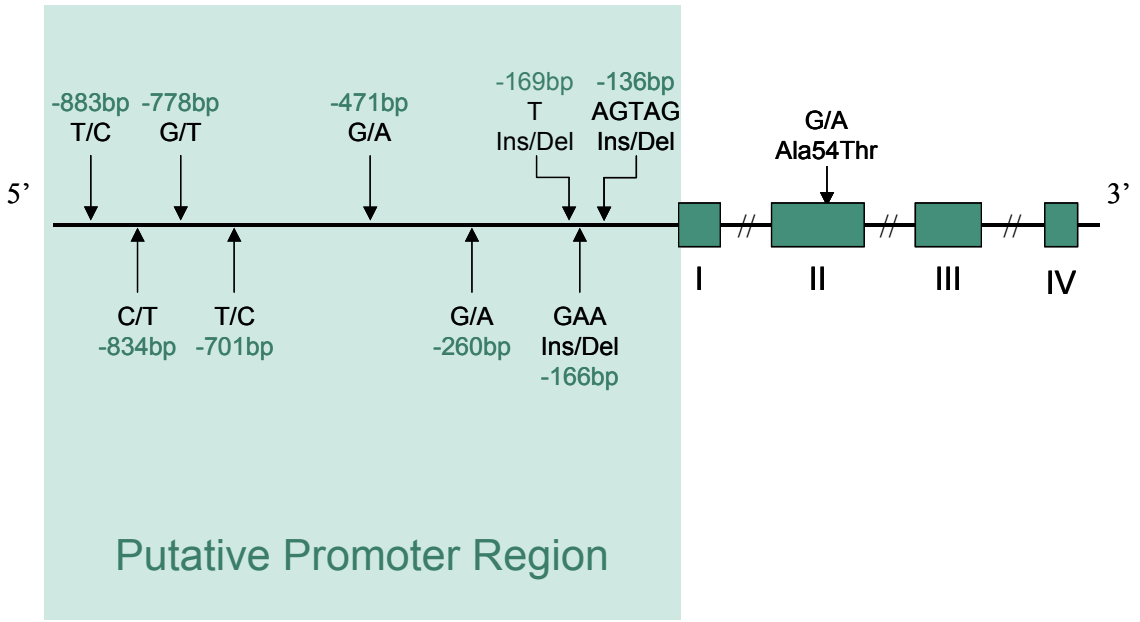

Figure 65: Polymorphic sites in the 5' Region of the FABP2 Gene

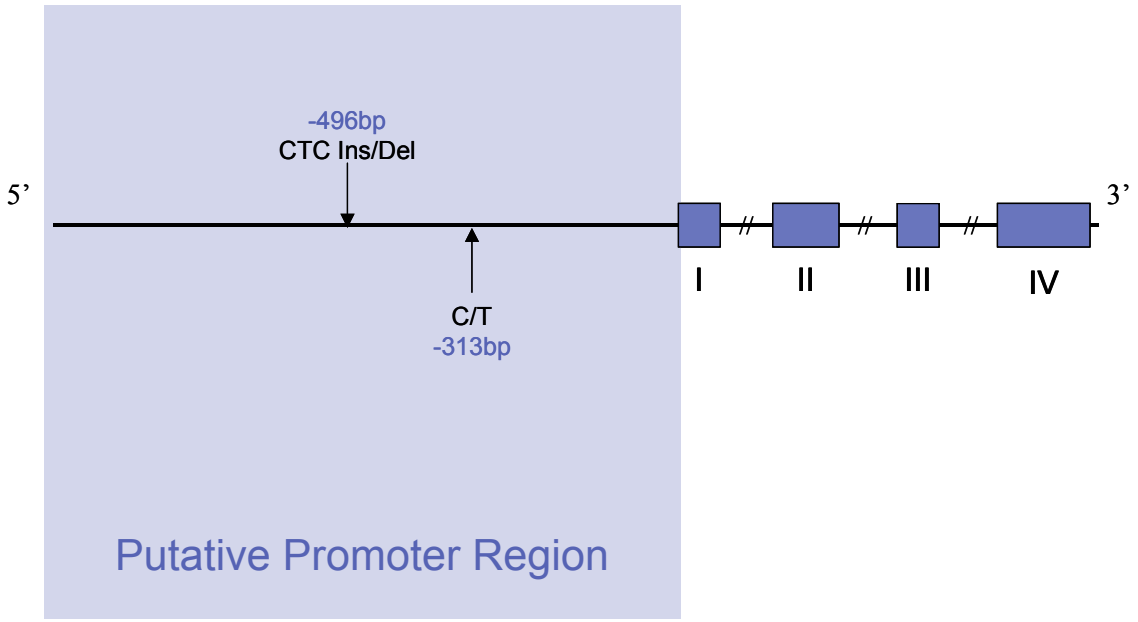

Figure 66: Polymorphic sites in the 5' Region of the FABP3 Gene

To determine if variation in the 5' regions of the FABP2 and FABP3 genes affects transcriptional activity, gene expression assays were performed using the Dual Luciferase Reporter Assay System (Promega). Two experimental constructs were prepared for each promoter by inserting fragments of opposite haplotypes into the pGL3-Basic plasmid vector (Figure 2). Figure 67 shows the layout of the FABP2 experimental constructs, FABP2 pGL3-Ins and FABP2 pGL3-Del. The polymorphic sites shaded in green are in complete LD and represent the two possible haplotype combinations. The polymorphisms shaded in blue are not in complete LD with the

insertion/deletion polymorphisms, so genotypes at these sites were held constant to avoid introducing additional variation to the experiment. The FABP3 experimental inserts, FABP3 pGL3-Ins and FABP3 pGL3-Del, are shown in Figure 68. These inserts represent the two most common FABP3 haplotype combinations. The pGL3-Basic vector, lacking a promoter, served as the background control. The pGL3 control vector, containing the SV40 promoter and enhancer sequences, was used as the positive control to which the experimental expression levels were compared.

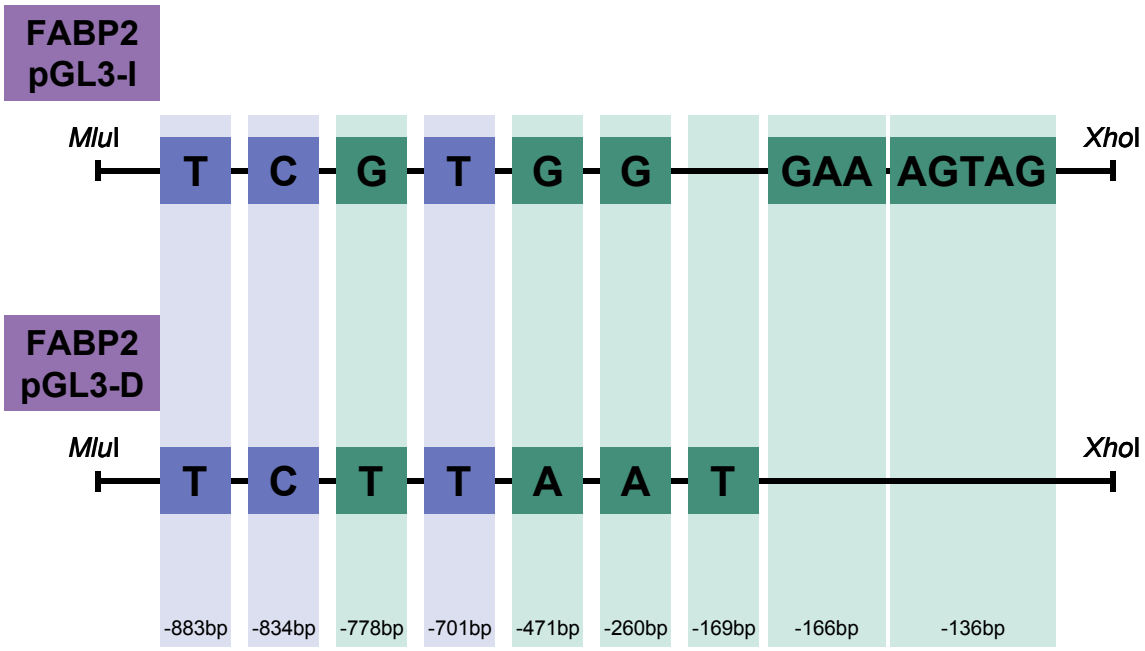

Figure 67: FABP2 Experimental Inserts

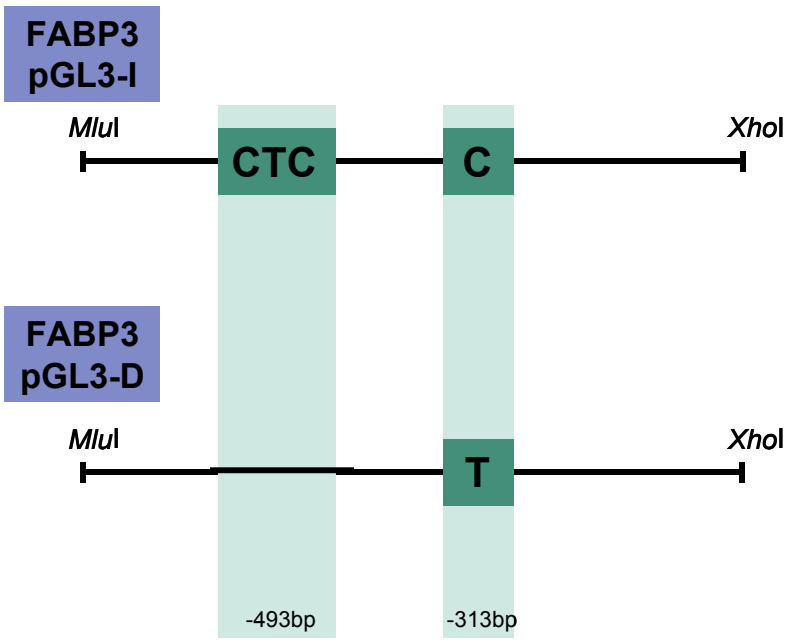

Figure 68: FABP3 Experimental Inserts

The FABP2 experimental plasmids were originally transfected into HT-29 cells, a human colorectal adenocarcinoma cell line; however, due to low transfection efficiency, this cell line was replaced with Caco-2 cells, a second cell line of colonic origin. Luciferase activity was measured after successful transfection of Caco-2 cells. Dual luciferase assay readings for the FABP2 constructs are shown in Table 73 of Appendix H. Figure 69 shows the mean relative luciferase activity (luciferase signal reading/*Renilla* signal reading) of the FABP2 experimental constructs as percentages of the pGL3-Control vector expression. The FABP2 pGL3-Ins plasmid produced ~0.21% of the control expression levels, while the FABP2 pGL3-Del construct produced ~0.11% of the control expression levels. The FABP2 pGL3 Ins construct shows a nearly two-

fold increase in expression over the FABP2 pGL3 Del, a statistically significant difference ($p<0.001$).

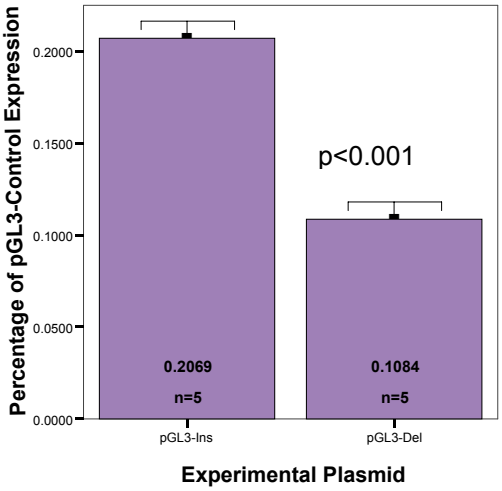

Figure 69: Relative Luciferase Expression of the FABP2 Experimental Constructs

Luciferase activity of the FABP3 constructs was measured after transfection of the HT-1080 fibroblast cell line. Dual luciferase assay readings for the FABP3 constructs are shown in Table 74 of Appendix H. Figure 70 shows the mean relative luciferase activity of the FABP3 experimental plasmids as a percentage of pGL3-Control vector expression. The FABP3 pGL3-Del and pGL3-Ins constructs produced ~1.62% and ~1.40% of the positive control level of expression, respectively. The difference in expression levels between the two experimental plasmids was not statistically significant ($p=0.545$).

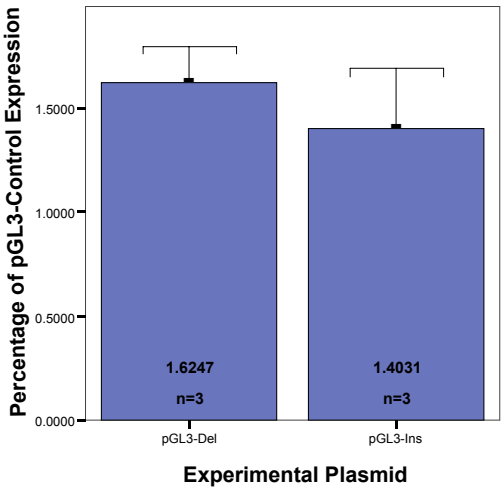

Figure 70: Relative Luciferase Expression of the FABP3 Experimental Constructs

V. SUMMARY AND CONCLUSIONS

This project was designed to explore the influences of candidate gene families on obesity- and diabetes-related phenotypes. The UCP and FABP gene families have been implicated as candidate genes due to roles in energy metabolism, fuel substrate partitioning and utilization, glucose metabolism, and insulin action. In this study, we identified variation in UCP and FABP genes, explored the influence of that variation on phenotype through multi-locus analysis, and assayed the functional consequences of promoter variation on gene expression levels.

A. SCREENING FOR VARIATION

The majority of the mutation screening efforts for this project focused on the 5' region of the UCP and FABP genes. In the UCP3 promoter region, a C to T substitution was identified at –55 bp, which was subsequently reported by Schrauwen et al. (1999a). This variant is potentially interesting due to its location four base pairs downstream of a PPAR regulatory element and six base pairs upstream from a TATA box. Schrauwen et al. (1999a) also reported a dramatic increase in UCP3 mRNA expression associated with the T allele.

The polymorphisms identified in the promoters of the FABP genes were all novel findings. The 5' region of the FABP2 gene was particularly interesting due to the identification of a series of insertion/deletion polymorphisms occurring within close proximity to the transcriptional start site (–136 bp to –169 bp). These insertion/deletion polymorphisms were in complete linkage disequilibrium with one another and with a

number of point mutations (FABP2p-ID). The 5' region of FABP3 contained a three base pair insertion/deletion polymorphism (FABP3p-ID) that was in partial linkage disequilibrium with a point mutation (FABP3p-313). In the FABP4 promoter region, two A to C point mutations in nearly perfect linkage disequilibrium were identified two base pairs away from one another. Only one of the sites was genotyped since the genetic effects of variation in one versus the other would be indistinguishable. Since transcription factors bind to sequence-specific motifs, each of these promoter variants has the potential to affect phenotypes related to the function of the gene.

B. DEVIATION OF UCP2-4 FROM HARDY-WEINBERG EQUILIBRIUM

The UCP2-4 variant showed statistically significant deviation from Hardy-Weinberg equilibrium in the Hispanic cohort, while a trend toward lack of Hardy-Weinberg equilibrium was shown in the non-Hispanic cohort. The consistency of this finding suggests the presence of selective pressures on genotype. In both Hispanics and non-Hispanics, there was an excess of heterozygotes. In general, the UCP2-4 heterozygous genotype was associated with conditions related to increased adiposity throughout the analysis. Historically, increased adiposity was advantageous in early populations to compensate for inconsistent food supplies and increased physical activity. Natural selection would have favored energy storage. The fact that the UCP2-4 heterozygote group in the SLVDS is disproportionately large and correlates with phenotypes related to increased adiposity suggests that selective pressures favored that genotype group. The mechanism by which this apparent heterozygote advantage manifested is unclear. In the future, it would be interesting to investigate the basis of this relationship further.

C. REGRESSION MODELING SPLIT BY SEX AND ETHNICITY

The data analysis plan was designed to examine associations between variation in the UCP and FABP gene families and specific outcome variables related to obesity and type 2 diabetes. In the preliminary analyses, there was suggestion of sex- and ethnic-specific differences in genetic influence on outcome variables. Thus, the data set was split by sex and ethnicity for the initial series of regression models.

1. Fat Mass in Non-Hispanic Females

The initial analyses, exploring single locus effects on fat mass in non-Hispanic females, identified the UCP3-5 variant as a significant predictor of fat mass. Alone, this variant exerts a relatively large influence over fat mass (R^2=0.062). Homozygosity for the UCP3-5 T allele was associated with the highest levels of fat mass (~32 kg), while the protective effect of the C allele considerably reduced fat mass levels to an average 27 kg. Regression models were constructed to explore the effects of interaction between the UCP3-5 variant and other polymorphisms in the UCP and FABP genes. We found that the UCP2-4 variant modifies fat mass levels in UCP3-5 T homozygotes to further define the phenotype in these individuals. In particular, the UCP2-4 T allele reduces fat mass levels in an additive fashion in UCP3-5 T/T individuals such that baseline levels of fat mass in the UCP2-4 T homozygotes are retained. The interactive relationship between the UCP2-4 and UCP3-5 variants was able to explain more than twice the variation in fat mass than the UCP3-5 variant alone. These results indicate

that interactive genetic variation in the UCP2/UCP3 chromosomal region is associated with fat mass in the non-Hispanic female cohort of the SLVDS.

2. Fat Mass in Hispanic Females

In the Hispanic females, preliminary analyses of single locus effects influencing fat mass identified UCP1-2 as a significant predictor. The UCP1-2 A allele was associated with increased fat mass over the UCP1-2 G homozygotes (~3.4 kg). Through regression modeling, we found that the UCP1-2 and UCP3-5 polymorphisms interact to significantly influence fat mass levels. Although the interaction was complex, it appears that the increase in fat mass associated with the UCP1-2 A allele is greatly intensified on the UCP3-5 T/T background. The protective effect of the UCP3-5 C allele in carriers of at least one UCP1-2 A allele is perplexing because the fat mass levels in the UCP3-5 heterozygotes are much lower than the C homozygotes. Perhaps the low number of individuals in both UCP3-5 homozygous groups on the UCP1-2 -/A background is having a confounding affect on the relationships among interacting groups. The UCP1-2 G homozygotes showed a net reduction in fat mass in comparison to carriers of the A allele; however, in this group, fat mass in the UCP3-5 heterozygotes is increased over both of the homozygous groups. The interactive relationship between UCP1-2 and UCP3-5 explains a relatively large percentage of the variation in fat mass in Hispanic females (~12.2%). These results show that two of the UCP genes, expressed in separate tissues, combine forces to influence an obesity-related phenotype.

3. Triglycerides in Non-Hispanic Males

Analysis of single locus effects on triglycerides in non-Hispanic males identified the UCP3p-55 variant as a significant predictor of triglycerides. The FABP2p-ID was marginally correlated with triglycerides. Homozygosity for the UCP3p-55 C allele is associated with increased levels of triglycerides. This elevation is intensified in FABP3p-ID heterozygous individuals, showing an interactive effect among variation in muscle-specific genes on triglycerides. Although the effect of the FABP2p-ID variant on triglycerides was not significant, the FABP2p-ID heterozygotes show a substantial reduction in triglyceride levels in comparison to the homozygous groups. Interaction of the UCP3-5 T allele with heterozygosity at FABP2p-ID results in a greater reduction in triglyceride levels. This model combines variation in muscle-specific genes with influence from the intestine-type FABP, showing an influential interaction between dietary uptake of lipids and target tissue utilization of lipids over plasma triglyceride levels in non-Hispanic males.

4. Triglycerides in Hispanic Males

In the initial analyses, the individual effects of each locus on triglyceride levels in Hispanic males were explored. We found that the FABP3p-313 and UCP3p-55 sites showed similar patterns of influence on triglycerides; however, the single locus effect of UCP3p-55 on triglycerides was not significant ($p=0.105$). Specifically, the presence of the T allele at either FABP3p-313 or UCP3p-55 was associated with increased triglyceride levels. Regression modeling identified an interaction between the FABP3p-

313 and the UCP3-5 variants. Since the UCP3-5 variant is in LD with the UCP3p-55, they may be marking the same effect on mean triglycerides. In the Hispanic male cohort, homozygosity for the C allele at FABP3p-313 and the T allele at UCP3-5 results in the lowest triglyceride levels. Presence of the UCP3-5 rare allele increases triglycerides by ~43 mg/dl, while in the presence of the FABP3p-313 C/C genotype. On the other hand, in the presence of the FABP3p-313 T allele, UCP3-5 shows the opposite trend in triglycerides with a dose dependent reduction with increasing presence of the UCP3-5 C allele. This model consists of interaction between variation in the muscle-specific genes from the UCP and FABP families, providing a possible mechanism by which muscle affects plasma triglyceride levels.

D. COMPARISON OF THE "SEX/ETHNICITY-SPLIT" AND "SEX-SPLIT" REGRESSION MODELING APPROACHES

The final regression models for fat mass in non-Hispanic and Hispanic females described above provide an example of the "sex/ethnicity-split" analysis for comparison to the "sex-split" final model for fat mass in the overall female cohort. Each of the "sex/ethnicity-split" models describes a relatively large percentage of the variation in fat mass (12-13%) for each female cohort. Both the final models for non-Hispanic and Hispanic females include the UCP3-5 variant with the T allele acting to increase fat mass, showing consistency in the effect of that polymorphism on the phenotype. However, the variants that the UCP3-5 polymorphism interacts with are different between the models. In the non-Hispanic female model for fat mass, the UCP3-5 variant interacts with the UCP2-4 polymorphism, while UCP3-5 interacts with the UCP1-2 variant in the Hispanic female model. It is possible that both of these models are showing an interactive effect on fat mass between genes expressed in the muscle and fat tissue. Since UCP2 is expressed in white adipocytes and UCP1 is expressed in brown adipocytes, this would suggest that there is an ethnic divergence in tissue response to adiposity signals. Perhaps the fat depots in Hispanic individuals contain a higher number of brown adipocytes or increased activity in brown adipocytes, making the BAT-specific genes more influential in adipocyte-related signaling. This theory is supported by the presence of UCP1 variants in several of the final models for outcome variables in both Hispanic females and males; however, physiological evidence is required for confirmation.

The comparison between the non-Hispanic and Hispanic male models for triglycerides is perplexing. These "sex/ethnicity-split" models of triglycerides are similar in that they include variants in the muscle-specific genes, UCP3 and FABP3. Although different polymorphisms appear in the models from those gene, they could be marking the same functional effect because they are in high linkage disequilibrium. However, the UCP3p-55 variant, which appears in both the non-Hispanic and Hispanic models, shows opposite influence on triglycerides in the two ethnic groups. In the non-Hispanic males, the T allele is protective, while it shows a deleterious effect on triglycerides in the Hispanic males. Therefore, this argues against the presence of similar mechanisms influencing triglycerides between non-Hispanic and Hispanic males. On the other hand, this discrepancy could be a result of spurious significant associations due to large sample size.

Although there are similarities among the final models resulting from the "sex/ethnicity-split" analyses, it seems that the effects of genetic variation on outcome in this population are both sex- and ethnicity-dependent. Thus, when we performed the "sex-split" analysis on the data set, it was important to adjust for the ethnic differences among individuals in each group. In an attempt to compensate for ethnic-specific effects, the outcome variables for the "sex-split" analyses were adjusted for skin reflectance. The outcome variables for the "sex-split" analyses were also adjusted for age, smoking status, and physical activity, whereas no adjustments were made to the outcome variables for the "sex-ethnicity split" analyses.

The final "sex-split" regression model for adjusted fat mass in females contained a diverse set of terms including polymorphisms in genes specific to several different

tissue types, including skeletal muscle, adipose tissue, and intestine. We compared the results of this model to the final “sex/ethnicity-split “ models for fat mass in non-Hispanic females and Hispanic females. Figure 71 shows a schematic of this comparison. The single locus terms shown in bold represent the sites shared by the “sex-split” model and at least one of the “sex/ethnicity-split” models. In this case the UCP1-2 variant appears in both the Hispanic female model and the overall “sex-split” female model. The UCP3-5 variant appears in each of the three models, maintaining a consistent association between the T allele and increased fat mass levels in females regardless of the analysis approach. One important feature to notice in the comparison between these analysis approaches is the resulting R^2 values. When the female groups are combined and adjusted for skin reflectance (“sex-split” analysis), the R^2 value drops more than two-fold. Thus, the “sex-split” model detects much less of the variation in fat mass due to genotype than the “sex/ethnicity-split” models. This observation is generally consistent across all of the outcome variables considered in the study, suggesting that the skin reflectance variable is unable to completely account for ethnic differences between individuals in this population.

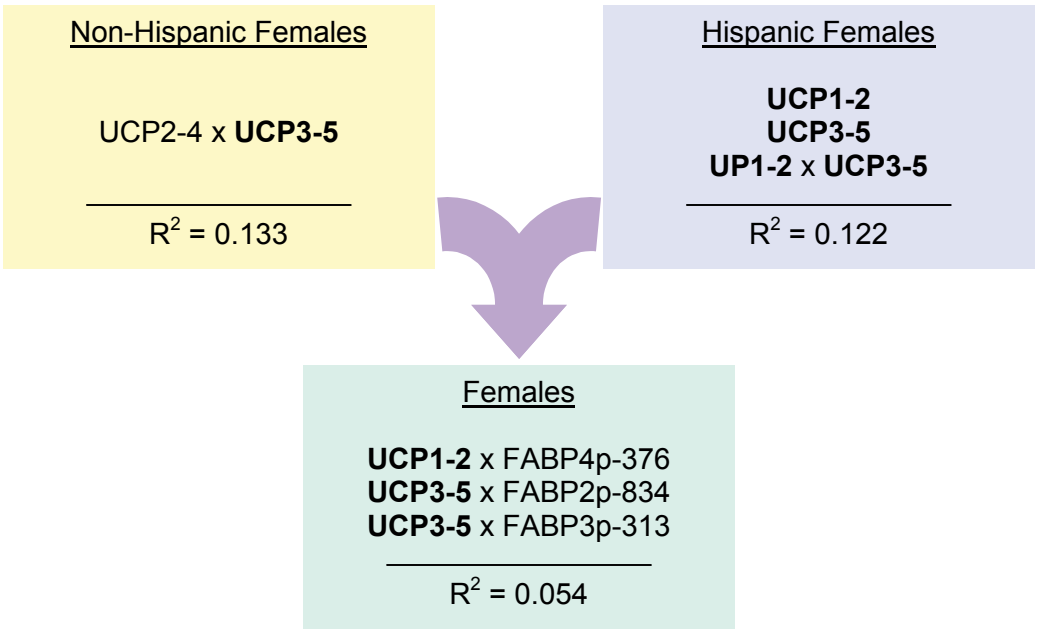

Figure 71: Comparison of "Sex/Ethnicity-Split" Fat Mass Models in Females to "Sex-Split" Fat Mass Model in Overall Female Cohort

The comparison between the "sex/ethnicity-split" final models and the "sex-split" final model for ln(triglycerides) in males is shown in Figure 72. The "sex/ethnicity-split" models contain variants predominantly from muscle-specific genes. While the FABP3p-313 variant appears in both the Hispanic male model and the overall "sex-split" male model, the effects of UCP3 variants on phenotype, seen in both "sex/ethnicity-split" models, are absent from the final "sex-split" model. The final "sex-split" model for triglycerides involved interaction between variation in a muscle-specific (FABP3) gene and an adipose-specific (FABP4) gene. Again, the "sex-split" model was only able to explain a fraction of the variation in triglycerides in males compared to the sex/ethnic-split models.

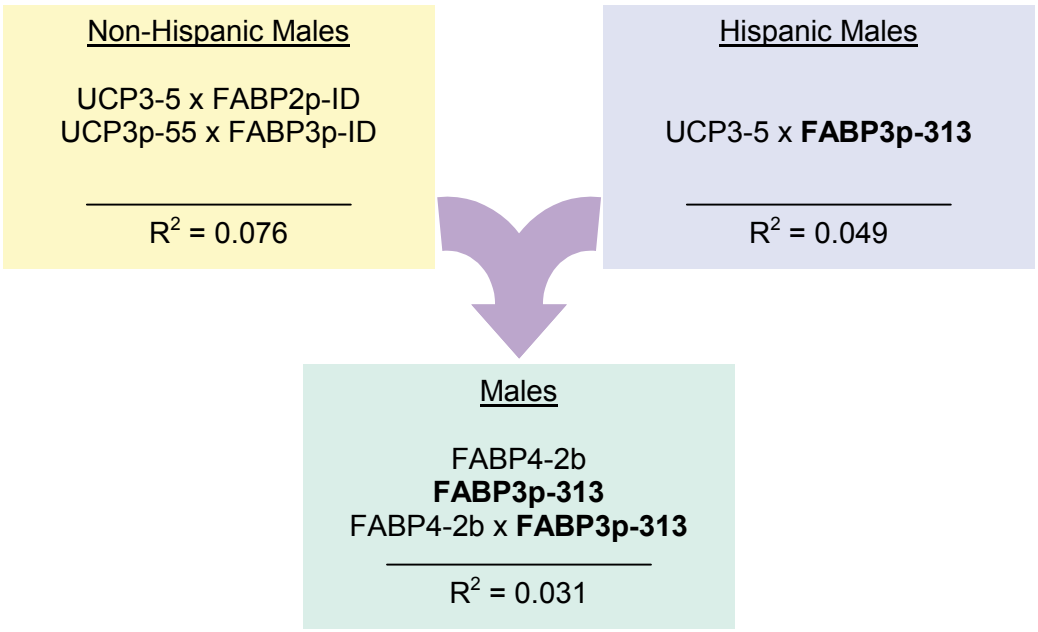

Figure 72: Comparison of "Sex/Ethnicity-Split" Triglyceride Models in Males to "Sex-Split" Triglyceride Model in Overall Male Cohort

E. EFFECTS OF "MUSCLE GENES" ON TRIGLYCERIDES AND HOMA IR IN NON-HISPANIC FEMALES

Insulin resistance is a condition of impaired insulin-mediated glucose uptake and metabolism in skeletal muscle and adipose tissue. Several studies have shown a direct relationship between insulin resistance and elevated plasma triglyceride and free fatty acid levels. These plasma lipids serve as alternate fuel sources to glucose and competitively inhibit glucose uptake. In the fasted state, these plasma lipids are normally elevated to serve as the primary fuel substrate (Baier et al. 1995; 1996). Chronic elevations in plasma lipids, as seen in obese individuals, leads to impaired insulin sensitivity in peripheral organs, suggesting a mechanism for the link between obesity and type 2 diabetes. The uncoupling proteins and fatty acid binding proteins have been shown to play a role in fuel partitioning and regulation of glucose and lipid metabolism.

This portion of the study investigated the impact of variation in UCP3 on features of glucose and lipid metabolism in the non-Hispanic white females from the SLVDS. Analysis of single locus effects on outcome identified the UCP3-5 and UCP3p-55 variants as significant predictors of insulin sensitivity and triglyceride levels, showing analogous relationships between each variant and outcome variable. Specifically, C homozygosity for either the UCP3-5 polymorphism or the UCP3p-55 variant is significantly associated with higher insulin sensitivity, a finding that corroborates the association observed by Otabe et. al. (1999) between diabetic status and UCP3-5 T homozygosity. The C/C genotype is also associated with reduced triglyceride levels for each variant. In the non-Hispanic female cohort, the UCP3-5 and UCP3p-55

polymorphisms influence insulin sensitivity and triglycerides in a similar manner, identifying a single gene (or gene region) influencing both traits. In addition, the UCP3-5 and UCP3p-55 variants show a high level of linkage disequilibrium, suggesting that these two variants may be marking a functional change in UCP3 affecting insulin sensitivity and triglyceride levels.

To explore this relationship further, we considered multi-locus and interactive effects among members of the UCP and FABP gene families on insulin sensitivity and triglyceride levels. The final regression models for both traits included polymorphisms from the UCP2/UCP3 region and the muscle-type FABP, FABP3. In comparing the effects of genotype on mean HOMA IR and mean triglycerides in the non-Hispanic females (see Figures 41 and 42), a similar trend is shown. The bar chart showing mean HOMA IR (Figure 41) represents the FABP3p-313 C homozygotes, while the bar chart for triglycerides (Figure 42) represents the FABP3p-ID D homozygotes. Since the two FABP3 promoter variants are in linkage disequilibrium with one another, both of the bar charts may be showing the same effect of FABP3 on each phenotype. In addition, UCP3-5 and UCP2-4 genotype shows similar effects on HOMA IR and triglycerides, respectively, when split by UCP3p-55 genotype. The UCP2-4 variant is in linkage disequilibrium with the UCP3-5 polymorphism. Therefore, it is possible that Figures 41 and 42 are showing the same overall genotypic effect on HOMA IR and triglycerides.

Since muscle is one of the major tissues affected by insulin resistance, it is not surprising to see a muscle-specific gene contribution to insulin sensitivity. Muscle is also a highly metabolically active tissue, which supports the triglyceride-/FFA-mediated mechanism described above as a major factor in the development of insulin resistance.

UCP2 and UCP3 have also been shown to be upregulated in muscle during fasting, supporting involvement in fuel partitioning. The similarities in patterns of influence of the “muscle genes” on both insulin resistance and triglycerides in this cohort suggests that elevated triglyceride levels influence insulin sensitivity through biochemical pathways involving the muscle-specific UCP and FABP genes.

F. EFFECTS OF THE UCP2/UCP3 REGION ON DIETARY INTAKE IN SLVDS FEMALES

In this portion of the study, we investigated the effects of genetic variation in the UCP2/UCP3 chromosomal region on measures of dietary intake in the female cohort of the SLVDS in order to explore how these "metabolic" genes may be involved in the development of overweight and/or obesity. Initially, we looked at the individual effects of each locus on total caloric intake and fat intake. We found that the UCP3-5 and UCP3p-55 sites were similarly correlated with both measures of intake, although the effect of UCP3p-55 on fat intake was only marginally significant ($p=0.063$). Specifically, the presence of the C allele at UCP3-5 or the T allele at UCP3p-55 was associated with increased total caloric and fat intake. The UCP2-4 variant showed no effect on dietary intake when considered alone. The linkage disequilibrium between the UCP3-5 and UCP3p-55 variants suggests that the UCP3-5 C allele and the UCP3p-55 T allele may be marking a single functional change in UCP3 affecting dietary intake. However, since the independent effects of the UCP3 polymorphisms were small, we considered the possibility that relationships among multiple sites within the UCP2/UCP3 region have a cumulative effect on total caloric and fat intake. Thus, regression models were constructed to consider the effects of each site and interactions among those sites. We found that the UCP3-5 and UCP3p-55 variants interact to influence both total caloric intake and fat intake, while the UCP2-4 variant modifies the effect of UCP3-5 on both measures on intake. In particular, homozygosity for either the C allele of UCP3p-55 or the T allele of UCP3-5 reduces total caloric intake (~200 calories) and fat intake (~10 grams), while the interaction between the two genotypes results in nearly double those

reductions. The predominant effect of the UCP2-4 variant seems to be slight alterations to intake levels of UCP3-5 heterozygotes. These results indicate that interactive genetic variation in the UCP2/UCP3 chromosomal region is associated with total caloric intake and fat intake. The regression models may not be representative of the precise effects exerted by the UCP2/UCP3 variation on intake, but it is clear that at least two loci and possibly all three loci are interacting to affect dietary intake.

To further investigate the implications of this study, we consider the phenotype displayed in the UCP3 overexpressing mouse reported by Clapham et al. (2000) in relation to the UCP3-5 variant in the female cohort of the SLVDS. The UCP3 overexpressing mouse is hyperphagic; therefore, to make a comparison between the transgenic mouse and the UCP3-5 variant, we consider the C allele, which is associated with increased dietary intake in this cohort. Despite an increase in appetite, fat mass is reduced in the UCP3 overexpressing mouse while plasma free fatty acids and triglycerides remain unchanged, theoretically to fuel increased metabolic rates. In the female cohort of the SLVDS, the UCP3-5 polymorphism was significantly associated with fat mass measured by DEXA ($p=0.006$). Presence of the C allele was associated with an ~3.4kg reduction in fat mass, showing a decrease in fat mass despite an increase in total caloric and fat intake similar to the transgenic mouse. Also, no significant change in plasma free fatty acids and triglycerides was observed across genotype groups in the cohort, suggesting an increase in lipid metabolism. The transgenic mouse also experiences lower plasma cholesterol levels and increased insulin sensitivity in comparison to wild-type littermates. In the SLVDS female cohort, the UCP3-5 C allele followed a trend toward decreased plasma cholesterol levels (mean

cholesterol: TT=211, TC=203, CC=199; p=0.088) and increased insulin sensitivity (mean HOMA IR: TT=15, TC=13, CC=13; p=0.195); however, statistical significance was not reached. In addition, the trend toward increased insulin resistance observed in T homozygotes of the SLVDS female cohort corroborates the finding by Otabe et al. (1999) of association between this variant and diabetic status. The similarities observed between the phenotypes of the overexpressing UCP3 mouse and the genotype-phenotype correlations at the UCP3-5 polymorphic site in this cohort suggest that the C allele may be a marker for increased UCP3 expression or a more functionally active form of the UCP3 protein.

The results presented here indicate the presence of interactive genetic variation within the UCP2/UCP3 region influencing overall caloric intake and nutrient selection. This suggests a role for UCP2 and UCP3 in fuel substrate management, which may play a role in body weight regulation. In addition, comparison between the UCP3-5 site and phenotypes of the UCP3 overexpressing mouse suggest that variation in the UCP2/UCP3 region marks increased activity of the UCP3 gene. Therefore, functional studies of the variation in this region could clarify the observed effects on dietary intake and uncover clues to the physiological role of the UCP2 and UCP3 genes.

G. TISSUE-SPECIFIC REGRESSION MODELING

The tissue-specific analysis approach allowed us to explore the effects of variation in genes expressed in specific tissue types on the outcome variables. These tissue-specific models were combined in a second round of regression analyses to obtain an overall final model for each outcome. Theoretically, the combined models identified the gene effects representative of the most influential tissue types on each outcome.

1. Free Fatty Acids in Males

In males, the final combined model for FFA was identical to the adipose-specific model for FFA. Although the intestine-specific model had a relatively large R^2 value, none of the terms from that model were included in the final combined model. This suggests that a large portion of the influence over FFA in males is specific to genes expressed in the adipose tissue. The final combined model for FFA in males is composed of complex interactions among UCP1, UCP2 and FABP4-2b variants. In UCP2-8 D homozygotes, average FFA levels were 532 μmol/L. Within this group, the UCP1-2 and FABP4-2b variants interact to influence FFA levels. Individuals homozygous form both the UCP1-2 G allele and the FABP4-2b I allele have reduced FFA levels below the average (~25 mg/dl). The UCP1-2 A allele and FABP4-2b D allele exert dose-dependent deleterious effects to dramatically increase FFA levels over the average.

2. Triglycerides in Males

The final combined model for triglycerides in males was a combination of the adipose-specific and intestine-specific models. The majority of the genetic influence on triglycerides appeared to originate from the adipose-specific genes. This model consists of a complex array of overlapping interactions between UCP2 and FABP4 variants, which is probably in part due to linkage disequilibrium between multiple sites within the UCP2 and FABP4 genes. In UCP2-4 C/C individuals, the FABP4-2b D allele and the FABP4p-376 C allele interact in a dose-dependent fashion to increase triglyceride levels. The UCP2-8 I allele shows a dose-dependent protective effect on triglycerides levels in FABP4p-376 A homozygotes. In UCP2-8 D homozygotes, a dramatic reduction in triglycerides is observed in FABP4-2b I homozygotes. The complex interactions between the UCP2 and FABP4 exert a sizable effect upon triglycerides in males, suggesting that these adipose-specific genes play an important role in managing plasma triglycerides.

3. Cholesterol in Males

This analysis approach did not detect significant association between genetic variation and cholesterol levels in males. Since the liver is the major organ of cholesterol synthesis, perhaps the addition of a liver-specific (FABP1) set of genes would help elucidate the genetic effects influencing this trait.

4. Free Fatty Acids in Females

In females, the final combined model for FFA included a mixture of genetic influences from each of the three tissue types. This suggests the presence of a complex signaling network between several tissues influencing plasma FFA levels. Since the intestine-specific model alone explained ~9.0% of the variation in FFA and most of the terms in the combined model originated from the intestine model, the majority of the effect seems to stem from the intestine-specific genes. The muscle component of this model consists of a heterozygote advantage-type effect of the UCP3-5 variant on PPARa5 C homozygotes. In the adipose-specific portion of the combined model, UCP1-2 G homozygosity exerts a protective effect over cholesterol levels, which is counteracted by the UCP2-8 D allele. The effects of the intestine-specific genes on cholesterol are very complex. This portion of the combined model includes interaction between two UCP2 variants that are in linkage disequilibrium and two FABP2 promoter variants that are also in linkage disequilibrium. This situation complicates interpretation of gene effect on phenotype because several of the multi-locus genotype groups are very small or were not observed. However, considering that such a large portion of the gene effects influencing FFA are a result of interaction among UCP2 and FABP2 variants, these genes probably play a pivotal role in managing FFA levels.

5. Triglycerides in Females

Complex interactions between UCP and PPAR genes expressed in adipose tissue influence triglyceride levels in females. The PPARg2 and UCP2-8 sites interact

in an additive fashion to result in a range of average triglycerides from 157 mg/dl to 185 mg/dl. The lowest level of triglycerides results form the protective effects of the PPARg2 G allele in combination with UCP2-8 I homozygosity. Further modification of triglycerides on the PPARg2/UCP2-8 background results from influence of UCP2-4 genotype. The interactive effects of all three polymorphic sites "muddies" the patterned effect of genotype on triglyceride levels (illustrated in Figure 60). UCP2-4 and UCP2-8 are in partial linkage disequilibrium with one another as well as with several UCP3 variants. Therefore, the individual effects of each variant, apart from any interactive effects, modify the phenotype to result in a complex pattern of triglyceride levels. Within this same model, the protective effect of UCP1-2 G homozygosity is also modified by UCP2-4 and UCP2-8 genotype in a similar manner. This model illustrates the complex nature of gene-gene interactions on phenotype.

6. Cholesterol in Females

The final combined model for cholesterol in females is a merger between the muscle-specific model and the intestine-specific model. The variation explained by the final combined model nearly equals that of the two tissue-specific models collectively. This suggests a strong influence from both tissue types on cholesterol levels. The muscle component of the model contains an interaction between two FABP3 promoter variants. On the FABP3p-313 C/C background, the FABP3p-ID I allele has a dose-dependent deleterious effect on cholesterol levels. This effect of FABP3p-ID genotype is completely suppressed by the presence of the FABP3p-313 T allele. The intestine-specific portion of the model results from complex interaction between variation in UCP2

and FABP2. UCP2-8 DD individuals show an ~24 mg/dl increase in cholesterol over carriers of the I allele. The UCP2-4 C allele completely counteracts that increase, retaining baseline levels of cholesterol. These interactions are complicated further by genotype at FABP2p-834. Cholesterol levels are elevated in UCP2-4 C homozygotes by FABP2p-834 homozygosity, which is a second example of complex interactive effects between UCP2 and FABP2 on plasma lipid levels in females.

7. Summary of Tissue-Specific Regression Analyses

The tissue-specific regression analyses uncovered a number of complex interactive relationships between genes expressed in the particular tissues. In several cases, the UCP2 variants interacted with either the FABP2 or FABP4 variants to produce obscure arrays of plasma lipid levels, which were complicated by linkage disequilibrium among polymorphisms. Both FFA and triglycerides in males were influenced to the largest extent by the adipose-specific genes. In females, the effects on outcome were varied among genes expressed in each of the three tissue types; however, the triglyceride model was influenced entirely by adipose-specific genes. Several of the gene effects remained consistent among the models. In general, the UCP2-8 D allele showed deleterious effects on plasma lipids, while the UCP1-2 G and FABP4-2b I alleles exerted protective influences. This analysis approach provided a means by which we could explore the effects of genetic variation on outcome variables using biological knowledge of the gene expression patterns.

H. PROMOTER ACTIVITY ASSAYS

Following the identification of statistical relationships, the next step in exploring the effects of genetic variation on phenotype is to perform functional assays to determine the potential biological effects of that variation. In this study, we investigated the consequences of variation in the 5' regions of the FABP2 (FABP2p-ID) and FABP3 (FABP3p-ID and FABP3p-313) genes on gene expression levels, using the Dual Luciferase Reporter Assay System.

The FABP2 expression studies showed that the FABP2p-ID insertion encoding allele was associated with an ~2-fold increase in mRNA expression over the FABP2p-ID deletion encoding allele. This difference in promoter activity was statistically significant. These results show that common genetic variation in the 5' region of FABP2 affects promoter activity, suggesting that the FABP2p-ID D allele is associated with a reduction in transcription of FABP2.

The FABP2p-ID polymorphism is in tight linkage disequilibrium with the FABP2-2 variant (D' = 0.904). A number of studies have explored genotype/phenotype relationships involving the FABP2-2 variant. *In vitro* expression studies in Caco-2 cells showed that Thr-encoding allele is associated with increased binding affinity and transport of long-chain fatty acids and increased secretion of triglycerides (Baier et al. 1996). In population studies, the Thr-encoding allele has been associated with elevated triglyceride levels, increased fat oxidation, and decreased insulin sensitivity (Baier et al. 1995; Pihlajamäki et al. 1997). Since the FABP2-2 polymorphism is in high linkage disequilibrium with the FABP2p-ID variant, the FABP2-2 may be marking functional consequences of altered promoter activity levels. In any case, promoter variation

affecting FABP2 expression levels potentially causes a wide range of phenotypic consequences. It would be interesting to take this study a step further and compare *in vivo* mRNA expression levels among individuals of different genotype groups for each of the FABP2 variants.

The FABP3 expression assays showed no statistically significant differences in expression levels between the FABP3 insertion encoding allele and the deletion encoding allele. This study was conducted using a fibroblast cell line because an immortalized skeletal muscle cell line is not available. Since the FABP3 gene is normally expressed in skeletal muscle, the fibroblast cell line may not have been able to provide essential transcription factors for FABP3 expression. Therefore, the accuracy of the experiment may have been compromised. However, the results of the FABP3 expression studies suggest that the FABP3p-ID and FABP3p-313 variants do not influence mRNA expression.

I. FUTURE STUDIES

Due to the exploratory nature of the analyses conducted for this study, the results should be viewed with caution. No corrections were made for multiple testing, so in the future, these results should be replicated in other population groups. It would be interesting to test some of the stonger models in other Hispanic and non-Hispanic populations to confirm our findings. The models should also be tested in other ethnic groups to determine if the effects were ethnic-dependent.

There were several variants identified in the 5' regions of the UCP and FABP genes. The promoter activity assays described above began to explore the functional effects of some of the variants by measuring differences in mRNA expression due to variation in FABP2 and FABP3. It would be interesting to investigate more of the promoter variants in that manner. Finally, to get the most informative picture of the effects of the promoter variants, *in vivo* studies should be done to assay differences in actual mRNA and protein levels in specific tissues.

J. CONCLUDING REMARKS

The analysis plan for this study was designed to identify interesting genotype/phenotype relationships involved in the development of obesity and type 2 diabetes. We explored several outcome variables using a multi-locus analysis scheme and performed the analysis using three different approaches. First, the data set was split by sex and ethnicity prior to analysis. This approach was followed by analysis of the data set split by sex with outcome variables adjusted for skin reflectance to account

for ethnic differences. The sex-split models consistently explained much less of the variation in phenotye, suggesting that the skin reflectance variable was an inadequate representative of ethnicity in this cohort. Therefore, the four sex/ethnic groups should be considered separately. The third analysis approach was designed to consider the effects of genes expressed in specific tissue types on phenotypes. To compliment the statistical analyses, functional studies were performed to assess the effects of promoter variation on promoter activity.

The overall results of this study suggest that a multi-locus approach to studying complex diseases is more informative than considering single locus effects individually. The non-Hispanic female model for fat mass, for example, explained approximately 13.3% of the variation, while UCP3 alone was only able to accout for approximately 6.2%. Several of the regression models were able to explain upwards of 10% of the variation in phenotype with the complex non-Hispanic male model for fat mass reaching 22.6%. Consideration of multiple gene families was also important to building the most parsimonious regression models. In addition to the statistical analyses, it was interesting to consider functional consequences of variation to determine potential biological effects. This study illustrates the importance of multi-locus analysis in understanding complex disease.

APPENDICES

APPENDIX A

MUTATION SCREENING

Table 40: SSCP and Sequencing Primers for UCP3 Exons

Primer Name	Primers (20μM)	Enzyme Digestion	$MgCL_2$ [ ]	Annealing Temp.
UCP3-1F UCP3-1R	5'-aggataaggtttcaggtcagc-3' 5'-tgacaagctgcagctagtga-3'	Hinf*I*	1.5mM	56°C
UCP3-2F UCP3-2R	5'-gacatcactccatcagcctt-3' 5'-ggatatgggagagaactagcc-3'	Nco*I*	1.0mM	57°C
UCP3-3F UCP3-3R	5'-cttgccttcccatctgagtc-3' 5'-tggctctgcctctgagtctag-3'	Nco*I*	1.0mM	58°C
UCP3-4F UCP3-4R	5'-agcatgtcccagagagctgc-3' 5'-agctctgcctaagaccgcct-3'	Nco*I*	1.0mM	59°C
UCP3-5F UCP3-5R	5'-cttgcagccagggcatccat-3' 5'-tgagggagagctgcctgcct-3'		1.0mM	62°C
UCP3-6F UCP3-6R	5'-acagtgcataacatatggacag-3' 5'-acccacggtagccacattc-3'	Rsa*I*	2.5mM	56°C
UCP3-7F* UCP3-7R*	5'-cctagcactccacctgatgtg-3' 5'-atgtgtgggtctgtgtccat-3'		1.0mM	58°C

*Sequenced only.

Table 41: Sequencing Primers for Promoter Screening

Primer Name	Primers (20μM)	$MgCl_2$ [ ]	Annealing Temp.
UCP3p1F UCP3p1R	5'-tacaggctccaacatggatg-3' 5'-ctgtggacgcttcctggtg-3'	2.0mM	60°C
UCP3p2F UCP3-1R	5'-gtacctatctcataggattgtg-3' 5'-tgacaagctgcagctagtga-3'	2.0mM	60°C
UCP3p3F UCP3p3R	5'-taggtcgggtgcagtggc-3' 5'-agtagagacgaggtcttg-3'	1.5mM	57°C
UCP3p4F UCP3p4R	5'-caggcagccttcggacttct-3' 5'-cattctctccaacatgacacttg-3'	1.0mM	60°C
UCP3p5F UCP3p5R	5'-gaacatccatgcttctgacc-3' 5'-ctccatacacattggtagtcac-3'	1.0mM	60°C
FABP2p1F FABP2p1R	5'-ctggcaatgctaaacacaat-3' 5'-ctgtaagctatctgtaatctcc-3'	1.5mM	62°C
FABP2p2F FABP2p2R	5'-ctagagcttctttcctgaccct-3' 5'-ctgggaaatgagaccatgac-3'	1.5mM	62°C
FABP3p1F FABP3p1R	5'-gacaaggtcagctcagccg-3' 5'-gctgtccactagcttccagg-3'	1.5mM	62°C
FABP3p2F3 FABP3fs-R	5'-agccctcagcatgcaataaatag-3' 5'-gaaattcttgctgtccactagctt-3'	1.0mM	56°C
FABP4pF FABP4pR	5'-ggagtacttctgaatcccat-3' 5'-aggtacctacaaaagcatcac-3'	1.5mM	56°C

General PCR Recipe:

50mM $MgCl_2$	1.0-2.0 µl
10X PCR Buffer	5.0 µl
1.25mM dNTP Mix	8.0 µl
20µM Forward Primer	0.5 µl
20µM Reverse Primer	0.5 µl
dH_2O	32.75-33.75µl
Taq Polymerase	0.25µl
DNA	1.0 µl
Total Volume	50.0 µl

Thermocycler Conditions:

1. 95°C, 5 min
2. 95°C, 30 sec
   Annealing Temp., 30 sec }35 cycles
   72°C, 30 sec*
3. 72°C, 2 min
4. 4°C, Soak

*The elongation step was increased to 1 minute for fragments ≥ 500bp.

General Restriction Enzyme Digestion Protocol:

2-5 units enzyme	0.2-0.5µl
10X Buffer	1.5µl
dH_2O	3.0-3.3µl
PCR Product	10.0µl
Total Volume	15.0µl

- When necessary, 0.125µl of 100X BSA was added per sample.
- Digests were incubated overnight at 37°C.

SSCP Reagent Recipes

Denaturing Solution

- 200µl of 0.5M EDTA
- 5ml of 1M NaOH
- 4.8ml of dH_2O

Formamide Dye

- 10ml Formamide
- 5mg Xylene Cyanol (0.05%)
- 5mg Bromophenol Blue (0.05%)
- 200µl of 0.5M EDTA

SYBR Green II

- Make a 1:10,000 by adding 4 µl of SYBR Green II to 50ml 1X TBE Buffer

APPENDIX B

GENOTYPING

Table 42: Genotyping Primers and PCR Conditions

Polymorphism	Primers (20μM)	$MgCl_2$ [ ]	Annealing Temp.
UCP1-2*	5'-aggtataaaggtgtcctgggaacaatcagc-3' 5'-ctgcggtgaggaactcctggac-3'	1.5mM	63°C
UCP1-5*	5'-cttatcgctggattttgcgcaaaag-3' 5'-gccgttggtccttcgttagtg-3'	1.5mM	60°C
UCP2-4*	5'-tcaggggccagtgcgcgctacgg-3' 5'-cagaatcatacaggccgatgcggacag-3'	1.5mM	69°C
UCP2-8	5'-gctgacctgatcacctct-3' 5'-gacgcttgggatcctggc-3'	1.5mM	59°C
UCP3-3a*	5'-cttcgcctccatccgcatcggcctcga-3' 5'-ctgggacatgctgttctctgcggggctgc-3'	2.0mM	69°C
UCP3-3b	5'-ctactgtgaccagcatggttg-3' 5'-ctgggacatgctgttctctgc-3'	2.0mM	62°C
UCP3-5*	5'-gacatcctcaaggagaagctgctggagta-3' 5'-accacaatgtacctggcacttttactagg-3'	1.5mM	68°C
UCP3p-55*	5'-aggactgaaccagatctggaactcactc-3' 5'-tctggcttggcactggtcttatacactc-3'	1.0mM	65°C
FABP2-2	5'-acaggtgttaatatagtgaaaag-3' 5'-taccctgagttcagttccgtc-3'	1.5mM	56°C
FABP2p-834*	5'-ctagctaccctctataccctgagcc-3' 5'-ccagtagagtcagaagccacagc-3'	1.5mM	64°C
FABP2p-ID	5'-ctcaggaatgtacagaacga-3' 5'-gatgtggaagcttaaagttc-3'	1.5mM	53°C
FABP3p-313 FABP3p-ID	5'-gacaaggtcagctcagccg-3' 5'-gctgtccactagcttccagg-3'	1.5mM	62°C
FABP4-2a FABP4-2b	5'-agtggctggcatggccaa-3' 5'-gtccagagtgttatacaa-3'	2.0mM	53°C
FABP4p-376	5'-cgaggcagttcttatgttcc-3' 5'-tgacagcttaatgctcagtgc-3' detection primer (10μM): 5'-cataactgcaatttaaataacacccc-3'	1.5mM	56°C

*Denotes primer set incorporating an engineered restriction enzyme site. Altered base is in bold.

General PCR Recipe:

50mM $MgCl_2$	1.0-2.0 µl
10X PCR Buffer	5.0 µl
1.25mM dNTP Mix	8.0 µl
20µM Forward Primer	0.5 µl
20µM Reverse Primer	0.5 µl
dH_2O	32.75-33.75µl
Taq Polymerase	0.25µl
DNA	1.0 µl
Total Volume	50.0 µl

Thermocycler Conditions:

1. 95°C, 5 min
2. 95°C, 30 sec
   Annealing Temp., 30 sec }35 cycles
   72°C, 30 sec*
3. 72°C, 2 min
4. 4°C, Soak

Table 43: Methods of Genotype Detection

Polymorphism	Method of Detection	Notes
UCP1-2	*Hha*I Digestion*	G=cut (129bp/27bp) A=uncut (156bp)
UCP1-5	*Hind*III Disgestion*	A=uncut (143bp) T=cut (117/26bp)
UCP2-4	*Eae*I Digestion*	C=cut (146bp/20bp) T=uncut (166bp)
UCP2-8	2% Agarose Gel (45bp InsDel)	Del: ~220bp Ins: ~265bp
UCP3-3a	*Drd*I Digestion*	T=uncut (228bp/25bp) C=cut (253bp)
UCP3-3b	*Asp*I Digestion	G=cut (301bp/175bp/46bp) A=uncut (344bp/178bp)
UCP3-5	*Rsa*I Digestion*	T=uncut (~180bp) C=cut (~154bp/26bp)
UCP3p-55	*Ava*I Digestion*	C=uncut (151bp) T=cut (120bp/31bp)
FABP2-2	*Hha*I Digestion	G=cut (98bp/82bp) A=uncut (180bp)
FABP2p-834	*Ban*II Digestion*	C=cut (42bp/20bp) T=uncut (62bp)
FABP2p-ID	3% Agarose Gel: 7bp overall size difference in I/D polymorphisms.	Genotypes at –778bp, -471bp, and –260bp inferred from linkage disequilibrium with I/D variants at –169bp, -166bp, and –136bp.
FABP3p-313	Direct Sequencing	
FABP3p-ID	Direct Sequencing	
FABP4-2a	*Afl*III Digestion	T=cut (~750bp/~380bp/~300bp) G=uncut (~1.3kb)
FABP4-2b	*Pvu*II Digestion	Ins=uncut (~800bp/~500bp) Del=cut(~800bp/~750bp/~500bp)
FABP4p-376	Fluorescence Polarization	

*Denotes engineered restriction enzyme site.

General Restriction Enzyme Digestion Protocol:

2-5 units enzyme	0.2-0.5µl
10X Buffer	1.5µl
dH_2O	3.0-3.3µl
PCR Product	10.0µl
Total Volume	15.0µl

- When necessary, 0.125µl of 100X BSA was added per sample.
- Digests were incubated overnight at 37^{o}C.
- Digestion products were run on 2% agarose gels and visualized under UV illumination.

Fluorescence Polarization Protocol

Amplification

PCR reaction mix:

dH_2O	6.7µl
10X PCR Buffer	1.0µl
50mM $MgCl_2$	0.5µl
1.25mM dNTP mix	0.2µl
2.5µM forward primer	0.2µl
2.5µM reverse primer	0.2µl
Taq polymerase	0.2µl
PCR product	1.0µl
	10.0µl

Thermocycler Conditions:

1. 95°C, 12 min
2. 95°C, 30 sec
   66°C (1°C step down/cycle), 30 sec }15 cycles
   72°C, 30 sec
3. 95°C, 30 sec
   50°C, 30 sec } 30 cycles
   72°C, 30 sec
4. 72°C, 6 min
5. 4°C hold

SAP Treatment

Reaction mix:

10X SAP buffer	1.0µl
SAP (1U/µl; Roche)	2.0µl
Exonuclease I (10U/µl; USB)	0.1µl
dH_2O	6.9µl
PCR product	10.0µl
	20.0µl

- Samples were incubated at 37^{o}C for 90 minutes.
- A 15-minute incubation followed at 95^{o}C to inactivate the enzymes.

Primer Extension

FABP4 promoter variant:

ddATP labeled with TAMARA dye

ddCTP labeled with R110 dye

Reaction mix:

25μM dye-labeled ddNTP	0.05μl
10μM detection primer	1.00μl
5X Thermosequenase buffer	1.00μl
Thermosequenase (8U/μl; USB)	0.20μl
dH_2O	7.75μl
SAP-Treated PCR product	20.00μl
	30.00μl

Thermocycler Conditions:

1. 94°C for 1 minute
2. 94°C for 10 seconds } 35 cycles
   55°C for 30 seconds
3. 4°C hold

APPENDIX C

PPAR & RXR GENOTYPING

Table 44: PPAR and RXR Allele Frequencies

Polymorphic Site	Allele	Overall Frequency	Frequency	
			Hispanics	Non-Hispanics
PPARγ γ2 specific exon	C (Pro)	0.883	0.884	0.882
	G (Ala)	0.117	0.116	0.118
PPARγ Exon 6	C	0.861	0.882	0.848
	T	0.139	0.118	0.152
PPARα Exon 5	C (Leu)	0.905	0.886	0.918
	G (Val)	0.095	0.114	0.082
PPARα Exon 6	T (Val)	0.980	0.965	0.991
	C (Ala)	0.020	0.035	0.009
RXRβ Exon 10 3' UTR	T	0.842	0.800	0.871
	A	0.158	0.200	0.129
RXRβ +140	A	0.721	0.704	0.732
	T	0.279	0.296	0.268
PPARβ Exon 6	C	0.869	0.863	0.873
	T	0.131	0.137	0.127

APPENDIX D

DESCRIPTIVE STATISTICS

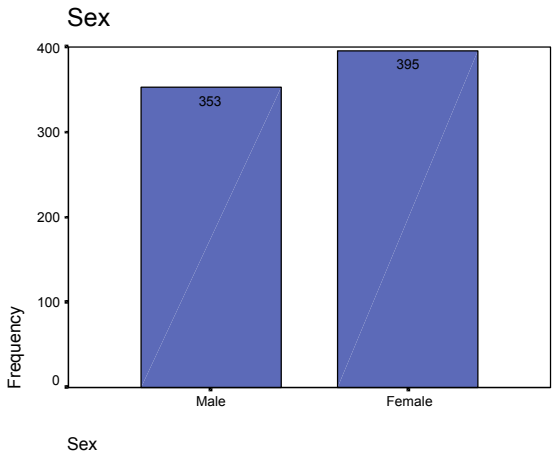

Figure 73: Bar Chart of Males vs. Females

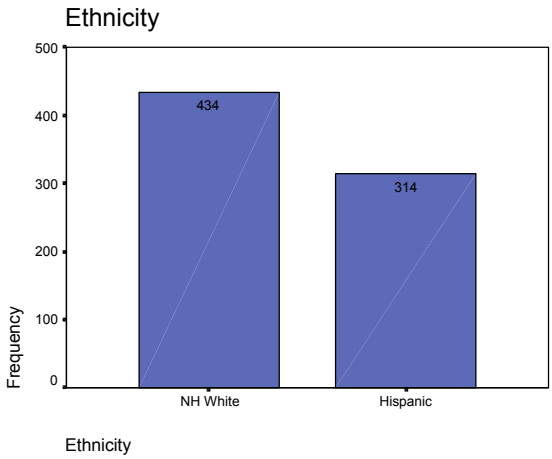

Figure 74: Bar Chart of Non-Hispanic Whites vs. Hispanics

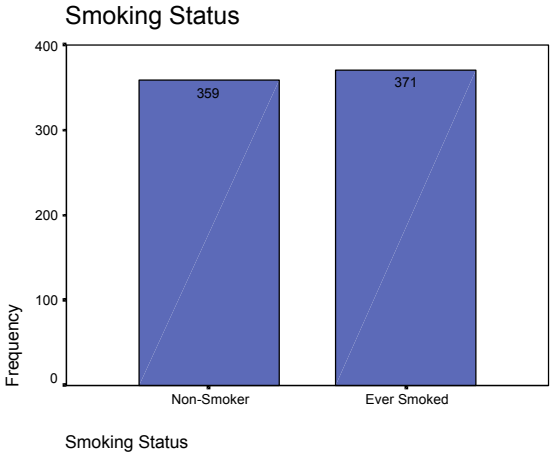

Figure 75: Bar Chart of Non-Smokers vs. Ever Smoked

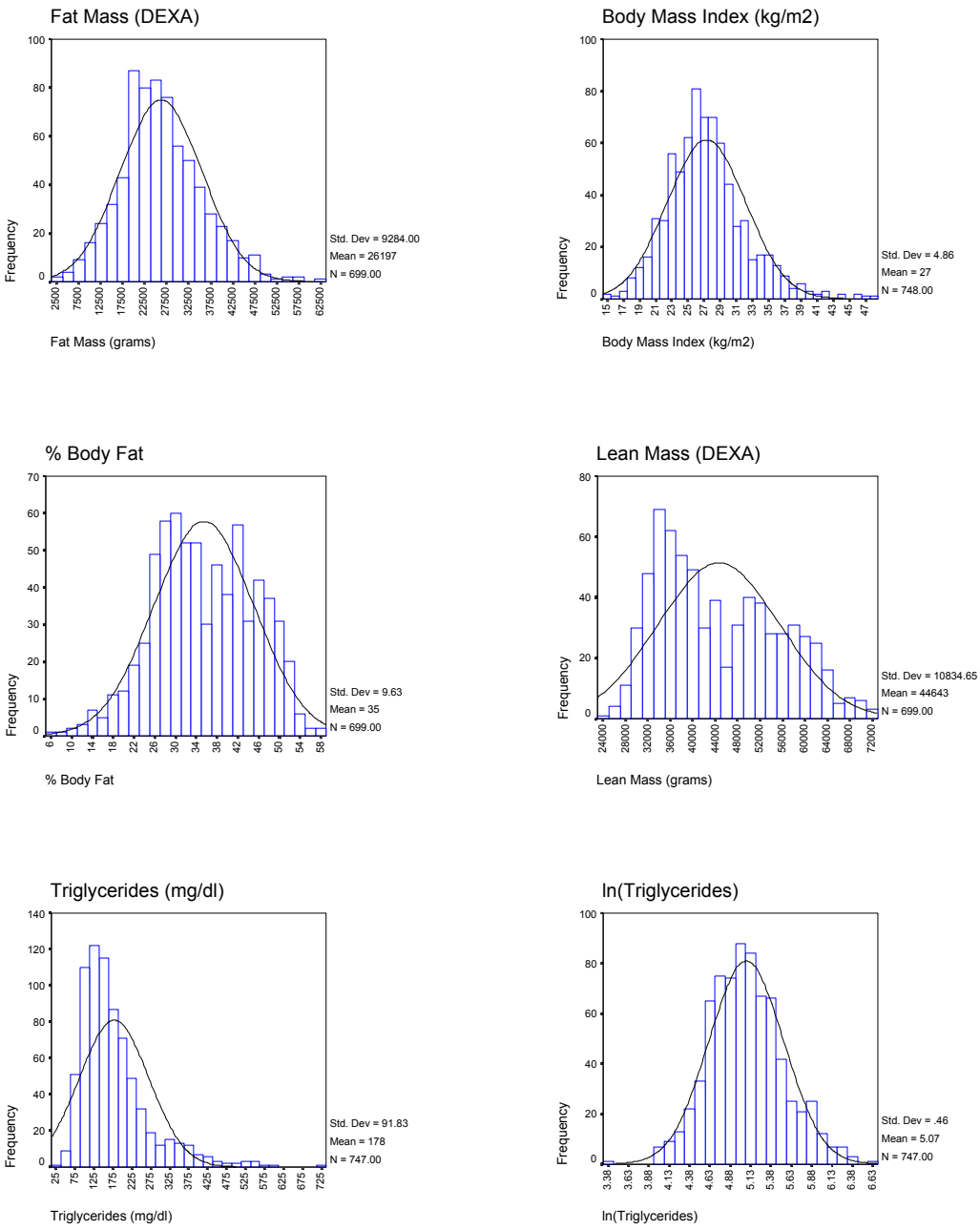

Figure 76: Histograms of Continuous Variables

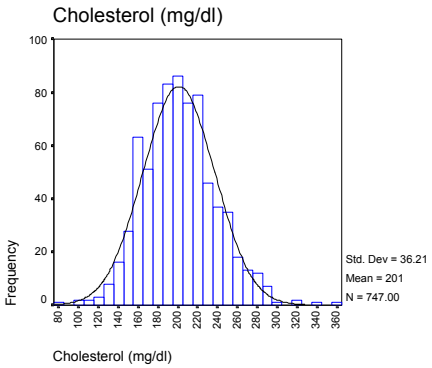

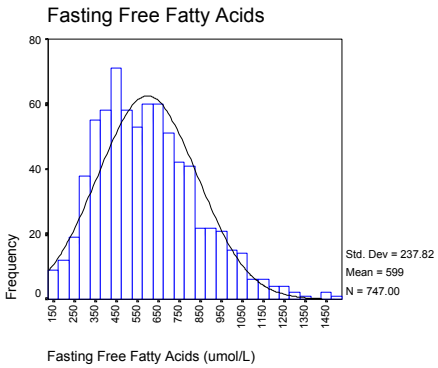

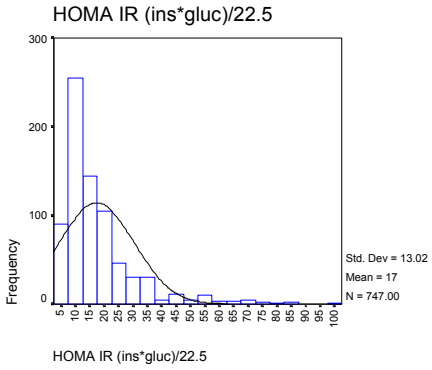

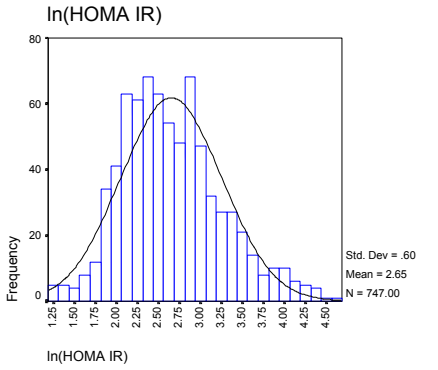

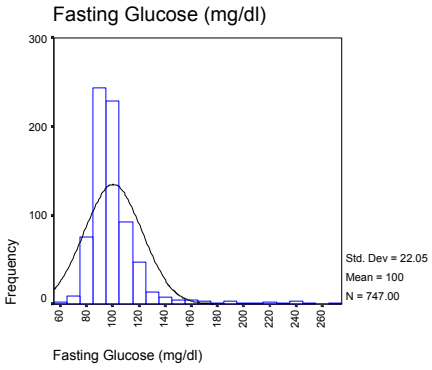

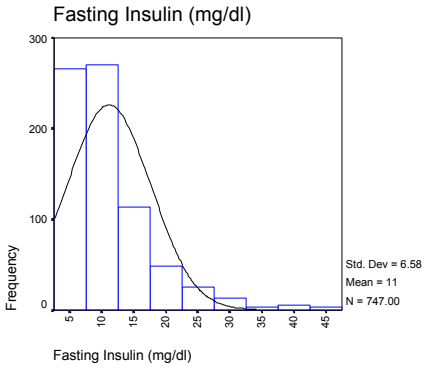

Figure 76: (continued)

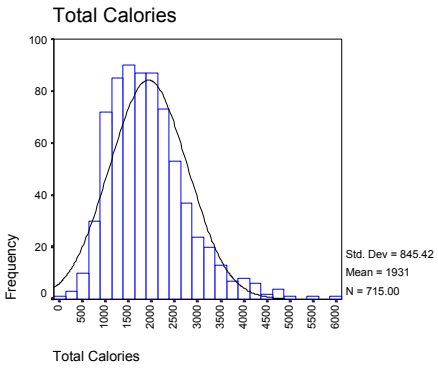

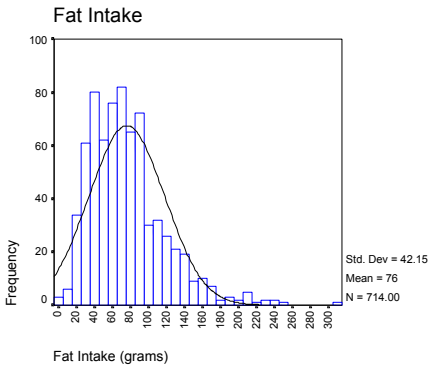

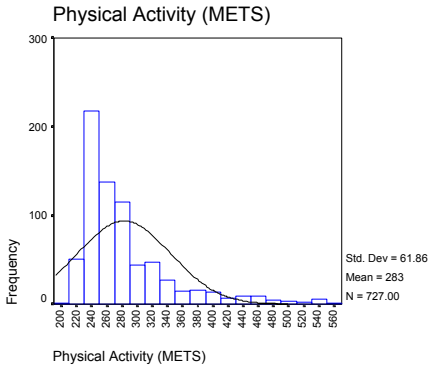

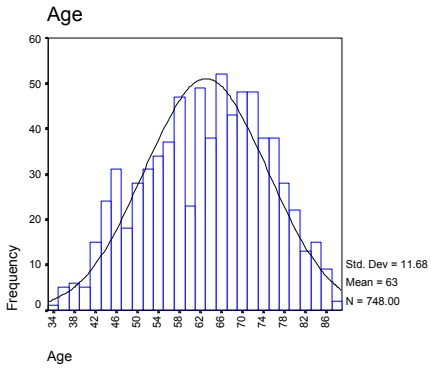

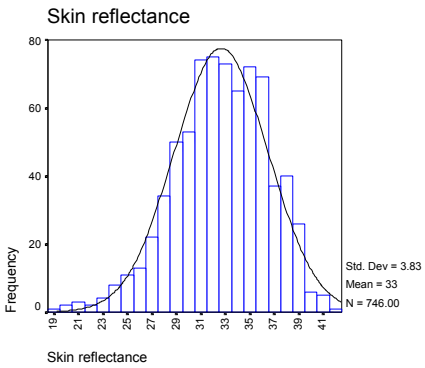

Figure 76: (continued)

Table 45: Correlation Matrix

	FM	FFA	TRIG	CHOL	H IR	CALIN	FATIN	PA	SKRF	AGE	SMK
FM	1.000	0.190	0.214	-0.002	0.466	-0.185	-0.128	-0.133	0.079	-0.120	-0.099
FFA	0.190	1.000	0.198	0.132	0.198	-0.278	-0.245	-0.157	-0.065	0.205	-0.042
TRIG	0.214	0.198	1.000	0.293	0.395	0.004	-0.028	-0.019	-0.074	-0.038	0.045
CHOL	-0.002	0.132	0.293	1.000	-0.059	-0.075	-0.017	-0.077	-0.031	0.034	-0.005
H IR	0.466	0.198	0.395	-0.059	1.000	-0.021	0.011	-0.072	-0.108	0.015	0.028
CALIN	-0.185	-0.278	0.004	-0.075	-0.021	1.000	0.878	0.194	0.008	-0.192	0.066
FATIN	-0.128	-0.245	-0.028	-0.017	0.011	0.878	1.000	0.155	-0.015	-0.171	0.078
PA	-0.133	-0.157	-0.019	-0.077	-0.072	0.194	0.155	1.000	0.036	-0.207	0.023
SKRF	0.079	-0.065	-0.074	-0.031	-0.108	0.008	-0.015	0.036	1.000	0.106	-0.116
AGE	-0.102	0.205	-0.038	0.034	0.015	-0.192	-0.171	-0.207	0.106	1.000	0.008
SMK	-0.099	-0.042	0.045	-0.005	0.028	0.066	0.078	0.023	-0.116	0.008	1.000

FM=Fat Mass; FFA=Free Fatty Acids; TRIG=ln(Triglycerides); CHOL=Cholesterol; H IR=ln(HOMA IR); CALIN=Total Caloric Intake; FATIN=Fat Intake; PA=Physical Activity; SKRF=Skin Reflectance; SMK=Smoking Status

APPENDIX E

REGRESSION MODELS SPLIT BY SEX AND ETHNICITY

Non-Hispanic Females

Table 46: Non-Hispanic Females – Final Regression Model for Free Fatty Acids

	β	p-value	R^{2*}
Constant	604	<0.001	0.058
UCP2-4 (CC) * UCP3-5 (TT)	240	0.004	
UCP2-4 (CT) * UCP3-5 (TT)	101	0.020	

*p=0.002

Table 47: Non-Hispanic Females - Final Regression Model for Cholesterol

	β	p-value	R^{2*}
Constant	210	<0.001	0.075
UCP3p-55 (CC)	11	0.050	
FABP2p-ID (ID)	-15	0.003	
UCP3p-55 (CC) * FABP3p-ID (DD)	-16	0.022	

*p=0.002

Non-Hispanic Males

Table 48: Non-Hispanic Males – Final Regression Model for Fat Mass

	β	p-value	R^{2*}
Constant	27678	<0.001	0.226
FABP2p-ID (II)	-5974	0.006	
FABP2p-ID (ID)	-3871	0.009	
FABP3p-ID (ID)	5446	0.005	
UCP1-2 (GG) * FABP3p-ID (DD)	7709	<0.001	
UCP2-8 (DD) * FABP3p-ID (DD)	-6612	0.006	
UCP2-8 (ID) * FABP3p-ID (DD)	-8352	<0.001	
UCP2-8 (ID) * FABP3p-ID (ID)	-3021	0.032	
FABP2p-ID (II) * FABP4p-376 (AA)	5322	0.015	
FABP3p-ID (ID) * FABP4p-376 (AA)	-7527	<0.001	

*p<0.001

Table 49: Non-Hispanic Males – Final Regression Model for Free Fatty Acids

	β	p-value	R^{2*}
Constant	515	<0.001	0.023
FABP3p-ID (DD)	-61	0.031	

*p=0.031

Table 50: Non-Hispanic Males – Final Regression Model for Cholesterol

	β	p-value	R^{2*}
Constant	203	<0.001	0.019
FABP3p-313 (CC)	-10	0.050	

*p=0.050

Table 51: Non-Hispanic Males – Final Regression Model for ln(HOMA IR)

	β	p-value	R^{2*}
Constant	2.968	<0.001	0.057
FABP2p-ID (II)	-0.568	0.007	
FABP3p-ID (DD)	-0.383	0.007	
FABP3p-ID (ID)	-0.377	0.006	
FABP2p-ID (II) * FABP3p-ID (DD)	0.689	0.006	
FABP2p-ID (II) * FABP3p-ID (ID)	0.686	0.003	

*p=0.044

Hispanic Females

Table 52: Hispanic Females – Final Regression Model for Free Fatty Acids

	β	p-value	R^{2*}
Constant	750	<0.001	0.117
UCP1-2 (GG) * UCP3p-55 (CC)	94	0.030	
UCP1-2 (GG) * FABP3p-ID (ID)	-161	0.001	
UCP3p-55 (CC) * FABP3p-ID (ID)	155	0.002	

*p<0.001

Table 53: Hispanic Females – Final Regression Model for ln(Triglycerides)

	β	p-value	R^{2*}
Constant	5.281	<0.001	0.074
UCP1-2 (GG)	-0.272	0.002	
UCP1-2 (GG) * UCP2-8 (DD)	0.225	0.004	

*p=0.002

Table 54: Hispanic Females – Final Regression Model for Cholesterol

	β	p-value	R^{2*}
Constant	201	<0.001	0.071
UCP3-5 (TT) * FABP3p-ID (ID)	26	0.001	

*p=0.001

Table 55: Hispanic Females – Final Regression Model for ln(HOMA IR)

	β	p-value	R^{2*}
Constant	2.835	<0.001	0.034
UCP3p-55 (CC) * FABP2p-834 (CC)	0.0150	0.072	
UCP3p-55 (CC) * FABP2p-834 (CT)	-0.107	0.090	

*p=0.061

Hispanic Males

Table 56: Hispanic Males – Final Regression Model for Fat Mass

	β	p-value	R^{2*}
Constant	20265	<0.001	0.054
UCP1-2 (GG) * FABP2-2 (GG)	3529	0.009	

*p=0.009

Table 57: Hispanic Males – Final Regression Model for Free Fatty Acids

	β	p-value	R^{2*}
Constant	508	<0.001	0.096
UCP2-4 (CT)	171	<0.001	
UCP2-8 (ID)	-99	0.030	

*p=0.001

Table 58: Hispanic Males – Final Regression Model for Cholesterol

	β	p-value	R^{2*}
Constant	228	<0.001	0.058
UCP2-8 (DD)	-36	0.007	
UCP2-8 (ID)	-36	0.006	

*p=0.018

APPENDIX F

REGRESSION MODELS SPLIT BY SEX

Females

Table 59: Females – Final Regression Model for Free Fatty Acids

	β	p-value	R^{2*}
Constant	639	<0.001	0.043
FABP2-2 (GG)	109	0.022	
UCP3-5 (TT) * FABP2-2 (GG)	-145	0.013	
UCP3-5 (TC) * FABP2-2 (GG)	-132	0.008	
UCP3-5 (TT) * FABP4-2b (II)	98	0.006	

*p=0.005

Table 60: Females – Final Regression Model for ln(Triglycerides)

	β	p-value	R^{2*}
Constant	5.096	<0.001	0.027
FABP4p-376 (AA)	-0.133	0.033	
UCP2-4 (CT) * FABP4p-376 (AA)	0.165	0.003	

*p=0.009

Table 61: Females – Final Regression Model for Cholesterol

	β	p-value	R^{2*}
Constant	193	<0.001	0.041
UCP2-4 (CT)	10	0.039	
UCP3-5 (TT)	20	<0.001	
UCP2-4 (CT) * UCP3-5 (TT)	-30	0.012	
UCP3-5 (TC) * FABP4-2b (II)	10	0.044	

*p=0.006

Table 62: Females – Final Regression Model for ln(HOMA IR)

	β	p-value	R^{2*}
Constant	2.163	<0.001	0.044
UCP3p-55 (CC)	0.444	0.051	
FABP2p-834 (CC)	0.513	0.008	
FABP2p-834 (CT)	0.654	0.001	
UCP3p-55 (CC)*FABP2p-834 (CC)	-0.510	0.038	
UCP3p-55 (CC)*FABP2p-834 (CT)	-0.762	0.003	

*p=0.007

Males

Table 63: Males – Final Regression Model for Fat Mass

	β	p-value	R^{2*}
Constant	24563	<0.001	0.038
UCP2-8 (ID) * FABP2-2 (GG)	4321	0.009	
UCP2-8 (ID) * FABP2p-ID (II)	-5591	0.005	
UCP2-8 (ID) * FABP2p-ID (ID)	-3554	0.002	

*p=0.008

Table 64: Males – Final Regression Model for Free Fatty Acids

	β	p-value	R^{2*}
Constant	453	<0.001	0.043
UCP3-5 (TT)	154	0.005	
FABP4p-376 (AA)	98	0.001	
UCP3-5 (TT) * FABP4p-376 (AA)	-169	0.006	

*p=0.003

Table 65: Males – Final Regression Model for Cholesterol

	β	p-value	R^{2*}
Constant	195	<0.001	0.031
UCP2-4 (CT)	13	0.011	
UCP2-4 (CT) * FABP3p-313 (CC)	-16	0.002	

*p=0.006

Table 66: Males – Final Regression Model for ln(HOMA IR)

	β	p-value	R^{2*}
Constant	2.775	<0.001	0.025
FABP2-ID (ID) * FABP3p-ID (DD)	-0.180	0.039	
FABP2-ID (ID) * FABP3p-ID (ID)	-0.182	0.013	

*p=0.016

APPENDIX G

TISSUE SPECIFIC ANALYSES: FAT MASS AND LEAN MASS MODELS

Table 67: Regression Model Summaries of Tissue-Specific Analyses for Adjusted Fat Mass in Males

Tissue	Genotype Terms	p-value	R^2
Muscle	No Model		
Adipose	PPARg2*FABP4-2b UCP1-2*FABP4-2b	0.017	0.027
Intestine	UCP2-8*FABP2p-ID UCP2-8*FABP2p-834 FABP2p-ID*FABP2p-834	0.003	0.057
Combined Model	UCP2-8 PPARg2*FABP4-2b UCP1-2*FABP4-2b UCP2-8*FABP2p-ID UCP2-8*FABP2p-834	<0.001	0.095

Table 68: Regression Model Summaries of Tissue-Specific Analyses for Adjusted Lean Mass in Males

Tissue	Genotype Terms	p-value	R^2
Muscle	PPARa5*UCP3-5	0.025	0.016
Adipose	UCP2-4*FABP4-2b	0.033	0.015
Intestine	PPARb6*UCP2-4 UCP2-4*FABP2p-834 UCP2-8*FABP2p-834	0.002	0.058
Combined Model	PPARb6*UCP2-4 UCP2-4*FABP4-2b UCP2-4*FABP2p-834 UCP2-8*FABP2p-834	0.001	0.074

Table 69: Regression Model Summaries of Tissue-Specific Analyses for Adjusted Fat Mass in Females

Tissue	Genotype Terms	p-value	R^2
Muscle	UCP3-5*FABP3p-313	0.001	0.033
Adipose	No Model		
Intestine	No Model		
Combined Model	UCP3-5*FABP3p-313	0.001	0.033

Table 70: Regression Model Summaries of Tissue-Specific Analyses for Adjusted Lean Mass in Females

Tissue	Genotype Terms	p-value	R^2
Muscle	No Model		
Adipose	FABP4p-376 UCP1-2*UCP2-8 UCP1-2*FABP4p-376 UCP2-4*UCP2-8	0.003	0.056
Intestine	UCP2-4 UCP2-8 PPARb6*UCP2-8 UCP2-4*FABP2p-834	<0.001	0.085
Combined Model	UCP2-4 FABP2p-834 FABP4p-376 PPARb6*UCP2-8 UCP1-2*UCP2-8 UCP1-2*FABP4p-376 UCP2-4*UCP2-8 UCP2-4*FABP2p-834	<0.001	0.155

APPENDIX H

PROMOTER ACTIVITY ASSAYS

Table 71: Protocol for Control Experiment

	pGL3 Control (µg)	pRL-TK (µg)	Lipofect-AMINE Reagent (µl)	PLUS Reagent (µl)	Media for Dilution (µl)
pGL3 Control	1.0	--	3.0	3.0	100
pRL-TK	--	1.0	3.0	3.0	100
pGL3 Control + pRL-TK	1.0	1.0	6.0	6.0	100

Table 72: Protocol for Transfection Experiment

	pGL3 Vector (µg)	pRL-TK (µg)	Lipofect-AMINE Reagent (µl)	PLUS Reagent (µl)	Media for Dilution (µl)
pGL3 Control	1.0	1.0	6.0	6.0	100
PGL3 Basic	1.0	1.0	6.0	6.0	100
pGL3-I	3.0	1.0	12.0	12.0	100
pGL3-D	3.0	1.0	12.0	12.0	100

Table 73: FABP2 Luciferase Assay Readings

	Luciferase Reading	*Renilla* Reading	Ratio (Luciferase:*Renilla*)	% of pGL3-Control Expression
Experiment 1				
pGL3-Control	1925	710.9	2.707835	
pGL3-Basic	0.951	1134.0	0.000839	
pGL3-Ins	1.798	298.1	0.006032	0.2228
pGL3-Del	1.044	494.9	0.002110	0.0779
Experiment 2				
pGL3-Control	2068	1446.0	1.430150	
pGL3-Basic	0.953	1542.0	0.000620	
pGL3-Ins	1.412	462.1	0.003050	0.2133
pGL3-Del	1.023	**659.1**	0.001550	0.1084
Experiment 3				
pGL3-Control*	8333	358.8	23.605069	
pGL3-Basic	54.61	7618.0	0.007169	
pGL3-Ins1	14.76	316.8	0.046591	0.1974
pGL3-Ins2	12.18	292.2	0.041684	0.1766
pGL3-Ins3	13.07	247.0	0.052915	0.2242
pGL3-Del1	8.277	264.5	0.031293	0.1326
pGL3-Del2	6.519	231.0	0.028221	0.1196
pGL3-Del3	7.344	301.2	0.024382	0.1033

Table 74: FABP3 Luciferase Assay Readings

	Luciferase Reading	*Renilla* Reading	Ratio (Luciferase:*Renilla*)	% of pGL3-Control Expression
pGL3-Control	3515	94.85	37.058513	
pGL3-Basic	4.486	247.5	0.181253	
pGL3-Del1	51.80	79.09	0.654950	1.7673
pGL3-Del2	41.47	87.47	0.474105	1.2793
pGL3-Del3	57.80	85.34	0.677291	1.8276
pGL3-Ins1	61.74	84.24	0.732910	1.9778
pGL3-Ins2	31.25	76.48	0.408604	1.1026
pGL3-Ins3	32.20	76.96	0.418399	1.1290

Phenol:Chloroform Purification

1. Prepare chloroform:isoamylalcohol was by adding 1 volume of isoamylalcohol to 24 volumes of chloroform.

2. Prepare phenol:chloroform was by adding equal volumes of phenol and the chloroform:isoamylalcohol mixture.

3. Dilute the plasmid DNA to a final volume of 200µl with dH_2O.

4. Add 200µl of phenol:chloroform.

5. Vortex the mixture and centrifuge for 4 minutes.

6. Transfer the aqueous phase to a clean tube.

7. Add 200µl of chloroform:isoamylalcohol (24:1).

8. Vortex the mixture and centrifuged for 4 minutes.

9. Transfer the aqueous phase to a clean tube.

10. Bring the volume of the extract back up to 200µl with dH_2O.

11. Add 700µl of chilled 100% ethanol, 100µl of 10M NH_4OAc, and of 3µl glycogen (20µg/µl) to the extract to precipitate the DNA.

12. Vortex the mixture and place it on dry ice for 15 minutes.

13. Centrifuge the mixture for 20 minutes and remove the ethanol.

14. Wash the pellet twice with 900µl of 70% ethanol and air-dry.

15. Resuspend the pellet in 40µl of dH_2O to a final concentration of ~100µg/ml.

Recipe for LB Broth/Agar

Bacto Tryptone	10g
Yeast Extract	5g
NaCl	9g
dH_2O	up to 1 Liter

1. Mix completely.
2. Pull off ~500ml for agar plates and add 7.5g Bacto Agar.
3. Cap both bottles (one of agar and one of broth) loosely and autoclave.
4. Cool to the touch.
5. Add Antibiotic:

   Ampicillin 500μl of a 50mg/ml stock (final [ ]: 50μg/ml)

6. Pour the LB Agar into petri plates.
7. Store agar plates and broth at 4^oC.

BIBLIOGRAPHY

BIBLIOGRAPHY

Acín A, Rodriguez M, Rique H, Canet E, Boutin JA, Galizzi JP (1999) Cloning and characterization of the 5' flanking region of the human uncoupling protein 3 (UCP3) gene. *Biochemical and Biophysical Research Communications* 258:278-283

Adams SH (2000) Uncoupling protein homologs: emerging views of physiological function. *Journal of Nutrition* 130:711-714

Agren JJ, Valve R, Vidgren H, Laakso M, Uusitupa M (1998) Postprandial lipemic response is modified by the polymorphism at codon 54 of the fatty acid binding protein 2 gene. *Arteriosclerosis, Thrombosis, and Vascular Biology* 18:1606-1610

American Diabetes Association (2002) Report of the expert committee on the diagnosis and classification of diabetes mellitus. *Diabetes Care* 25:S5-S20

Argyropoulos G, Brown AM, Willi SM, Zhu J, He Y, Reitman M, Gevao SM, Spruill I, Garvey WT (1998) Effects of mutations in the human uncoupling protein 3 gene on the respiratory quotient and fat oxidation in severe obesity and type 2 diabetes. *Journal of Clinical Investigaton* 102:1345-1351

Arsenijevic D, Onuma H, Pecqueur C, Raimbault S, Manning BS, Miroux B, Couplan E, Alves-Guerra MC, Goubern M, Surwit R, Bouillaud F, Richard D, Collins S, Ricquier D (2000) Disruption of the uncoupling protein-2 gene in mice reveals a role in immunity and reactive oxygen species production. *Nature Genetics* 26:435-439

Astrup A, Toubro S, Dalgaard LT, Urhammer SA, Sorensen TIA, Pedersen O (1999) Impact of the v/v 55 polymorphism of the uncoupling protein 2 gene on 24-h energy expenditure and substrate oxidation. *International Journal of Obesity* 23:1031-1034

Baier LJ, Sacchettini JC, Knowler WC, Eads J, Paolisso G, Tataranni PA, Mochizuki H, Bennett PH, Bogardus C, Prochazka M (1995) An amino acid substitution in the human intestinal fatty acid binding protein is associated with increased fatty acid binding, increased fat oxidation, and insulin resistance. *Journal of Clinical Investigation* 95:1281-1287

Baier LJ, Bogardus C, Sacchettini JC (1996) A polymorphism in the human intestinal fatty acid binding protein alters fatty acid transport across Caco-2 cells. *The Journal of Biological Chemistry* 271:10892-10896

Bao S, Kennedy A, Wojciechowski B, Wallace P, Ganaway E, Garvey T (1998) Expression of mRNAs encoding uncoupling proteins in human skeletal muscle: effects of obesity and diabetes. *Diabetes* 47:1935-1940

Barsh GS, Farooqi IS, O'Rahilly S (2000) Genetics of body-weight regulation. *Nature* 404:644-651

Bernlohr DA, Simpson MA, Vogel Hertzel A, Banaszak LJ (1997) Intracellular lipid-binding proteins and their genes. *Annual Review of Nutrition* 17:277-303

Binas B, Danneberg H, McWhir J, Mullins L, Clark AJ (1999) Requirement for the heart-type fatty acid binding protein in cardiac fatty acid utilization. *FASEB Journal* 13:805-812

Birnbaum MJ (2001) Dialogue between muscle and fat. *Nature* 409:672-673

Bouchard C, Perusse L, Chagnon YC, Warden C, Ricquier D (1997) Linkage between markers in the vicinity of the uncoupling protein 2 gene and resting metabolic rate in humans. *Human Molecular Genetics* 6:1887-1889

Boss O, Samec S, Paoloni-Giacobino A, Rossier C, Dulloo A, Seydoux J, Muzzin P, Giacobino JP (1997) Uncoupling protein-3: a new member of the mitochondrial carrier family with tissue-specific expression. *FEBS Lett* 408:39-42

Boss O, Samec S, Kuhne F, Bijlenga P, Assimacopoulos-Jeannet F, Seydoux J, Giacobino JP, Muzzin P (1998a) Uncoupling protein-3 expression in rodent skeletal muscle is modulated by food intake but not by changes in environmental temperature. *Journal of Biological Chemistry* 273:5-8

Boss O, Bobbioni-Harsch E, Assimacopoulos-Jeannet F, Muzzin P, Munger R, Giacobino JP, Golay A (1998b) Uncoupling protein-3 expression in skeletal muscle and free fatty acids in obesity. *The Lancet* 351:1933

Boss O, Giacobino JP, Muzzin P (1998c) Genomic structure of uncoupling protein-3 (UCP3) and its assignment to chromosome 11q13. *Genomics* 47:425-426

Boss O, Hagen T, Lowell BB (2000) Uncoupling proteins 2 and 3: Potential regulators of mitochondrial energy metabolism. *Diabetes* 49:143-156

Brand MD, Chien LF, Ainscow EK, Rolfe DFS, Porter RK (1994) The causes and functions of mitochondrial proton leak. *Biochimica et Biophysica Acta* 1187:132-139

Brand MD, Brindle KM, Buckingham JA, Harper JA, Rolfe DFS, Stuart JA (1999) The significance and mechanism of mitochondrial proton conductance. International Journal of Obesity and Related Metabolic Disorders 23:S4-S11

Brownlee M (2001) Biochemistry and molecular cell biology of diabetic complications. *Nature* 414:813-820

Brun S, Carmona MC, Mampel T, Vinas O, Giralt M, Iglesias R, Villarroya F (1999) Uncoupling protein-3 gene expression in skeletal muscle during development is regulated by nutritional factors that alter circulating non-estrified fatty acids. *FEBS Letters* 453:205-209

Cadenas S, Buckingham JA, Samec S, Seydoux J, Din N, Dulloo AG, Brand MD (1999) UCP2 and UCP3 rise in starved rat skeletal muscle by mitochondrial proton conductance is unchanged. *FEBS Letters* 462:257-260

Carlsson M, Orho-Melander M, Hedenbro J, Almgren P, Groop L (2000) The T 54 allele of the intestinal fatty acid binding protein 2 is associated with a parental history of stroke. *The Journal of Clinical Endocrinology & Metabolism* 85:2801-2804

Cassard AM, Bouillaud F, Mattei MG, Hentz E, Raimbault S, Thomas M, Ricquier D (1990) Human uncoupling protein gene: structure, comparison with rat gene, and assignment to the long arm of chromosome 4. *Journal of Cellular Biochemistry* 43:255-265

Cassell PG, Neverova M, Janmohamed S, Uwakwe N, Qureshi A, McCarthy MI, Saker PJ, Albon L, Kopelman P, Noonan K, Easlick J, Ramachandran A, Snehalatha C, Pecqueur C, Picquier D, Warden C, Hitman GA (1999) An uncoupling protein 2 gene variant is associated with a raised body mass index but not type II diabetes. *Diabetologia* 42:688-692

Chan CB, MacDonald PE, Saleh MC, Johns DC, Marbàn E, Wheeler MB (1999) Overexpression of uncoupling protein 2 inhibits glucose-stimulated insulin secretion from rat islets. *Diabetes* 48:1482-1486

Chan CB, De Leo D, Joseph JW, McQuaid TS, Ha XF, Xu F, Tsushima RG, Pennefather PS, Salapatek AMF, Wheeler MB (2001) Increased uncoupling protein-2 levels in β-cells are associated with impaired glucose-stimulated insulin secretion: mechanism of action. *Diabetes* 50:1302-1310

Chen X, Levine L, Kwok PY (1999) Fluorescence polarization in homogeneous nucleic acid analysis. *Genome Research* 9:492-498

Chevillotte E, Rieusset J, Roques M, Desage M, Vidal H (2001) The regulation of uncoupling protein-2 gene expression by ω-6 polyunsaturated fatty acids in human skeletal muscle cells involves multiple pathways, including the nuclear receptor peroxisome proliferator-activated receptor β. *The Journal of Biological Chemistry* 276:10853-10860

Chiu KC, Chuang LM, Yoon C (2001) Fatty acid binding protein 2 and insulin resistance. *European Journal of Clinical Investigation* 31:521-527

Claffey KP, Herrera VL, Brecher P, Ruiz-Opazo N (1987) Cloning and tissue distribution of rat heart fatty acid binding protein mRNA: identical forms in heart and skeletal muscle. *Biochemistry* 26:7900-7904

Clapham JC, Arch JRS, Chapman H, Haynes A, Lister C, Moore GBT, Piercy V, Carter SA, Lehner I, Smith SA, Beeley LJ, Godden RJ, Herrity N, Skehel M, Changani KK, Hockings PD, Reid DG, Squires SM, Hatcher J, Trail B, Latcham J, Rastan S, Harper AJ, Cadenas S, Buckingham JA, Brand MD, and Abuin A (2000) Mice overexpressing human uncoupling protein-3 in skeletal muscle are hyperphagic and lean. *Nature* 406: 415-418

Clement K, Ruiz J, Cassard-Doulcier AM, Bouillaud F, Ricquier D, Basdevant A, Guy-Grand B, Froguel P (1996) Additive effect of A→G (-3826) variant of the uncoupling protein gene and the Trp64Arg mutation of the beta 3-adrenergic receptor gene on weight gain in morbid obesity. *International Journal of Obesity and Related Metabolic Disorders* 20:1062-1066

Cortright RN, Zheng D, Jones JP, Fluckey JD, DiCarlo SE, Grujic D, Lowell BB, Dohm GL (1999) Regulation of skeletal muscle UCP-2 and UCP-3 gene expression by exercise and denervation. *American Journal of Physiology* 276:E217-E221

Crisman TS, Claffey KP, Saouaf R, Hanspal J, Brecher P (1987) Measurement of rat heart fatty acid binding protein by ELISA: tissue distribution, developmental changes and subcellular distribution. *Journal of Molecular and Cellular Cardiology* 19:423-431

Dalgaard LT, Sorensen TIA, Andersen T, Hansen T, Pedersen O (1999) An untranslated insertion variant in the uncoupling protein 2 gene is not related to body mass index and changes in body weight during a 26-year follow-up in Danish Caucasian men. *Diabetologia* 42:1413-1416

Dalgaard LT & Pedersen O (2001a) Uncoupling proteins: functional characteristics and role in the pathogenesis of obesity and type 2 dibetes. *Diabetologia* 44:946-965

Dalgaard LT, Sørensen TIA, Drivsholm T, Borch-Johnsen K, Andersen T, Hansen T, Pedersen O (2001b) A prevalent polymorphism in the promoter of the UCP3 gene and its relationship to body mass

index and long term body weight change in the Danish population. *The Journal of Clinical Endocrinology & Metabolism* 86:1398-1402

Devlin B & Risch N (1995) A comparison of linkage disequilibrium measures for fine-scale mapping. *Genomics* 29:311-322

Dreyer C, Keller H, Mahfoudi A, Laudet V, Krey G, Wahli W (1993) Positive regulation of the peroxisomal beta-oxidation pathway by fatty acids through activation of peroxisome proliferator-activated receptors (PPAR). *Biology of the Cell* 77:67-76

Dutta-Roy AK (2000) Cellular uptake of long-chain fatty acids: role of membrane-asociated fatty-acid-binding/transport proteins. *Cellular and Molecular Life Sciences* 57:1360-1372

Elbrecht A, Chen Y, Cullinan CA, Hayes N, Leibowitz MD, Moller DE, Berger J (1996) Molecular cloning, expression and characterization of human peroxisome proliferator activated receptors gamma-1 and gamma-2. *Biochemical and Biophysical Research Communications* 224:431-437

Enerback S, Jacobsson A, Simpson EM, Guerra C, Yamashita H, Harper ME, Kozak LP (1997) Mice lacking mitochondrial uncoupling protein are cold-sensitive but not obese. *Nature* 387:90-94

Esterbauer H, Oberkofler H, Liu YM, Breban D, Hell E, Krempler F, Patsch W (1998) Uncoupling protein-1 mRNA expression in obese human subjects: the role of sequence variations at the uncoupling protein-1 gene locus. *Journal of Lipid Research* 39:834-844

Esterbauer H, Oberkofler H, Dallinger G, Breban D, Hell E, Krempler F, Patsch W (1999) Uncoupling protein-3 gene expression: reduced skeletal muscle mRNA in obese humans during pronounced weight loss. *Diabetologia* 42:302-309

Esterbauer H, Schneitler C, Oberkofler H, Ebenbichler C, Paulweber B, Sandhofer F, Ladurner G, Hell E, Strosberg AD, Patsch JR, Krempler F, Patsch W (2001) A common polymorphism in the promoter of UCP2 is associated with decreased risk of obesity in middle-aged humans. *Nature Genetics* 28:178-183

Evans D, Minouchehr S, Hagemann G, Mann WA, Wendt D, Wolf A, Beisiegel U (2000) Frequency of and interaction between polymorphisms in the beta3-adrenergic receptor and in uncoupling proteins 1 and 2 and obesity in Germans. *International Journal of Obesity and Related Metabolic Disorders* 24:1239-1245

Flier JS & Lowell BB (1997) Obesity research springs a proton leak. *Nature Genetics* 15:223-224

Fleury C, Neverova M, Collins S, Raimbault S, Champigny O, Levi-Meyrueis C, Bouillaud F, Seldin MF, Surwit RS, Ricquier D, Warden CH (1997) Uncoupling protein-2: a novel gene linked to obesity and hyperinsulinemia. *Nature Genetics* 15:269-272

Friedman JM (2000) Obesity in the new millennium. *Nature* 404:632-634

Fujimoto WY (2000) The importance of insulin resistance in the pathogenesis of type 2 diabetes mellitus. *American Journal of Medicine* 108:9S-14S

Fumeron F, Durack-Bown I, Betoulle D, Cassard-Doulcier AM, Tuzet S, Bouillaud F, Melchior JC, Ricquier D, Apfelbaum M (1996) Polymorphisms of uncoupling protein (UCP) and beta 3 adrenoreceptor genes in obese people submitted to low calorie diet. *International Journal of Obesity and Related Metabolic Disorders* 20:1051-1054

Gagnon J, Lago F, Chagnon YC, Pérusse L, Näslund I, Lissner L, Sjöström L, Bouchard C (1998) DNA polymorphism in the uncoupling protein 1 (UCP1) gene has no effect on obesity related phenotypes in the Swedish Obese Subjects cohorts. *International Journal of Obesity* 22:500-505

Galluzzi JR, Cupples LA, Otvos JD, Wilson PWF, Schaefer EJ, Ordovas JM (2001a) Association of the A/T54 polymorphism in the intestinal fatty acid binding protein with variations in plasma lipids in the Framingham Offspring Study. *Atherosclerosis* 159:417-424

Galluzzi JR, Cupples LA, Meigs JB, Wilson PWF, Schaefer EJ, Ordovas JM (2001b) Association of the ala54-thr polymorphism in the intestinal fatty acid binding protein with 2-h postchallenge insulin levels in the Framingham Offspring Study. *Diabetes Care* 24:1161-1166

Gardner LI, Stern MP, Haffner SM, Gaskill SP, Hazuda HP, Relethford JH, Eifler CW (1984) Prevalence of diabetes in Mexican Americans: relationship to percent of gene pool derived from Native American sources. *Diabetes* 33:86-92

Georgopoulos A, Aras O, Tsai MY (2000) Codon-54 polymorphism of the fatty acid biding protein 2 gene is associated with elevation of fasting and postprandial triglyceride in type 2 diabetes. *The Journal of Clinical Endocrinology & Metabolism* 85:3155-3160

Gimeno RE, Dembski M, Weng X, Deng N, Shyjan AW, Gimeno CJ, Iris F, Ellis SJ, Woolf EA, Tartaglia LA (1997) Cloning and characterization of an uncoupling protein homolog: a potential molecular mediator of human thermogenesis. *Diabetes* 46:900-906

Glatz JFC, Vork MM, Cistola DP, van der Vusse GJ (1993) Cytoplasmic fatty acid binding protein: Significance for intracellular transport of fatty acids and putative role in signal transduction pathways. *Prostaglandins Leukotrienes and Essential Fatty Acids* 48:33-41

Glatz JFC, Borchers T, Spener F, van der Vusse GJ (1995) Fatty acids in cell signalling: modulation by lipid binding proteins. *Prostaglandins Leukotrienes and Essential Fatty Acids* 52:121-127

Glatz JFC, Luiken JJFP, van Nieuwenhoven FA, van der Vusse GJ (1997) Molecular mechanism of cellular uptake and intracellular translocation of fatty acids. *Prostaglandins Leukotrienes and Essential Fatty Acids* 57:3-9

Glatz JFC & Storch J (2001) Unravelling the significance of cellular fatty acid-binding proteins. *Current Opinion in Lipidology* 12:267-274

Gong DW, He Y, Karas M, Reitman M (1997) Uncoupling protein-3 is a mediator of thermogenesis regulated by thyroid hormone, β3-adrenergic agonists, and leptin. *The Journal of Biological Chemistry* 272:24129-24132

Gong DW, He Y, Reitman ML (1999) Genomic organization and regulation by dietary fat of the uncoupling protein 3 and 2 genes. *Biochemical and Biophysical Research Communications* 256:27-32

Gong DW, Monemdjou S, Gavrilova O, Leon LR, Marcus-Samuels B, Chou CJ, Everett C, Kozak LP, Li C, Deng C, Harper ME, Reitman ML (2000) Lack of obesity and normal response to fasting and thyroid hormone in mice lacking uncoupling protein-3. *The Journal of Biological Chemistry* 275:16251-16257

Gura, T (1998) Uncoupling proteins provide new clue to obesity's causes. *Science* 280:1369-1370

Hamilton JA & Kamp F (1999) How are free fatty acids transported in membranes? Is it by proteins or by free diffusion through the lipids? *Diabetes* 48:2255-2269

Hamann A, Tafel J, Büsing B, Münzberg H, Hinney A, Mayer H, Siegfried W, Ricquier D, Greten H, Hebebrand J, Matthaei S (1998) Analysis of the uncoupling protein-1 (UCP1) gene in obese and lean subjects: identification of four amino acid variants. *International Journal of Obesity* 22:939-941

Hamman RF, Marshall JA, Baxter J, Kahn LB, Mayer EJ, Orleans M, Murphy JR, Lezotte DC (1989) Methods and prevalence of non-insulin-dependent diabetes mellitus in a biethnic Colorado population: The San Luis Valley Diabetes Study. *American Journal of Epidemiology* 129:295-311

Harper ME & Himms-Hagen J (2001) Mitochondrial efficiency: lessons learned from transgenic mice. *Biochimica et Biophysica Acta* 1504:159-172

Hashimoto L, Habita C, Beressi JP, et al. (1994) Genetic mapping of susceptibility locus for insulin-dependent dibetes mellitus on chromosome 11q. *Nature* 371:161-164

Heilbronn LK, Kind KL, Pancewicz E, Morris AM, Noakes M, Clifton PM (2000) Association of –3826 G variant in uncoupling protein-1 with increased BMI in overweight Australian women. Diabetologia 43:242-244

Helledie T, Antonius M, Sørensen RV, Hertzel AV, Bernlohr DA, Kølvraa S, Kristiansen K, Mandrup S (2000) Lipid-binding proteins modulate ligand-dependent *trans*-activation by peroxisome proliferator-activated receptors and localize to the nucleus as well as the cytoplasm. *Journal of Lipid Research* 41:1740-1751

Hotamisligil GS, Johnson RS, Distel RJ, Ellis R, Papaioannou VE, Spiegelman BM (1996) Uncoupling of obesity from insulin resistance through a targeted mutation in aP2, the adipocyte fatty acid binding protein. *Science* 274:1377-1379

Issemann I, Prince R, Tugwood J, Green S (1992) A role for fatty acids and liver fatty acid binding protein in peroxisome proliferation? *Biochemical Society Transactions* 20:824-827

Kahn CR, Vicent D, Doria A (1996) Genetics of non-insulin-dependent (Type II) diabetes mellitus. *Annual Review of Medicine* 47:509-531

Kersten S, Desvergne B, Wahli W (2000) Roles of PPARs in health and disease. *Nature* 405:421-424

Khalfallah Y, Fages S, Laville M, Langin D, Vidal H (2000) Regulation of uncoupling protein-2 and uncoupling protein-3 expression during lipid infusion in human skeletal muscle and subcutaneous adipose tissue. *Diabetes* 49:25-31

Klaus S, Casteilla L, Bouillaud F, Ricquier D (1991) The uncoupling protein UCP: a membraneous mitochondrial ion carrier exclusively expressed in brown adipose tissue. *International Journal of Biochemistry* 23:791-801

Klingenberg M (1999) Uncoupling protein: a useful energy dissipator. *Journal of Bioenergetics and Biomembranes* 31:419-430

Kopelman PG (2000) Obesity as a medical problem. *Nature* 404, 635-643

Kozak LP & Harper ME (2000) Mitochondrial uncoupling proteins in energy expenditure. *Annual Review of Nutrition* 20:339-363

Lanouette CM, Chagnon YC, Rice T, Pérusse L, Muzzin P, Giacobino JP, Gagnon J, Wilmore JH, Leon AS, Skinner JS, Rao DC, Bouchard C (2002) Uncoupling protein 3 gene is associated with body composition changes with training in HERITAGE study. *Journal of Applied Physiology* 92:1111-1118

Lawrence JW, Kroll DJ, Eacho PI (2000) Ligand-dependent interaction of hepatic fatty acid-binding protein with the nucleus. *Journal of Lipid Research* 41:1390-1401

Life Technologies. LipofectAMINE PLUS Reagent Specification Sheet and Protocol. Form #18057N.

LjL Biosystems. SNP Genotyping with an HEFP-Based Assay. Application Notes.

Lönnqvist F, Nordfors L, Schalling M (1999) Leptin and its potential role in human obesity. *Journal of Internal Medicine* 245:643-652

Lowell BB & Spiegelman BM (2000) Towards a molecular understanding of adaptive thermogenesis. *Nature* 404:652-660

Matthews DR, Hosker JP, Rudenski AS, Naylor BA, Treacher DF, Turner RC (1985) Homeostasis model assessment: insulin resistance and β-cell function from fasting plasma glucose and insulin concentrations in man. *Diabetologia* 28:412-419

Moffett SP (2002) The PPAR pathway to obesity and type 2 diabetes: a multi-locus approach to understanding complex disease. PhD Thesis, University of Pittsburgh Department of Human Genetics, Pittsburgh, PA.

Monemdjou S, Kozak LP, Harper ME (1999) Mitochondrial proton leak in brown adipose tissue mitochondria of *Ucp1*-deficient mice is GDP insensitive. *American Journal of Physiology-Endocrinology and Metabolism* 276:E1073-E1082

Monemdjou S, Hofmann WE, Kozak LP, Harper ME (2000) Increased mitochondrial proton leak in skeletal muscle mictochondria of UCP1-deficient mice. *American Journal of Physiology-Endocrinology and Metabolism* 279:E941-E946

Moore GBT, Himms-Hagen J, Harper ME, Clapham JC (2001) Overexpression of UCP-3 in skeletal muscle of mice results in increased expression of mitochondrial thioesterase mRNA. *Biochemical and Biophysical Research Communications* 283:785-790

Mori H, Okazawa H, Iwamoto K, Maeda E, Hashiramoto M, Kasuga M (2001) A polymorphism in the 5' untranslated region and a $met^{229}\rightarrow leu$ variant in exon 5 of the human UCP1 gene are associated with susceptibility to type II diabetes mellitus. *Diabetologia* 44:373-376

Millet L, Vidal H, Andreelli F, Larrouy D, Riou JP, Ricquier D, Laville M, Langin D (1997) Increased uncoupling protein-2 and –3 mRNA expression during fasting in obese and lean humans. *Journal of Clinical Investigation* 100:2665-2670

National Cholesterol Education Program (2001) Executive Summary of the Third Report of the National Cholesterol Education Program (NCEP) Expert Panel on Detection, Evaluation, and Treatment of High Blood Cholesterol in Adults (Adult Treatment Panel III). *JAMA* 285:2486-2497

Oberkofler H, Dallinger G, Liu YM, Hell E, Krempler F, Patsch W (1997) Uncoupling protein gene: quantification of expression levels in tissues of obese and non-obese humans. *Journal of Lipid Research* 38:2125-2133

Oberkofler H, Liu YM, Esterbauer H, Hell E, Krempler F, Patsch W (1998) Uncoupling protein-2 gene: reduced mRNA expression in intraperitoneal adipose tissue of obese humans. *Diabetologia* 41:940-946

Oppert JM, Vohl MC, Chagnon M, Dionne FT, Cassard-Doulcier AM, Ricquier D, Pérusse L, Bouchard C (1994) DNA polymorphism in the uncoupling protein (UCP) gene and human body fat. *International Journal of Obesity and Related Metabolic Disorders* 18:526-531

Otabe S, Clement K, Rich N, Warden C, Pecqueur C, Neverova M, Raimbault S, Guy-Grand B, Basdebant A, Ricquier D, Froguel P, Vasseur F (1998) Mutation screening of the human UCP2 gene in normoglycemic and NIDDM morbidly obese patients: lack of association between new UCP2 polymorphisms and obesity in French Caucasians. *Diabetes* 47:840-842

Otabe S, Clement K, Dubois S, Lepretre F, Pelloux V, Leibel R, Chung W, Boutin P, Guy-Grand B, Froguel P, Vasseur F (1999) Mutation screening and association studies of the human uncoupling protein 3 gene in normoglycemic and diabetic morbidly obese patients. *Diabetes* 48:206-208

Otabe S, Clement K, Dina C, Pelloux V, Guy-Grand B, Froguel P, Vasseur F (2000) A genetic variation in the 5' flanking region of the UCP3 gene is associated with body mass index in humans in interaction with physical activity. *Diabetologia* 43:245-249

Pecqueur C, Cassard-Doulcier AM, Raimbault S, Miroux B, Fleury C, Gelly C, Bouillaud F, Ricquier D (1999) Functional organization of the human uncoupling protein-2 gene, and juxtaposition to the uncoupling protein-3 gene. *Biochemical and Biophysical Research Communications* 255:40-46

Pihlajamäki J, Rissanen J, Heikkinen S, Karjalainen L, Laakso (1997) Codon 54 polymorphism of the human intestinal fatty acid binding protein 2 gene is associated with dyslipidemias but not with insulin resistance in patients with familial combined hyperlipidemia. *Arteriosclerosis, Thrombosis, and Vascular Biology* 17:1039-1044

Poirier H, Niot I, Monnot MC, Braissant O, Meunier-Durmort C, Costet P, Pineau T, Wahli W, Willson TM, Besnard P (2001) Differential involvement of peroxisome-proliferator-activated receptors α and δ in fibrate and fatty-acid-mediated inductions of the gene encoding liver fatty-acid-binding protein in the liver and the small intestine. *Biochemistry Journal* 355:481-488

Promega Corporation (1999) Dual-Luciferase Reporter Assay System. Technical Manual No. 040.

Promega Corporation (2001) pGL3 Luciferase Reporter Vectors. Technical Manual No. 033.

Promega Corporation (2000) pRL-TK Vector. Technical Bulletin No. 240.

Razzaghi H & Kamboh MI (2001) A highly sensitive and nonradioactive mutation detection method based on vertical gradient temperature single-stranded conformation polymorphism. *Electrophoresis* 22:2665-2669

Ribarik Coe N, Simpson MA, Bernlohr DA (1999) Targeted disruption of the adipocyte lipid-binding protein (aP2 protein) gene impairs fat cell lipolysis and increases cellular fatty acid levels. *Journal of Lipid Research* 40:967-972

Ricquier D & Bouillaud F (2000) Mitochondrial uncoupling proteins: from mitochondria to the regulation of energy balance. *Journal of Physiology* 529:3-10

Samec S, Seydoux J, Dulloo AG (1998a) Interorgan signaling between adipose tissue metabolism and skeletal muscle uncoupling protein homologs: Is there a role for circulating free fatty acids? *Diabetes* 47:1693-1698

Samec S, Seydoux J, Dulloo AG (1998b) Role of UCP homologues in skeletal muscles and brown adipose tissue: Mediators of thermogenesis or regulators of lipids as fuel substrate? *The FASEB Journal* 12:715-724

Samec S, Seydoux J, Dulloo AG (1999) Skeletal muscle UCP3 and UCP2 gene expression in response to inhibition of free fatty acid flux through mitochondrial ß-oxidation. *European Journal of Physiology* 438:452-457

Schäffler A, Palitzsch KD, Watzlawek E, Drobnik W, Schwer H, Schölmerich J, Schmitz G (1999) Frequency and significance of the A→G (-3826) polymorphism in the promoter of the gene for uncoupling protein-1 with regard to metabolic parameters and adipocyte transcription factor binding in a large population-based Caucasian cohort. *European Journal of Clinical Investigation* 29:770-779

Schrauwen P, Xia J, Walder K, Snitker S, Ravussin E (1999a) A novel polymorphism in the proximal UCP3 promoter region: Effect on skeletal muscle UCP3 mRNA expression and obesity in male non-diabetic Pima Indians. *International Journal of Obesity Related Metabolic Disorders* 23:1242-1245

Schrauwen P, Xia J, Bogardus C, Pratley RE, Ravussin E (1999b) Skeletal muscle uncoupling protein 3 expression is a determinant of energy expenditure in Pima Indians. *Diabetes* 48:146-149

Silva JE & Rabelo R (1997) Regulation of the uncoupling protein gene expression. *European Journal of Endocrinology* 136:251-264

Sipilainen R, Uusitupa M, Heikkinen S, Rissanen A, Laakso M (1997) Variants in the human intestinal fatty acid binding protein 2 gene in obese subjects. *Journal of Clinical Endocrinology and Metabolism* 82:2629-2632

Solanes G, Vidal-Puig A, Grujic D, Flier JS, Lowell BB (1997) The human uncoupling protein-3 gene: Genomic structure, chromosomal localization, and genetic basis for short and long form transcripts. *The Journal of Biological Chemistry* 272:25433-25436

Stuart JA, Cadenas S, Jekabsons MB, Roussel D, Brand MD (2001) Mitochondrial proton leak and the uncoupling protein 1 homologues. *Biochimica et Biophysica Acta* 1504:144-158

Surwit RS, Wang S, Petro AE, Sanchis D, Raimbault S, Ricquier D, Collins S (1998) Diet-induced changes in uncoupling proteins in obesity-prone and obesity-resistant strains of mice. *Proceedings of the National Academy of Science USA* 195:4061-4065

Sweetser DA, Birkenmeier EH, Klisak IJ, Zollman S, Sparkes RS, Mohandas T, Lusis AJ, Gordon JI (1987) The human and rodent intestinal fatty acid binding protein genes: a comparative analysis of their structure, expression, and linkage relationships. *The Journal of Biological Chemistry* 262:16060-16071

Taber CW. *Taber's Cyclopedic Medical Dictionary*. Philadelphia: F.A. Davis Company, 1997.

Tsuboyama-Kasaoka N, Tsunoda N, Maruyama K, Takahashi M, Kim H, Ikemoto S, Ezaki O (1998) Up-regulation of uncoupling protein 3 (UCP3) mRNA by exercise training and down-regulation of UCP3 by denervation in skeletal muscles. *Biochemical and Biophysical Research Communications* 247:498-503

Tu N, Chen H, Winnikes U, Reinert I, Marmann G, Pirke KM, Lentes KU (1999) Structural organization and mutational analysis of the human uncoupling protein-2 (hUCP2) gene. *Life Sciences* 64:PL41-PL50

Tu N, Chen H, Winnikes U, Reinert I, Marmann G, Pirke KM, Lentes KU (2000) Functional characterization of the 5'-flanking and the promoter region of the human UCP3 (hUCP3) gene. *Life Sciences* 67:2267-2279

Urhammer SA, Fridberg M, Sorensen TIA, Echwald SM, Andersen T, Tybjaerg-Hansen A, Clausen JO, Pedersen O (1997a) Studies of genetic variability of the uncoupling protein 1 gene in Caucasian subjects with juvenile-onset obesity. *Journal of Clinical Endocrinology and Metabolism* 82:4069-4074

Urhammer SA, Dalgaard LT, Sorensen TIA, Moller AM, Andersen T, Tybjaerg-Hansen A, Hansen T, Clausen JO, Vestergaard H, Pedersen O (1997b) Mutational analysis of the coding region of the uncoupling protein 2 gene in obese NIDDM patients: Impact of a common amino acid polymorphism on juvenile and maturity onset forms of obesity and insulin resistance. *Diabetologia* 40:1227-1230

Urhammer SA, Dalgaard LT, Sorensen TIA, Tybjaerg-Hansen A, Echwald SM, Andersen T, Clausen JO, Pedersen O (1998) Organisation of the coding exons and mutational screening of the uncoupling protein 3 gene in subjects with juvenile-onset obesity. *Diabetologia* 41:241-244

Valve R, Heikkinen S, Rissanen A Laakso M, Uusitupa M (1998) Synergistic effect of polymorphisms in uncoupling protein 1 and β3-adrenergic receptor genes on basal metabolic rate in obese Finns. *Diabetologia* 41:357-361

Vassileva G, Huwyler L, Poirier K, Agellon LB, Toth MJ (2000) The intestinal fatty acid binding protein is not essential for dietary fat absorption in mice. *FASEB Journal* 14:2040-2046

Vidal H, Langin D, Andreelli F, Millet L, Larrouy D, Laville M (1999) Lack of skeletal muscle uncoupling protein 2 and 3 mRNA induction during fasting in type-2 diabetic subjects. *American Journal of Physiology* 277:E830-E837

Vidal-Puig A, Solanes G, Grujic D, Flier JS, Lowell BB (1997) UCP3: an uncoupling protein homologue expressed preferentially and abundantly in skeletal muscle and brown adipose tissue. *Biochem Biophys Res Commun* 235:79-82

Vidal-Puig AJ, Grujic D, Zhang CY, Hagen T, Boss O, Ido Y, Szczepanik A, Wade J, Mootha V, Cortright R, Muoio DM, and Lowell BB (2000) Energy metabolism in uncoupling protein 3 gene knockout mice. *The Journal of Biological Chemistry* 275:16258-16266

Walder K, Norman FA, Hanson RL, Schrauwen P, Neverova M, Jenkinson CP, Daslick J, Warden CH, Pecqueur C, Raimbault S, Picquier D, Harper M, Silver K, Shuldiner AR, Solanes G, Lowell BB, Chung WK, Leibel RL, Pratley R, Ravussin E (1998) Association between uncoupling protein polymorphisms (UCP2-UCP3) and energy metabolism/obesity in Pima Indians. *Human Molecular Genetics* 7:1431-1435

Warden CH, Fisler JS, Shoemaker SM, Wen PZ, Svenson KL, Pace MJ, Lusis AJ (1995) Identification of four chromosomal loci determining obesity in a multifactorial mouse model. *Journal of Clinical Investigation* 95:1545-1552

Weigle DS, Selfridge LE, Schwartz MW, Seeley RJ, cummings DE, Havel PJ, Kuijper JL, BeltrandelRio H (1998) Elevated free fatty acids induce uncoupling protein 3 expression in muscle: A potential explanation for the effect of fasting. *Diabetes* 47:208-302

Willson TM, Brown PJ, Sternbach DD, Henke BR (2000) The PPARs: from orphan receptors to drug discovery. *Journal of Medicinal Chemistry* 43:527-550

Wolfrum C, Borrmann CM, Börchers T, Spener F (2001) Fatty acids and hypolipidemic drugs regulate peroxisome proliferator-activated receptors α- and γ-mediated gene expression via liver fatty acid binding protein: a signaling path to the nucleus. *Biochemistry* 98:2323-2328

World Health Organization. (1997) Obesity: Preventing and Managing the Global Epidemic. World Health Organization, Geneva

Yamada K, Yuan X, Ishiyama S, Koyama K, Ichikawa f, Koyanagi A, Koyama W, Nonaka K (1997) Association between ala54thr substitution of the fatty acid-binding protein 2 gene with insulin resistance and intra-abdominal fat thickness in Japanese men. *Diabetologia Arteriosclerosis, Thrombosis, and Vascular Biology* 40:706-710

Young ME, Patil S, Ying J, Depre C, Ahuja HS, Shipley GL, Stepkowski SM, Davies PJA, Taegtmeyer H (2001) Uncoupling protein 3 transcription is regulated by peroxisome proliferator-activated receptor in the adult rodent heart. *The FASEB Journal* 15:833-845

Zhang CY, Hagen T, Mootha VK, Slieker LJ, Lowell BB (1999) Assessment of uncoupling activity of uncoupling protein 3 using a yeast heterologous expression system. *FEBS Letters* 449:129-134

Zhang CY, Baffy G, Perret P, Krauss S, Peroni O, Grujic D, Hagen T, Vidal-Puig AJ, Boss O, Kim YB, Zheng XX, Wheeler MB, Shulman GI, Chan CB, Lowell BB (2001) Uncoupling protein-2 negatively regulates insulin secretion and is a major link between obesity, β cell dysfunction, and type 2 diabetes. *Cell* 105:745-755